MECHANOREGULATION OF CHONDROCYTES AND CHONDROPROGENITORS: THE ROLE OF TGF-BETA AND SMAD SIGNALING

A Dissertation
Presented to
The Academic Faculty

By

Janna Kay Mouw

In Partial Fulfillment
Of the Requirements for the Degree
Doctor of Philosophy in Bioengineering

Georgia Institute of Technology
December 2005

MECHANOREGULATION OF CHONDROCYTES AND CHONDROPROGENITORS: THE ROLE OF TGF-β AND SMAD SIGNALING

Approved by:

Marc E. Levenston, Ph.D., Advisor
School of Mechanical Engineering
Georgia Institute of Technology

Andrés J. García, Ph.D.
School of Mechanical Engineering
Georgia Institute of Technology

Barbara D. Boyan, Ph.D.
School of Biomedical Engineering
Georgia Institute of Technology

Harish Radhakrishna, Ph.D.
School of Biology
Georgia Institute of Technology

Christopher R. Jacobs, Ph.D.
School of Mechanical Engineering
Stanford University

To my mother and father.

Without the love and support of my mother and father, this PhD would never have been possible. They stood by my side through countless trials and tribulations, lifting me up and encouraging me every single day. There were many times when I was convinced that this degree would never get completed, that I just simply did not have the necessary elements required to persevere through 7+ years. Time and time again my mother and father held a mirror up to me, showing me that I could, in fact, successfully navigate the journey that was my doctoral work.

Thank you, mom and dad. I was blessed with your love.

ACKNOWLEDGEMENTS

I would like to thank my advisor, Dr. Marc E. Levenston, for guiding me through my PhD experience. Through many projects, and even more hair colors and styles, he gave an endless amount of positive energy and encouragement. On a more personal note, he went above and beyond to help me through some very difficult life experiences.

I would also like to thank my committee members: Dr. Barbara D. Boyan, Dr. Andrés J. García, Dr. Christopher Jacobs, and Dr. Harish Radhakrishna. I appreciate their time and patience throughout this whole process. I am especially grateful to Dr. García, who helped guide and shape my project. Watching him navigate the rough terrain of teaching his class (for which I was a teaching assistant) during the fall of 2001, in wake of 9/11, was truly an inspiration. He handled one of history's worst American tragedies, in front of a class of young undergraduates, with grace and dignity.

This work was funded by the ERC program of the NSF through the Georgia Tech/Emory Center for the Engineering of Living Tissues (GTEC). I was personally funded through a National Science Foundation Graduate Research Fellowship, a President's Fellowship from the Georgia Institute of Technology and a George W. Woodruff Mechanical Engineering Fellowship.

The most rewarding aspect of my PhD experience was working with such incredibly bright, creative and kind people. What might have been a difficult and frustrating experience was turned into an enjoyable and worthwhile journey through the interactions with multiple amazing people. The first person I need to thank is Erica Ooten Biediger, my best friend from "way back" at Texas A&M University. She traveled

the long distance from our native Texan soil to pursue her PhD at Georgia Tech with me. She held my hand during difficult experiences, gave me a shoulder to cry on and lent an ear for all of my inappropriate stories. Thanks, E! A big hug and thanks goes out to Dr. Stacy Marie Imler! Quite possible THE sweetest and most organized person on the entire planet, she allowed me to share a brain with her when ours were only working at 50%. Upon her graduation, I felt as if I had been separated from my co-joined head. Quite possibly she took the brain with her when she left! I thank Christopher "Topher" Hunter for being an awesome friend and a wonderful mentor. I have since realized that everything he taught me was crap, but I appreciate the effort nevertheless. I thank Natasha Case for her friendship and all the fiery interactions we had while working together into the wee hours of the morning. Without her knowledge, my project would simply not exist. She is the epitome of what I believe a scientist should be: a sharing, open-minded explorer. I thank Eric Vanderploeg for bringing in the Dutch connection, as well as an endless well of patience and trouble-shooting energy. Taller and blonder IS better! I also thank Kathryn Brodkin for her friendship and willingness to eat at Taqueria at the drop of a hat!

On to those who I will always consider the "newbies": Ashley Wells Palmer, Christoper Wilson and John "John Connelly oops sorry John" Connelly. For as much as we butted heads initially, I would like to thank Ashley Wells for showing me that you can't always judge people via first impressions. She could ALWAYS be counted on to genuinely care about your well-being and to remember to ASK about it. And, YES, two alpha females CAN exist in the same space, as long as the space is BIG. I thank Wilson for reminding me how fun science can be. He was always willing to put the paradigm

aside for the sake of a thought-provoking discussion. Plus, he was darn fun to tease! And last, but not least, is the incredibly intelligent and hardworking John Connelly. For as necessary as Natasha's input was in the life of my project, John was equally important. He took my rough ideas and transformed them into something USEFUL, helping me to focus my energy in necessary directions. He also provided excellent gossip time in the hood during long passaging days.

I would like to give a big thanks to everyone in the Guldberg and García laboratories as well. Beyond my immediate lab mates, these fellow students have built a community full of diverse backgrounds and expertise, willing to share and wanting to further good science. There are several people in particular that I need to recognize. Rhima Coleman has been one of my best friends during my time at Tech. While quite possibly the most difficult person in the entire world to get to know (and to get along with), once she is on your side, her loyalty is impenetrable. Her ideas and help are dispersed throughout my dissertation, from the organizing of ideas before I ever proposed, to helping shape the background and introductory materials in Chapter 2. She can be counted on for an honest perspective and many crazy stories. I thank Blaise "BP" Porter for always being there. He provided an endless amount of unconditional love and support. My mom loves you, Blaise! I thank Kristin Michael for her willingness to discuss science WHILE shopping or getting our hair done. She was also an amazing support system and a valuable asset to my research.

I thank Kristine Knox Hermann for being one of my best friends for the past 16 years. She loved and supported me when all I wanted was to be left alone. She also knows of all the fashion mistakes that I have made over the majority of my fashion life. I

thank Kimberly Noel Smith for her love and friendship for the past 12 years. It seems like just yesterday that I walked into my sweet-mate's room in Mosher Hall at TAMU and met this exotic girl with the name that didn't match her. Her friendship opened my eyes to parts of life that I was blind to. I thank Rob Williams for distracting and picking on me endlessly during the work day. In addition to being able to make me giggle when all I wanted to do was cry, he also had the strangest, most accurate intuition when it came to members of the opposite sex (opposite from mine, that is). I thank Andrew Lydon for encouraging me through all of my terrible thesis moods, sending flowers and candy when I needed it most and for allowing me to take out my stress on him. I also thank Amy Dosen-Black and Nicole Fann, my roommates in Washington DC, for being eternally patient with the prolonged conclusion to my PhD.

I thank Dr. Benjamin Byers, Dr. Kathryn Vogel and JudeAnn Smith for helping shape the person I am today. Without each of them, I quite possibly would not know the depth of my strength. I grew emotionally through my experiences with each of these people.

I would like to thank my superheros: Jesus Christ, Joan Jett, Wonder Woman, Marie Curie, Maude Menten, Dorothy Crowfoot Hodgkin, Sofia Kovalevskaia, Rosalind Franklin, Ellen Swallow Richards, Barbara McClintock, Rosalyn Yalow, Jocelyn Bell Burnell, Amelia Earhart and Erica Ray. Of my superhero collection, only Erica Ray is an interactive part of my life. I thank Erica for traveling 2+ tough years with me. Her strength and courage are extraordinary and inspirational.

I believe that it was the great Gloria Steinem who said, "We're not only going to change women to fit the world, but the world to fit women" (Ms. Foundation Fundraiser,

2004). In the past 80 or so years, great strides have been made to release American society from the patriarchy that that still pervades much of the rest of the world. The fact that I live in a society…♀free from female genital mutilation, ♀where I am not forced to cover my body from head to toe, and ♀where it is unacceptable to stone a women to death after she has been sexually abused due to the disgrace that it may bring here family...has not escaped my consciousness. I can only think, with as rampant as sexism still is in the world today, women must have a terrifically powerful spirit to incite such stifling. Globally, I have been blessed to live in a society where freedom and equality is a concept that is openly debated and, for the most part, revered. Specifically, I have been blessed to be mentored by, and work alongside, some incredibly intelligent, creative and assertive women. My experience with my undergraduate co-op mentor, Jackie Chesnutt Robison, gave me the courage to use my voice. She gave me the space to excel and grow in an environment that was not the most liberal, a manufacturing plant in conservative east Texas. Luckily in my emulation of her, I didn't pick up her awful habit of chewing tobacco, although if anyone could dip with grace, she did. I would like to thank Dr. Margaret Wooldridge, for whom I was an undergraduate research assistant at Texas A&M, for inspiring and encouraging me to further my education through graduate school. But greater than an individual experience I may have had, working with an awesome collection of women in my 7.5 years at Georgia Tech was an absolutely unbelievable experience. Never once in my time at Tech did I feel set apart for being female. On the contrary, I felt accepted, heard and appreciated.

I thank my brother Daniel and sister-in-law Melinda for supporting me though the past 10 years. Along with their two lovely children, my nephew Preston and niece

Corinne, they provided endless amounts of love and a refreshing perspective on life. Many moons ago, I traveled on the handlebars of Dan's bike, jumped on his friend's trampoline and burned myself while riding a motorcycle with him, all before the age of 5. He was (and still is) the best big brother a little sister could ask for. I also thank my "sister" Nelva Gonzales Ramos for allowing me to witness her amazing journey from high school through to her position as a Nueces County District Court judge.

My mother and father were the glue and the backbone to my doctoral experience. I cannot count how many times I called home asking for something: advice, a shoulder to lean on, $50. These two people are my true heroes. The kindness and generosity that my mom, Evonne Kathryn Mouw, brings into this world cannot be explained with words. She is quite simply an angel with a heart of gold; to know her is to be touched by the grace of God. I thank my mom for giving of herself every time the phone rang and I needed something. While my dad passed away a couple years before I finished my PhD, his spirit has remained in my heart as the very energy that has driven me through these final days in my doctoral experience. He was my favorite person in the entire world. He never wavered in his support and love for me, and always let me know that I could achieve anything.

Finally, I thank my creator God. He sustained me through this experience. His Light guided me through the dark times, of which there were many. As an engineer, I realize that He is the ORIGINAL engineer that we seek to emulate. He gave us the beautifully synchronized hierarchical masterpiece of cells, tissues and organs which constitutes the human body. Thank you, Lord, for carrying me. I am indebted to you eternally.

Thy Word is a lamp unto my feet, and a light unto my path.

Psalm 119: 105

TABLE OF CONTENTS

ACKNOWLEDGEMENTS iv

LIST OF TABLES xv

LIST OF FIGURES xvi

LIST OF ABBREVIATIONS xix

SUMMARY xx

CHAPTER 1 INTRODUCTION 1

1.1 MOTIVATION 1

1.2 RESEARCH OBJECTIVES 2

1.3 SCIENTIFIC CONTRIBUTION 8

CHAPTER 2 BACKGROUND AND SIGNIFICANCE 10

2.1 ARTICULAR CARTILAGE 10

2.1.1 Structure and Function 10

2.1.2 Disease and Treatment Options 16

2.2 ARTICULAR CHONDROCYTES 22

2.2.1 Biomechanical Influences 22

2.2.2 Mechanotransduction 23

2.3 CARTILAGE TISSUE ENGINEERING 24

2.3.1 Scaffolding 25

2.3.2 Cell Source 26

2.4 CHONDROGENESIS 27

2.4.1 Transforming Growth Factor β and Smad Signaling 27

2.4.2 Biomechanical Influences 29

CHAPTER 3 INFLUENCE OF VARIOUS TISSUE-ENGINEERING SCAFFOLD MATERIALS ON THE ECM PRODUCTION BY BOVINE ARTICULAR CHONDROCYTES 30

3.1 INTRODUCTION 30

3.2 MATERIALS AND METHODS 33

3.2.1 Construct assembly and cell culture 33

3.2.2 Analytical Techniques 35

3.3 RESULTS 37

3.3.1 Histology 37

3.3.2 DNA Content 39
3.3.3 sGAG Production 41
3.3.4 Δ-Disaccharide Composition 44
3.4 DISCUSSION 48
CHAPTER 4 INFLUENCE OF VARIOUS ION-CHANNEL MECHANOTRANSDUCTION PATHWAYS ON THE BIOSYNTHESIS OF BOVINE ARTICULAR CHONDROCYTES **52**
4.1 INTRODUCTION 52
4.2 MATERIALS AND METHODS 54
4.2.1 Explant and construct culture 54
4.2.2 Experimental Design 56
4.2.3 Analytical Techniques 59
4.3 RESULTS 61
4.3.1 Dose Response 61
4.3.3 Gel Response 66
4.3.4 Static Compression 67
4.3.5 Dynamic Compression 68
4.4 DISCUSSION 69
CHAPTER 5 INFLUENCE OF THE TGF-β SIGNALING PATHWAY ON THE CHONDROCYTE RESPONSE TO DYNAMIC COMPRESSIVE LOADING **72**
5.1 INTRODUCTION 72
5.2 MATERIALS AND METHODS 73
5.2.1 Construct culture 73
5.2.2 TGF-β Inhibitor 73
5.2.3 Experimental Design 74
5.2.4 Analytical techniques 75
5.3.1 Dose Response 78
5.3.3 Mechanical Stimulation: Gene Expression 82
5.3.4 Mechanical Stimulation: Matrix Synthesis Rates 84
5.4 DISCUSSION 86
CHAPTER 6 INFLUENCE OF PASSAGING, MEDIA SUPPLEMENTS AND SCAFFOLD ENVIRONMENT ON CHONDROGENESIS OF BMSCs **91**
6.1 INTRODUCTION 91
6.2 MATERIAL AND METHODS 92

6.2.1 Cell Isolation 92
6.2.2 Experimental Design 93
6.2.3 Analytical techniques 94
6.3 RESULTS 96
6.3.1 Passaging Study 96
6.3.2 Seeding Density Study 99
6.3.3 Alginate Time Course 104
6.3.4 Agarose Time Course 107
6.4 DISCUSSION 117
CHAPTER 7 INTERACTION BETWEEN THE TGF-β SIGNALING PATHWAY AND DYNAMIC COMPRESSIVE LOADING IN THE CHONDROGENESIS OF BONE MARROW STROMAL CELLS 121
7.1 INTRODUCTION 121
7.2 MATERIALS AND METHODS 123
7.2.1 Cell Isolation 123
7.2.2 Experimental Design 125
7.2.3 Analytical Techniques 126
7.3 RESULTS 126
7.3.1 Day 8 Short Term Loading 126
7.3.2 Day 16 Short Term Loading 131
7.3.3 Long Term Loading 146
7.4 DISCUSSION 150
CHAPTER 8 CONCLUSIONS AND RECOMMENDATIONS 153
8.1 SUMMARY 153
8.2 CONCLUSIONS 157
8.3 RECOMMENDATIONS AND FUTURE WORK 165
APPENDIX A MATERIALS AND REAGENTS 170
APPENDIX B TISSUE CULTURE METHODS 173
B.1 ARTICULAR CHONDROCYTES IN GEL CULTURE 173
B.2 BONE MARROW STROMAL CELLS ISOLATION AND PASSAGING 173
B.3 TISSUE ENGINEERING SCAFFOLDS AND MEDIA 175
APPENDIX C FLUOROPHORE-ASSISTED CARBOHYDRATE ELECTROPHORESIS (FACE) 179

C.1 MATERIALS 179
C.2 EXPERIMENTAL PROCEDURE 180
C.3 NOTES 182
APPENDIX D MECHANICAL LOADING SYSTEM **186**
D.1 DESIGN 186
D.2 SET-UP PROTOCOL FOR DYNAMIC LOADING 187
D.3 DYNAMIC COMPRESSION PROGRAM 190
APPENDIX E WESTERN BLOTTING PROTOCOL **191**
E.1 BUFFERS AND SOLUTIONS 191
E.2 AGAROSE GEL TAKE-DOWN 192
E.3 WESTERN BLOTTING 194
APPENDIX D IMMUNOHISTOCHEMISTRY PROTOCOL **196**
D.1 FIXED FROZEN SAMPLE PREPARATION 196
D.2 FORMALIN FIXED, PARAFFIN EMBEDDED SAMPLE PREPARATION 196
D.3 IMMUNOHISTOCHEMISTRY 197
D.4 IMAGING 198
APPENDIX E STATISTICAL ANALYSIS **199**

LIST OF TABLES

Table 3-1: GAG Δ-disaccharide contents derived from CS and DS after 20 and 40 days of culture. 47

Table 4-1: Ion-channel inhibitors and levels used in dose-response, recovery and compression experiments. 58

Table 5-1: Primer sequences for real-time RT-PCR for bovine β-actin, aggrecan, biglycan, collagen type I, collagen type II, collagen type X, decorin, GAPDH, TGF- β1 and TGF- β receptor type I (TβRI). 77

LIST OF FIGURES

Figure 2.1: Articular cartilage constituents and hierarchy from the triple helix to the organ level. (Pictures included with the permission of Dr. Stacy Marie Imler) 15

Figure 2.2: Proposed TGF-β signaling pathways in chondrocytes (TRE: TGF-β responsive element, VDR/RXR: vitamin D receptor/retinoic acid X receptor, AP-1: activation protein-1). 28

Figure 3.1: Representative interior sections stained with Safranin O from A) articular cartilage and B-F) constructs cultured for 20 days. 38

Figure 3.2: Construct DNA contents. 40

Figure 3.3: Construct sGAG content normalized to DNA content after 20 and 40 days of culture. 42

Figure 3.4: Average sGAG release rates during four 10-day intervals. 43

Figure 3.5: Construct ΔDi-6S/ΔDi-4S ratios after 20 and 40 days of culture. 46

Figure 4.1: Dose-dependent inhibition of cartilage explant protein (L-5-^{3}H-proline incorporation) and sGAG (^{35}S-sodium sulfate incorporation) synthesis rates for each of the ion-channel inhibitors. 62

Figure 4.2: Representative Live/Dead images of cartilage explants exposed to the ion-channel inhibitors for 24 hours. 64

Figure 4.3: Protein and sGAG synthesis rates of cartilage explants during recovery from 24 hours of exposure to the ion-channel inhibitors. 65

Figure 4.4: Protein and sGAG synthesis rates of free-swelling gels after 44 hours of exposure to the ion-channel inhibitors. 66

Figure 4.5: Protein (A) and sGAG (B) synthesis rates for gels subjected to varying grades of static compression for 20 hours in the presence of ion-channel inhibitors. 67

Figure 4.6: Protein (A) and sGAG (B) synthesis rates for gels subjected to static and dynamic compression for 20 hours in the presence of ion-channel inhibitors. 68

Figure 5.1: Dose-dependent inhibition of BAC construct protein (L-5-^{3}H-proline incorporation) and sGAG (^{35}S-sodium sulfate incorporation) synthesis rates for the inhibitor SB431542. 79

Figure 5.2: Recovery response of BAC construct protein (L-5-^{3}H-proline incorporation) and sGAG (^{35}S-sodium sulfate incorporation) synthesis rates for the inhibitor SB431542. 81

Figure 5.3: Gene expression for BAC constructs dynamically compressed for 20 hours in the absence (BASAL) or presence of the inhibitor SB431542 (BASAL+SB). 83

Figure 5.4: Matrix synthesis rates for BAC constructs dynamically compressed for 20 hours in the absence or presence of the inhibitor SB431542. 85

Figure 6.1: Gene expression results for BMSCs passaged 2, 3 and 4 times and seeded in 2% alginate. 97

Figure 6.2: sGAG per DNA accumulation for BMSCs passaged 2, 3 and 4 times and seeded in 2% alginate. 98

Figure 6.3: Gene expression for BMSCs seeded at three different cellular densities in 2% alginate (LOW=12.5x10^6, MID=25x10^6 and HIGH=50x10^6 cells/mL). 101

Figure 6.4: sGAG per DNA accumulated for BMSCs seeded at three different cellular densities in 2% alginate. 103

Figure 6.5: Gene expression time course for passage 3 BMSCs seeded 25x10^6 cells/mL in 2% alginate. 105

Figure 6.6: sGAG per DNA time course for passage 3 BMSCs seeded 25x10^6 cells/mL in 2% alginate. 106

Figure 6.7: Viability staining for BMSCs in agarose cultured for 16 days. Green indicates live cells; red indicates dead cells. (N=4) 108

Figure 6.8: Gene expression for BMSCs in agarose cultured for 8 and 16 days. 110

Figure 6.9: Matrix synthesis rates for BMSCs in agarose cultured for 8 and 16 days. 112

Figure 6.10: sGAG accumulation for BMSCs in agarose cultured for 8 and 16 days. 113

Figure 6.11: Safranin O staining for BMSCs in agarose cultured for 8 and 16 days (20X objective). (N=4) 115

Figure 6.12: Representative Safranin O stained sections for BMSCs in agarose cultured for 8 and 16 days (10X objective). 116

Figure 7.1: Gene expression for BMSCs seeded in agarose and subjected to 3 hours of mechanical stimulation on day 8. 128

Figure 7.2: Matrix synthesis rates for BMSCs seeded in agarose and subjected to 20 hours of mechanical stimulation on day 8. 130

Figure 7.3: Day 16 gene expression for BMSCs seeded in agarose and subjected to 3 hours of mechanical stimulation. 132

Figure 7.4: Day 16 matrix synthesis rates for BMSCs seeded in agarose and subjected to 20 hours of mechanical stimulation. 134

Figure 7.5: Total Smad2/3 immunohistochemical staining after 1 hour of mechanical stimulation. 136

Figure 7.6: Total Smad 2/3 (Smad 2/3) immunohistochemical staining. 137

Figure 7.7: Smad 2/3 levels. 138

Figure 7.8: Phosphorylated Smad2/3 immunohistochemical staining after 1 hour of mechanical stimulation. 141

Figure 7.9: Phosphorylated Smad 2/3 (pSmad 2/3) immunohistochemical staining. 142

Figure 7.10: Phosphorylated Smad 2/3 (pSmad 2/3) levels. 143

Figure 7.11: TGF-β Receptor I (TGF-β RI) levels. 145

Figure 7.12: DNA content after loading from day 8 to day 16. 146

Figure 7.13: sGAG per DNA accumulation after loading from day 8 to day 16. 147

Figure 7.14: Collagen I / II co-localization after loading from day 8 to day 16. 149

LIST OF ABBREVIATIONS

2-D	two-dimensional
3-D	three-dimensional
4AP	4-aminopyridine
ACA	ε-aminocaproic acid
ANOVA	analysis of variance
bFGF	fibroblast growth factor-basic
BAC	bovine articular chondrocyte
BMSC	bone marrow stromal cell
BSA	bovine serum albumin
DEX	dexamethasone
DMEM	Dulbecco's modified eagle's medium
DMMB	1,9-dimethylmethylene blue
DNA	deoxyribonucleic acid
ECM	extracellular matrix
FBS	fetal bovine serum
GAG	glycosaminoglycan
GAPDH	glyceraldehyde-3-phosphate dehydrogenase
Gd	gadolinium
MPC	mesenchymal progenitor cell
NEAA	non-essential amino acids
Nf	nifedipine
PBS	phosphate buffered saline
RNA	ribonucleic acid
RT-PCR	reverse-transcription polymerase chain reaction
sGAG	sulfated glycosaminoglycan
Tg	thapsigargin
TGF-β1	transforming growth factor-beta 1

SUMMARY

In pathological states such as osteoarthritis, the complex metabolic balance of cartilage is disrupted leading to a loss in the integrity and biomechanical function of cartilage[1]. Osteoarthritis affects more than 20 million Americans, costing the United States economy over $60 billion yearly[2]. Risk factors for osteoarthritis include age, excessive joint loading, and joint injury. Tissue engineering offers a potential solution for the replacement of diseased and/or damaged cartilage[3,4]. Unfortunately, plentiful donor cell populations are difficult to assemble, as chondrocytes have a well characterized lack of expansion potential[5]. Mesenchymal progenitor cells (MPCs) offer an alternative with a high expansion potential capable of supplying large quantities of cells. Using an immature bovine model, the chondrogenic differentiation of articular chondrocytes (BACs) and bone marrow stromal cells was found to be scaffold, media and mechanical stimulation dependent. Mechanisms modulating mechanotransduction in BACs were explored, including ion-channel and TGF-β signaling.

TGF-β signaling participated in the response of articular chondrocytes to dynamic compressive loading, as well as enhanced the chondrogenesis of bovine BMSCs, through interactions between loading and TGF-β/Smad signaling. Also, dynamic loading altered gene expression, matrix synthesis rates and intracellular phosphorylation for bovine BMSCs. However the response of the cells to dynamic loading depends on both media supplementation and the duration of unloaded culture. These studies establish signaling through the TGF-beta pathway as a mechanotransduction pathway for chondrocytes and chondroprogenitors in 3D culture.

CHAPTER 1 INTRODUCTION

1.1 MOTIVATION

In pathological states such as osteoarthritis, the complex metabolic balance of cartilage is disrupted leading to a loss in the integrity and biomechanical function of cartilage[1]. Osteoarthritis affects more than 20 million Americans, costing the United States economy over $60 billion yearly[2]. Risk factors for osteoarthritis include age, excessive joint loading, and joint injury. Tissue engineering offers a potential solution for the replacement of diseased and/or damaged cartilage[3,4]. Unfortunately, plentiful donor cell populations are difficult to assemble, if not impossible. Chondrocytes have a well characterized lack of expansion potential[5]. Mesenchymal progenitor cells (MPCs) offer an alternative with a high expansion potential capable of supplying large quantities of cells. MPCs can be easily isolated, offer high proliferation potential and are capable of differentiating into a distinct phenotype through a series of discrete steps, finishing with cells involved in the production of a distinct tissue type[6,7]. Understanding the behavior of chondrocytes and chondroprogenitors in response to physiologically relevant biomechanical and biochemical stimuli is central to understanding normal tissue maintenance, as well as elucidating potential mechanisms for repair of diseased or damaged cartilage.

1.2 RESEARCH OBJECTIVES

The overall goal of this dissertation is to elucidate the mechanotransduction of bovine articular chondrocytes (BACs) and bone marrow stromal cells (BMSCs) through the interaction between TGF-β signaling and dynamic compression. The central hypothesis of this dissertation is that interactions between loading and TGF-β/Smad signaling will regulate the response of articular chondrocytes to dynamic compressive loading, as well as enhance the chondrogenesis of bovine BMSCs.

1.2.1 Specific Aims

There were three hypotheses and five specific aims to elucidate the mechanotransduction of BMSCs through the interaction between TGF-β signaling and dynamic compression. Bovine articular chondrocytes (BACs) were used to establish a 3D model for investigating mechanotransduction in specific aims 2 and 3. The 3D model developed with BACs was used to investigate the relationship and interaction between TGF-β signaling and dynamic compression in BMSCs in specific aim 5. The work identified in specific aim 1 focused on investigating the influence of scaffold choice on ECM production by BACs. The work identified in specific aim 4 focused on establishing *in vitro* conditions for the chondrogenic differentiation of bovine BMSCs. The results from specific aims 1 and 4 provided justification for cell isolation and seeding procedures of subsequent studies in the dissertation and aided in the interpretation of results.

Specific Aim 1: Examine the influence of various tissue engineering scaffold materials on the extracellular matrix production by bovine articular chondrocytes.

Multiple scaffold materials have been used for tissue engineering cartilage. In specific aim 1, scaffold materials commonly used for cartilage tissue engineering were evaluated to determine whether scaffold material directly or indirectly influences chondrocyte matrix synthesis, specifically glycosaminoglycan (GAG) Δ-disaccharide composition. Articular chondrocytes from two donors were isolated and seeded at $15x10^6$ cells/mL into the following tissue engineering scaffolds:. 1.5% LMP agarose, 0.75% sodium alginate, 2 mg/mL type I collagen (rat tail), and 50 mg/mL fibrin (n=8/scaffold/timepoint). Cells were also seeded on polyglycolic acid (PGA) felt at a target density of $15x10^6$ cells/mL, although poor seeding efficiency yielded approximately 1/3 of the intended density. Native cartilage samples from the same joints were maintained in identical culture conditions for the comparison of the GAG Δ-disaccharide composition. Constructs were cultured for either 20 or 40 days, after which they were assayed for total DNA and sGAG contents, as well as for Δ-disaccharide composition using fluorophore-assisted carbohydrate electrophoresis (FACE).

Hypothesis 1: Mechanotransduction mechanisms established with articular chondrocytes in monolayer will be critical in the response of articular chondrocytes in 3D culture subjected to dynamic compressive loading. Perturbing these pathways will inhibit the upregulation of protein and proteoglycan (PG) synthesis due to dynamic compressive loading.

Specific Aim 2: Examine the influence of various ion-channel mechanotransduction pathways on the biosynthesis of bovine articular chondrocytes.

Mechanotransduction studies have been performed on chondrocytes in monolayer. However, important differences exist between chondrocyte behavior in monolayer and 3D (3D) cultures. The extent to which these same ion channels are involved in the transduction of mechanical stimuli in 3D culture has not yet been addressed. In specific aim 2, the roles four ion-channels play in the signal transduction of bovine articular cartilage and BACs was investigated using inhibitory media supplements including: 4-Aminopyridine (4AP), a potassium channel blocker; Nifedipine (Nf), a calcium channel blocker; Gadolinium (Gd), a stretch-activated channel blocker; and Thapsigargin (Tg), which releases intracellular Ca^{2+} stores by inhibiting ATP-dependent Ca^{2+} pumps.

The response of bovine articular cartilage to stimulation with a range of ion channel inhibitor doses was examined using articular cartilage tissue explants using radiolabel incorporation to monitor both protein and sGAG synthesis rates and LIVE/DEAD® imaging to investigate cell viability. Recovery from the inhibition of protein and sGAG synthesis rates was examined over 3 days post-exposure to a single level of each inhibitor. Agarose gels seeded with $20x10^6$ BACs/mL were mechanically stimulated in the presence of a single level of each of ion channel inhibitor. To examine the influence of the ion-channels on the response of chondrocytes to mechanical stimulation, agarose gels seeded with $20x10^6$ BACs/mL chondrocytes were cultured for 5 weeks prior to the application of mechanical stimulation. Constructs were then cultured

in basal media supplemented with both an inhibitor and radiolabeled precursors under the following conditions: static compression (10%), 1Hz oscillatory compression (10%±3%) and unloaded.

Hypothesis 2: TGF-β1 modulated pathways regulate the response of bovine articular chondrocytes to dynamic compressive loading through the Smad2/3 signaling pathway. Perturbing TGF-β signaling through chemical inhibition will inhibit the upregulation of protein and PG synthesis and gene expression due to loading.

Specific Aim 3: Examine the influence of the TGF-β signaling pathway on the chondrocyte response to dynamic compressive loading.

Transforming growth factor-beta 1 (TGF-β1) has been shown to have an anabolic affect on articular chondrocytes. In specific aim 3, the role the TGF-β1/Smad signaling pathway has in the BAC response to dynamic compressive loading was investigated. BACs seeded at $20x10^6$ cells/mL in 3% agarose were used the study. This study examined the effects of mechanical loading in the absence or presence of the TGF-β1 inhibitor SB431542. SB431542 is proposed to block the signaling cascade of TGF-β and activin type receptors after ligand binding occurs by inhibiting the kinase activity of the TGF-β type I Receptor (ALK5). Four concentrations of SB431542 were used ranging from 100nM-100μM, as well as a no-inhibitor control, to establish a dose response of the inhibitor on both protein and sGAG synthesis rates. Recovery from the inhibition of protein and sGAG synthesis rates was examined over 3 days post-exposure to a single

level of the inhibitor. To examine the influence of TGF-β1 signaling pathway on the response of BACs to mechanical stimulation, agarose gels were cultured for 24 hours prior to the application of mechanical stimulation. Constructs were then cultured in basal media ± 1 μM SB431542 under the following conditions: static compression (10%), 1Hz oscillatory compression (10%±3%) and unloaded controls. Following growth factor supplementation and/or dynamic loading, samples will be taken down and assayed for radiolabel incorporation and gene expression.

Specific Aim 4: Examine effects of passaging, media supplements and scaffold environment on chondrogenesis of bovine BMSCs.

Previous studies have shown that members of the transforming growth factor (TGF) family induce chondrogenic differentiation of stromal cells, but the optimal *in vitro* conditions within which BMSCs can achieve the most chondrogenic response have yet to be explored in depth for the bovine model. In specific aim 4, various media conditions, passage number, seeding density and the temporal differentiation of BMSCs were examined in alginate and agarose gel systems. The results from this aim were used to pursue specific aim 5. A 2% alginate gel system was used to examine the effects of passaging, seeding density and temporal differentiation due to the ease and consistency of obtaining RNA from these samples. The temporal differentiation was also investigated in 3% agarose due to the ease of getting consistent dimension suitable for loading. Following growth factor supplementation, samples were assayed for sulfated GAG (sGAG) content, DNA content, gene expression, and cell viability.

Hypothesis 3: Modulation of the chondrogenic differentiation of bovine BMSCs by dynamic compressive loading is dependent on TGF-β1 signaling through the Smad2/3 signaling pathway. Dynamic compressive loading will increase Smad2/3 phosphorylation and nuclear accumulation, leading to an increase in chondrogenic genes and protein production.

Specific Aim 5: Examine the influence and interaction of TGF-β1 and dynamic compressive loading on the chondrogenic differentiation of bovine BMSCs.

The differentiation of BMSCs can be influenced by various stimuli including growth factors, cell-cell interactions, and cell-matrix interactions. Mechanical stimulation has been shown to be important in the development of certain tissues and may influence differentiation of BMSCs. It has been suggested that the combination of chondrogenic media and dynamic compressive loading may enhance chondrogenesis of BMSCs over the addition of exogenous factors alone. In specific aim 5, the influence of TGF-β1 and oscillatory compressive loading on the gene expression, matrix synthesis rates and Smad phosphorylation/translocation of BMSCs was investigated. This study examined the response of agarose gels seeded with BMSCs to oscillatory compression with and without TGF-β1 supplementation. Constructs were cultured in basal media consisting of high glucose DMEM plus antibiotic/antimycotic, non-essential amino acids, 1% ITS+, 50μg/mL ascorbate and 0.4mM proline (BASAL), basal media plus 10ng/mL TGF-β1 (TGF-β1), or basal media plus 10ng/mL TGF-β1 and 100nM dexamethasone

(TGF-β1+DEX). After a preculture period of either 8 or 16 days, samples were either left unloaded or subjected to 10% static compression or 10%±3% oscillatory compression. Samples were analyzed for gene expression, matrix synthesis rates and Smad phosphorylation and translocation. The effects of long term loading from day 8 to day 16 were also investigated. Samples were analyzed for sGAG accumulation and immunohistochemistry (IHC) for collagen I and II localization.

1.3 SCIENTIFIC CONTRIBUTION

Investigation of the influence of transforming growth factor β1 (TGF-β1) signaling in the response of chondrocytes and BMSCs to dynamic compressive loading may provide clues to the mechanisms involved in chondrocyte differentiation and define other potential targets to regulate this process. The mechanisms through which mechanotransduction occurs in chondrocytes and chondroprogenitor cells remain largely elusive. This work addresses a potential pathway through which mechanotransduction occurs in these cells.

The work presented in this dissertation demonstrates that there are marked differences in the phenotypic expressions between the responses of BACs and bovine BMSCs to mechanical stimulation in 3D culture. Additionally, interactions between TGF-β signaling and dynamic compression in BACs and BMSCs have been demonstrated. While speculative, there are multiple potential regulatory mechanisms through which TGF-β1 signaling and mechanical stimulation interact. Understanding the relationship between mechanical loading and TGF-β signaling may provide potential

targets for manipulating cell differentiation, as well as for treating diseased and injured cartilage. To this end, this work is important for understanding *in vitro* development of 3D scaffolds for cartilage regeneration. It has been hypothesized that the loading environment in the knee is too harsh to allow an immature construct lacking mechanical integrity to survive and develop into a tissue capable of successful load bearing[8]. Facilitating a tissue-engineered construct capable of functioning successfully in vivo will involve matching mechanical and biochemical properties of native cartilage as closely as possible.

While this work supports the importance of TGF-β signaling in articular chondrocytes and BMSCs, the TGF-β signaling pathway is only one of many growth factor mediated signaling pathways that regulate articular chondrocyte metabolism. These studies establish a paradigm for exploring interactions between mechanical stimulation and a specific growth factor mediated signaling pathway. While *in vitro* mechanical stimulation may end up improving both the mechanical and biochemical properties of constructs, it may not prove to be practical or even feasible for purposes other than scientific investigation. Understanding the pathways through which mechanotransduction occurs offers the possibility of regulating these mechanisms biochemically, as opposed to biomechanically.

CHAPTER 2 BACKGROUND AND SIGNIFICANCE

2.1 ARTICULAR CARTILAGE

2.1.1 Structure and Function

Articular cartilage is a hyaline cartilage found at the ends of diarthrodial joints and provides resistance to compressive, shear and tensile forces that occur during normal joint motion[9]. This ability arises from the unique architecture of the matrix elements found in articular cartilage. The tissue consists of four major components: collagen, proteoglycans, water, and cells. It is through the highly delicate and complex interactions of these constituents that articular cartilage maintains its resiliency and near frictionless properties[10]. Because articular cartilage is mostly avascular, chondrocytes receive nourishment from the synovial fluid through diffusion[9]. This avascularity also contributes to the limited healing properties of this tissue[11].

Collagen

The extracellular matrix component most responsible for the resistance to tensile forces is collagen[12]. Several types of collagen have been found in articular cartilage (II, V, VI, IX, X, XI, XII, XIV). Collagen type II is 80-90% of the total collagen content, making it the most abundant collagen in articular cartilage[12-14]. It is a homotrimer composed of three α_1(II) chains that bind into a helical structure. These helical molecules bind end to end to form microfibrils. In combination with collagen types IX and XI, the microfibrils are arranged into fibrils ranging from 20-120nm in diameter in normal hyaline cartilage

(Figure 2.2). Type IX collagen makes up approximately 2% of the collagen in articular cartilage; its proposed function is as a mechanical spacer within collagen fibrils, as well as to provide a location where the fibrils can interact with proteoglycans. Collagen types V and XI are thought to regulate fiber size[9,12].

Proteoglycans

The fibrillar collagen network is organized and stabilized through molecular cross-links that restrain the swelling pressure exerted by a high concentration of negatively charged sulfated glycosaminoglycans (sGAGs). In articular cartilage, the GAGs are mainly chondroitin sulfate (CS) and keratan sulfate (KS), as well as a small proportion of dermatan sulfate (DS) chains[15]. Aggrecan is the predominant proteoglycan found in articular cartilage, constituting ~10% of the dry weight of articular cartilage[16]. It consists of a protein core with attached CS chains containing predominately 4- or 6-sulfated disaccharides[17,18] and a small amount of KS chains near the binding site for hyaluronan[9]. These negatively charged GAGs attract the influx of water into the tissue, which makes up 60-90% of cartilage weight[10]. The close interactions of aggrecan and collagen II prevent full swelling of the proteoglycan molecules, creating a swelling pressure that gives articular cartilage its compressive stiffness and maintains tensile stress in the type II collagen network[19]. While the collagen network is somewhat metabolically static[20], aggrecan undergoes a distinct turnover process[21,22] in which catabolic cleavage[23,24] and removal of molecules from the extracellular matrix are in balance with synthesis and deposition of new molecules[25,26].

In addition to large, aggregating proteoglycans, human articular cartilage also contains smaller proteoglycans know as small leucine-rich repeat proteoglycans (SLRPs). Human articular cartilage has been shown to contain 2 DS proteoglycans – biglycan and decorin – and one KS proteoglycan – fibromodulin[27]. These SLRPs have been shown to interact with the fibrillar collagens of the extracellular matrix, though their sites and strengths of interaction may vary[27]. For example, decorin binds collagen type II and is thought to regulate collagen fibril size[9].

Chondrocytes

The cells of articular cartilage are called articular chondrocytes and they are responsible for the balanced maintenance of the extracellular matrix proteins that affords this tissue its highly specialized properties[28]. Chondrocytes make up 2-5% of total articular cartilage volume[9,13,29], are mostly senescent, and slowly turn over their extracellular matrix[30]. The interactions of chondrocytes with their extracellular matrix allow them to maintain tissue homeostasis as well as provide links to intracellular signal transduction pathways[29]. Links to the extracellular matrix include, but are not limited to, the CD44 receptor which binds hyaluronan and annexin V (anchorin CII) and the $\alpha_1\beta_1$ and $\alpha_2\beta_2$ integrins which bind type II collagen[9,28,31]. Integrin interaction with the cytoskeleton provides cells with the ability to sense changes in their environment and also to change the affinity of specific integrins for extracellular matrix components[31]. Chondrocyte-matrix associations are crucial for cell survival[31]. Blocking the ability of CD44 to bind hyaluronan causes chondrolysis of chondrocytes in articular cartilage slices

in vitro and cartilage degradation[29,31]. Deprivation of collagen-derived signals has been shown to induce apoptosis[31].

Architecture

The microstructure of articular cartilage varies from the joint surface to the subchondral bone (Figure 2.1). The zonal distinctions include the degree of cellularity, the ratios of extracellular matrix components, growth factor concentrations, and hydrostatic pressures induced by loading[9,13]. In the surface zone, the cells are flattened and run parallel to the surface. The collagen in this zone is arranged in a "lamina splendens" layer of thin, tightly packed fibrils that also run parallel to the surface[13]. The high fibrillar nature of this zone affords this zone with the highest tensile properties[9,13]. The proteoglycan content in this zone is the lowest and decorin and biglycan content is highest here. Additionally, the cells in the superficial zone produce a specialized molecule unique to this region, lubricin, which is thought to contribute to lubrication[9]. In the middle zone, cellularity decreases and the cells have a more rounded morphology[9]. Here, the predominant proteoglycan is aggrecan and the collagen fibrils are larger and more randomly organized as the load distribution within the tissues transitions from predominantly shear to predominantly compressive forces. Below this zone, the deep zone contains the lowest cell density and aggrecan content. The collagen fibrils in the deep zone are thickest and are oriented perpendicular to the surface of the joint[9,13]. The calcified zone between below the deep zone provides transitional mechanical properties between the cartilage and the subchondral bone. Cells here have the hypertrophic phenotype, specifically expression of collagen type X[12]. Unlike, the growth plate this

region resists vascular invasion restricting nutritional flow into the cartilage from this surface. Finally, the subchondral bone, which is much like cortical bone in structure, separates the articular cartilage from the underlying trabecular bone.

In addition to the zonal variability in the extracellular matrix components and distribution, there are also variations on the cellular level as well. The chondrocytes are surrounded by a pericellular or cell associated matrix that has a different composition from the further removed or interterritorial matrix[9,31]. In general, the pericellular region is 2μm thick, fairly amorphous, and contains few collagen fibrils. In this region, decorin and aggrecan are expressed and collagen Type VI is predominant, but types VI, IX, and XI have also been found[28]. The collagen is arranged in a thin filamentous network that interacts with decorin and hyaluronan.

Chondrocyte proliferation, differentiation, and homeostasis are not only governed by interactions with extracellular matrix, but also by soluble growth factors within the matrix. Several growth factors are stored within the matrix of articular cartilage in active and inactive forms. Bone morphogenetic proteins (BMPs) and transforming growth factor-β (TGF-β) are both stored in articular cartilage[30,31]. Proteoglycans are known to indirectly influence chondrocyte activity, either through cell-matrix interactions or by binding specific growth factors in the extracellular matrix, thereby modifying their temporal and spatial effects[15,32]. For instance, the sequestering of TGF-β by proteoglycans within the extracellular matrix regulates the availability of this factor to chondrocytes[31]. Similarly, insulin-like growth factor–I (IGF-I), fibroblastic growth factors (FGFs), and bone morphogenetic protein-2 (BMP-2) are also sequestered in articular cartilage[31]. The roles of their interactions with various matrix proteins are still

being investigated. There is, however, evidence that the formation of focal adhesions due to integrin binding is necessary for chondrocytes to be responsive to some growth factors[31]. This evidence demonstrates the important interplay between cells, extracellular matrix proteins and growth factors to maintain tissue properties.

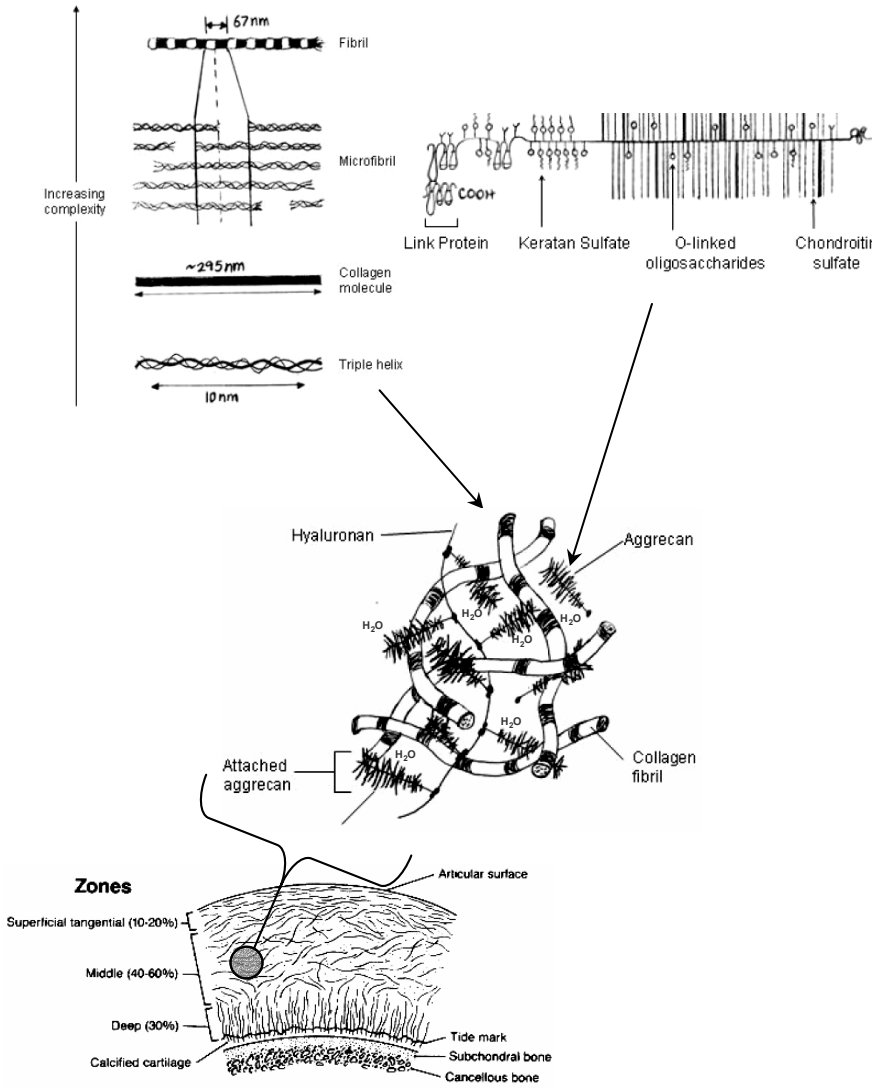

Figure 2.1: Articular cartilage constituents and hierarchy from the triple helix to the organ level. (Pictures included with the permission of Dr. Stacy Marie Imler)

2.1.2 Disease and Treatment Options

Age, Injury and Disease

Articular cartilage undergoes several cellular and molecular changes with age. The surface becomes fibrillated, proteoglycan structure and composition are altered, and collagen matrices become increasingly cross-linked. Cell proliferation, as well as matrix production, and response to growth factors all decrease[9,33]. The loss of chondrocyte function with age is associated with telomere erosion and/or oxidative injury due to mitochondrial damage[32].

The exact incidence of injury to articular cartilage is unclear, which is most likely due to the asymptomatic nature of many of these injuries[14]. In a study by Shelbourne *et al.*, patients with chondral lesions discovered at the time of ACL reconstructions resulted in a lower subjective healing score over a period of 8.7 years than those with patients with healthy cartilage[34]. Radiographic evidence presented in recent studies demonstrates progression of cartilage degeneration of full-thickness defects treated by debridement. Advances in cartilage-specific MRI technology can determine location, size, and depth of cartilage lesions and, using contrast agents, biochemical and biomechanical changes can be diagnosed[13,14].

Martin *et al.*. defined mechanical damage to the articular surface by three classifications: damage to cells and extracellular matrix proteins with no visible disruption of the cartilage surface, chondral fissures involving only the articular cartilage (partial-thickness defects), and full-thickness defect that includes the entire thickness of the cartilage and the subchondral bone[32]. It has been shown that impact loads greater than 25 MPa cause chondrocyte death and cartilage fissures. Several investigators have

demonstrated that loads in the patellar femoral joint exceed 25MPa during normal joint loading showing the importance of rate of the applied load as well as its magnitude. Rapidly applied loads occur too fast for fluid movement out of the matrix, exposing matrix molecules and cells to damaging levels of mechanical stress. Damage to cells can lead to decreased proteoglycan concentration, increased hydration, and disruption of collagen structure. This, in turn, results in an uneven distribution of force transmission to the subchondral bone, leading to an increase in subchondral bone stiffness. The greater stiffness of the subchondral bone transmits more load onto the damaged cartilage and this damaging spiral continues[14]. Decrease in proteoglycan content or organization occurs before other signs of injury and may be due to increase degradation or decreased synthesis[32,33,35]. Following injury, chondrocytes increase proliferation and matrix synthesis, but this healing response is insufficient to complete fill the defect and can lead to altered joint mechanics[32].

In full thickness injuries, blood enters the cavity resulting in hematoma formation and an inflammatory response. Growth factors released from platelets and from the fractured bone matrix stimulate matrix production and attract stem cells to the site. Unfortunately, this repair response results in fibrocartilagenous tissue formation and the resultant tissue has inferior resilience, poor wear characteristics, and inferior stiffness[11,14,32].

The ultimate goal of the early detection and treatment of traumatic articular cartilage injuries and the restoration of the normal joint mechanical environment is the prevention of cartilage degeneration and osteoarthritis (OA). OA is the most common joint disease and it is characterized by joint pain and stiffness. In later stages, muscle

atrophy and joint deformities may result[2,36]. The disease is characterized by articular cartilage loss, osteophyte formation, and in some cases increased subchondral bone density. Unfortunately, the pathophysiology is poorly understood and therefore reliable clinical preventive measures are difficult to design. Primary OA frequently occurs with no known cause of degeneration and rarely occurs in younger patients[2,36]. Secondary OA can develop in younger patients due to injury or a variety of hereditary, inflammatory, developmental, or metabolic disorders[2,11,37].

Instability of the joint can contribute short-term abnormal loading, which may lead to degenerative diseases such as OA in the long-term[38]. It has been shown that the results of cartilage repair techniques are lower if join instability is not corrected[14]. For example, the meniscus reduces the very high contact stresses seen within the joint, thereby protecting articular cartilage from OA[38]. It has been shown that loss of 20% of the meniscus can lead to 350% increase in contact forces in articular cartilage and, after partial meniscectomy, up to 6.5% loss of articular cartilage volume per year has been noted[14].

Treatment Options

Lavage and Debridement

Lavage involves irrigation of the surface of joint arthroscopically[39]. Debridement, popularized by Magnusson[14], was the first arthroscopic treatment of chondral injuries to reduce mechanical symptoms and inflammation. This procedure involves the arthroscopic removal of inflammatory tissue from the surface cartilage. Both procedures

alleviate pain through the removal of debris, but are only beneficial for injuries due to minimal energy trauma in a highly stable joint[14,39].

Marrow stimulation

The idea behind marrow stimulation is to stimulate the healing response of a full-thickness cartilage defect, providing a stable filler containing progenitor cells and growth factors that will stimulate a natural healing response[14,32,40]. Perforating the subchondral bone to repair articular cartilage lesions has been in practice since the concept was introduced by Pridie in 1956[14,32]. Abrasion arthroplasty is performed arthroscopically and involves removal of 1-2mm of bone down to the vasculature. Unfortunately, this procedure is technique sensitive and involves uncontrolled destruction of the subchondral bone, leading to variable clinical outcomes. Standardization of this technique, microfracture, was introduced by Steadman *et al.* in 1997[41]. It involves using arthroscopic picks to perforate the subchondral bone in a controlled pattern without drilling. This allows for more controlled depth of penetration and placement. This procedure achieves the best results in traumatic lesions surrounded by healthy tissue and is more successful in younger patients, presumably due to higher progenitor cell content of their bone marrow[13,14]. In a 11 year follow-up study, Steadman *et al.* found that 80% of patients reported improvement after this procedure[41].

Osteochondral Transfer

The transfer of cartilage autografts with intact subchondral bone was first published in 1985 with progression to arthroscopic methods in 1993[14,42]. In this

procedure, small subchondral bone plugs covered with healthy hyaline cartilage are removed from low-weight bearing areas and press fit into the recipient site. Defects from 1 to 4 cm can be filled depending on the availability of donor tissue. The advantages of this technique are that tissue harvest and implantation can occur in one arthroscopic procedure, tissue availability and disease transmission is not an issue, and the procedure is relatively inexpensive[14]. Overall, studies have demonstrated 80-90% good to excellent outcomes in follow-up studies[14,43]. For larger defects, multiple plugs are transferred to the defects site in a procedure known as mosaicplasty. In cases where insufficient tissue is available, allogenic sources for implantation are necessary[11].

Autologous Chondrocyte Implantation

This treatment method of articular cartilage lesions was introduced by Grande *et al.* in 1989 and clinical application of this technique was pioneered by Brittberg *et al.* in 1994[19]. Implantation of chondrocytes is generally applied to shallow, partial-thickness lesions 2 to 10 cm^2 in size and is indicated when the above treatments have failed. Cartilage tissue is removed arthroscopically from non-weight bearing surfaces of articular cartilage and the are cells released from the matrix and expanded *in vitro*. After expansion, the patient undergoes a second procedure in which cells are injected underneath a autologous periosteal patch that is sutured to the surrounding intact cartilage[14,39]. Recent studies comparing autologous chondrocyte implantation to osteochondral transfer noted significantly better subjective and histological outcomes with the implantation of chondrocytes[13,14]. Optimization of the number of cells to be

implanted has not been studied; currently in the clinical setting, the aim is to implant $30x10^6$ cells/mL[14,39].

Limitations of Cartilage Defect Treatment Options

Though the marrow stimulation techniques introduce growth factor and progenitor cells capable of adapting the chondrogenic phenotype into the cartilage lesion, the resultant tissue formed is mostly fibrocartilaginous[39]. The newly formed tissue is composed of predominantly collagen type I, has inferior mechanical properties to healthy articular cartilage, and rarely fills more than 75% of the defect area[14].

Growth factor delivery is an attractive an option to increase cell proliferation and matrix synthesis. Through *in vitro* and *in vivo* studies, the function of various growth factors has been discovered in recent years, but the clinical application of growth factors has not yet been implemented[13]. New evidence that increased proliferation and matrix production by these cells may lead to degeneration due to enhanced senescence of chondrocytes may deter their application in the treatment of cartilage lesions without the introduction of a younger cell population into the area[32].

Osteochondral transfer has demonstrated good clinical results in follow-up studies. Unfortunately, there remain several limitations to the procedure, the most predominant of which is availability of healthy donor tissue[14]. Significant research has been done to identify harvest locations for healthy tissue, but the harvesting of tissue for osteochondral transfer can lead to donor site morbidity, and the use of allogenic tissue increases the chances of infection transfer[14,39]. Additionally, the fixation strength of osteochondral plugs has been shown to decrease after soaking of plugs in saline *in vitro*

over a period of 7 days, increasing the chances of graft failure. Matching the original contours of the recipient type is also generally difficult, which may lead to localized regions of abnormal stresses and eventual cartilage degeneration[14].

Autologous transfer of articular chondrocytes has yet to gain wide acceptance in the United States and it is estimated that only 10,000 procedures have been performed worldwide. Therefore little long-term data are available on this procedure. Several follow-up studies have demonstrated good to excellent subjective improvements, but the variability in these results is site dependent. Currently, this procedure is only recommended for shallow cartilage lesions not involving the subchondral bone[14,39,44].

Though great strides have been made in the clinical treatment of cartilage lesions, the limitations of these techniques do not completely inhibit formation of fibrocartilaginous tissue and do not fully address the poor integration of the replacement tissue [11]. Long-term studies are demonstrating the need for alternative strategies to treat cartilage lesions and much research is still taking place in this field with a focus on tissue engineering.

2.2 ARTICULAR CHONDROCYTES

2.2.1 Biomechanical Influences

The biomechanical environment contributes to the regulation of cartilage development, maturation and maintenance. Articular cartilage has been shown to be responsive to changes in mechanical loading across the joint. Experimental studies have indicated that moderate exercise leads to increased proteoglycan content, while joint

immobilization leads to loss of proteoglycan content[45,46]. *In vitro* studies have provided important information regarding how mechanical loading influences articular chondrocyte metabolism[8,47]. Static compression of cartilage explants inhibits both protein and sGAG synthesis, while dynamic compression increases both protein and sGAG synthesis within given frequency and deformation ranges[48]. Studies with isolated chondrocytes in hydrogels have demonstrated that the length of culture time preceding exposure to mechanical loading influences cellular response[49]. The ability of a cell to sense mechanical stimulation after formation of a pericellular matrix, but before formation of an interconnected extracellular matrix, has been shown to be dramatically decreased. For hydrogels subjected to loading after multiple weeks in culture, static compression was found to decrease both protein and sGAG synthesis, while dynamic loading increased synthesis[50-52].

2.2.2 Mechanotransduction

The mechanisms by which chondrocytes sense changes in their local mechanical environment produced by these macroscopic stimuli are largely unknown. Studies with articular chondrocytes in monolayer suggest that mechanosensitive ion channels may participate in chondrocyte mechanotransduction. It has been demonstrated that fluid flow, which chondrocytes experience in vivo and which results in a variety of morphological and metabolic changes in cultured articular chondrocytes, can stimulate a rise in intracellular calcium concentration due to both G-protein modulation and the release of Ca^{2+} stores, possibly through an inositol 1,4,5-trisphosphate (IP3)-dependent mechanism[53]. It has also been suggested that transient increases in intracellular Ca^{2+}

concentrations may be one of the earliest events involved in the response of chondrocytes to mechanical stress through deformation-induced Ca^{2+} waves initiated through mechanosensitive ion channels[54]. Stretch-activated channels have been suggested to participate in the control of chondrocyte proliferation. Also, blocking the Ca^{2+}-senstitive K^{+} channels has been demonstrated to have an effect on both proliferation and mRNA level of certain proteins[55]. However, important differences exist between chondrocyte behavior in monolayer and three dimensional cultures. The extent to which these same ion channels are involved in the transduction of mechanical stimuli in three-dimensional culture is unclear.

2.3 CARTILAGE TISSUE ENGINEERING

In pathological states such as osteoarthritis, the complex metabolic balance of cartilage is disrupted, marked by increased catabolism and decreased synthesis of matrix proteins by chondrocytes. This leads to a loss in the integrity and biomechanical function of cartilage[1]. Tissue engineering offers a potential solution for the replacement of diseased and/or damaged cartilage[3,4]. Unfortunately, plentiful donor cell populations are difficult to assemble, if not impossible. It has been demonstrated that chondrocytes lack the ability to be expanded in monolayer culture without a parallel loss of phenotype[5]. Mesenchymal progenitor cells offer an alternative with a far greater expansion potential capable of supplying large quantities of cells.

2.3.1 Scaffolding

The criteria for scaffold design in general is that the material must exhibit biocompatibility, provide mechanical support during the healing process, and support ingrowth of native cells and matrix. When addressing biocompatibility, consideration must be given to not only how the recipient tissue will respond to the intact scaffold, but also to its degradation products as the tissue regenerates[11,56]. For example, the build up of acidic products during the degradation of lactic acid based scaffolds has been shown to be detrimental to the surrounding tissue. During the early stages of healing, the scaffold must be able to withstand the complex mechanical environment of articular cartilage, especially if cells and/or growth factors are to be delivered to the site[56]. In articular cartilage, lack of integration with the surrounding cartilage has been the focus of much research. Loosening of constructs due to the hypertrophic shear environments at the implant/cartilage interface may impede integration and implant stability is usually obtained by suturing or press fitting[14]. Sites of uneven integration with the host tissue may later become the nucleation site of arthritic degeneration[11]. Finally, ease of handling in the clinical setting is of critical importance for any tissue engineered application[8].

Several types of scaffolds are being investigated by articular cartilage tissue-engineering researchers. These include natural scaffolds (autologous or allogenic tissues), woven scaffolds like polyglycolic acid (PGA) and polylactic acid (PLA), and gels made from natural proteins like collagen, fibrin, chitosan, agarose, and alginate[11,57].

Materials derived from PLA and PGA are attractive because they have been USDA approved for *in vivo* applications for many years[11,56,57]. They support cell attachment and matrix production of several different cell types involved in

osteochondral tissue engineering[56]. They have been shown to support significant matrix accumulation by young bovine chondrocytes in rotating wall and perfusion bioreactors *in vitro*[8]. Hydrogels are also attractive because their high hydration provides the construct with initial mechanical stability and allows diffusion of nutrients and waste products to and from the encapsulated cells. The ability of these gels to be injected into a defect site and polymerized *in situ* make hydrogels ideal for easy delivery clinically. A great deal of research has been performed to on the ability of alginate and agarose to recover and/or maintain the chondrocytic phenotype of cells derived from cartilaginous tissues[8,58].

2.3.2 Cell Source

Though much has been learned from articular chondrocytes *in vitro*, the applicability in the clinical setting is limited by the fact that there are limited sites from which donor tissue can be harvested[13]. Additionally, despite evidence that the chondrocytic phenotype lost by articular chondrocytes during expansion can be recovered by placing these cells in a 3D environment, poor expansion is still a characteristic of these cells. MPCs can be easily isolated and offer high proliferation potential. These undifferentiated MPCs are capable of differentiating into a distinct phenotype through a series of discrete steps, finishing with cells involved in the production of a distinct tissue type[7,59]. The *in vitro* chondrogenesis of bone marrow derived MPCs has been described using the aggregate culture (i.e. pellet[60]) and gel culture (agarose[61], alginate[62]) of MPCs in media supplemented with transforming growth factor-beta 1 (TGF-β1)[63]. Fibroblast growth factor 2 (FGF-2) has been found to maintain cells in a more proliferative state,

allowing *in vitro* expansion of BMSCs[64]. BMSCs have been shown to retain some level of chondrogenic potential through 20 or more passages[65].

2.4 CHONDROGENESIS

2.4.1 Transforming Growth Factor β and Smad Signaling

Both biochemical and biomechanical stimulation have been shown to influence the growth and differentiation of BMSCs. Much effort investigating the effect of growth factor and cytokine supplementation on the chondrogenesis of BMSCs has focused around members of the transforming growth factor β (TGF-β) family[66]. Multiple members of the TGF-β family, including TGF-β1, have been shown to induce *in vitro* chondrogenesis of BMSCs[67,68]. The transforming growth factor β (TGF-β) superfamily is involved in the regulation of multiple cellular processes, including cell proliferation, differentiation and apoptosis[69]. TGF-β transmits its signal from the cell surface via a transmembrane serine/threonine kinase receptor complex[70,71]. Upon ligand binding, the type II receptor subunit engages and transphosphorylates a type I receptor subunit (TβRI), which in turn phosphorylates the receptor-activated Smad proteins (R-Smads) Smad2 and Smad3 (Figure 2.2). A protein complex with Smad4 is formed with the activated R-Smads and translocated into the nucleus where they interact with additional transcription factors, binding to the promoters of responsive genes and regulate their expression by cooperating with other activators or repressors[72]. In addition to the Smad pathway, TGF-β has been shown to activate other signaling pathways including p38 mitogen-activated protein kinase (MAPK)[73] and protein kinase C (PKC)[74]. TGF-β

signaling has been demonstrated through the p38 MAPK pathway through activation of mitogen-activated protein kinase 1 (MEK1) and subsequent ERK/ELK signaling[75,76]. It has also been shown that G-protein-dependent activation of PKC results from TGF-β stimulation of growth plate chondrocytes[74]. It has been suggested that TGF-β responsiveness requires the activation of the R-Smad2/4 complexes as well as other signaling pathways.

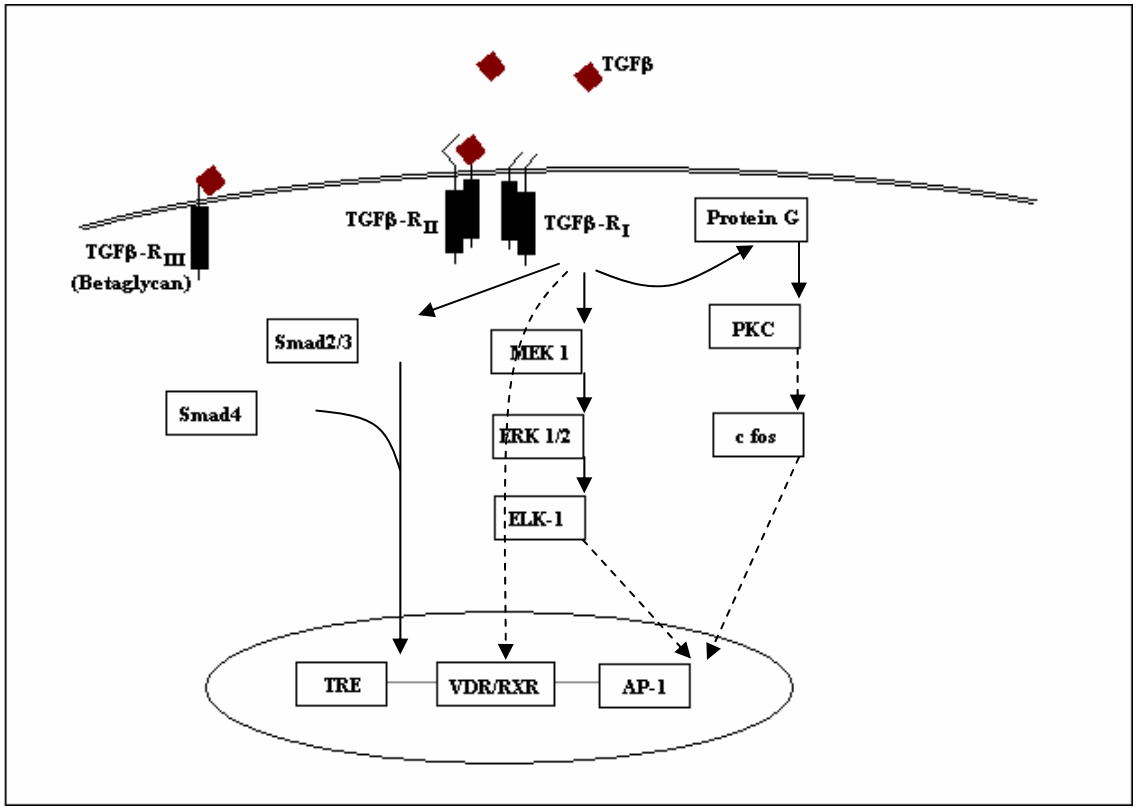

Figure 2.2: Proposed TGF-β signaling pathways in chondrocytes (TRE: TGF-β responsive element, VDR/RXR: vitamin D receptor/retinoic acid X receptor, AP-1: activation protein-1).
(Adapted from Grimaud *et al.*[77])

2.4.2 Biomechanical Influences

Mechanical stimulation has been shown to be important in the development of certain tissues and may influence differentiation of BMSCs[78]. It has been suggested that the combination of chondrogenic media and dynamic compressive loading may enhance chondrogenesis of BMSCs over the addition of exogenous factors alone[79]. Dynamic compressive loading has been shown to increase the expression of chondrogenic markers, aggrecan and collagen II, in rabbit BMSCs in agarose culture[79]. Dynamic compressive loading has also been shown to induce chondrogenesis in chick-bud mesenchymal cells[80,81]. Human BMSCs cultured under conditions promoting chondrogenesis found that the application of cyclic hydrostatic pressure for multiple days increased proteoglycan and collagen content after 14 days in culture[82]. Mechanical loading has been found to be critical in the differentiation of other tissue types, including bone. BMSCs cultured on partially demineralized bone subjected to four-point bending loading experienced elevated osteogenic differentiation, compared to unloaded controls[83]. Combined with the substantial knowledge base that mechanical stimulation can affect the maintenance of cartilage, these studies suggest that controlled mechanical stimulation may direct differentiation and subsequent matrix assembly in engineered cartilage derived from mesenchymal progenitor cells.

CHAPTER 3 INFLUENCE OF VARIOUS TISSUE-ENGINEERING SCAFFOLD MATERIALS ON THE ECM PRODUCTION BY BOVINE ARTICULAR CHONDROCYTES

3.1 INTRODUCTION

The function of healthy cartilage resides in its ability to provide resistance to compressive, shear and tensile forces that occur during normal joint motion. This ability arises from the unique architecture of the matrix components found in articular cartilage. The fibrillar collagen network is organized and stabilized through molecular cross-links that restrain the swelling pressure exerted by a high concentration of negatively charged proteoglycans. Proteoglycans are known to indirectly influence chondrocyte activity, either through cell-matrix interactions or by binding specific growth factors in the extracellular matrix, thereby modifying their temporal and spatial effects[15]. Many of these biological interactions involve the highly negative glycosaminoglycan (GAG) chains, which are covalently attached to the protein cores of individual proteoglycan molecules[15]. In articular cartilage, the GAGs are mainly chondroitin sulfate (CS) and keratan sulfate chains found on the large, aggregating proteoglycan aggrecan, as well as a small proportion of dermatan sulfate (DS) chains[15]. Aggrecan monomers consist of a protein core to which are attached CS chains containing predominately 4- or 6-sulfated disaccharides[84,85]. These negatively charged GAGs produce a swelling pressure through interactions with the ionic interstitial fluid[15], contributing to the compressive stiffness of the tissue and maintaining tensile stress in the type II collagen network. While the collagen network is somewhat metabolically static[86], aggrecan undergoes a distinct

turnover process[21,87] in which catabolic cleavage[88,89] and removal of molecules from the extracellular matrix are in balance with synthesis and deposition of new molecules[90,91]. Maintenance of the appropriate structure and concentration of the proteoglycans is critical for maintaining healthy cartilage capable of resisting compressive loads.

Alterations in glycosaminoglycan sulfation have been associated with aging and degeneration of articular cartilage. Changes include a decreased keratan sulfate to CS ratio and a decrease in overall glycosaminoglycan chain length[15,92]. The internal disaccharide (Δ-disaccharide) composition of CS chains shifts with age, with an increased ratio of 6-sulfated (ΔDi-6S) to 4-sulfated (ΔDi-4S) disaccharides and a decrease in unsulfated (ΔDi-0S) disaccharides[15]. The non-reducing termini of CS chains from aggrecan purified from fetal to elderly human cartilage contain distinctly different ratios of variably sulfated galNAc residues which are characteristic of the age of the patient[93], with an age related increase in 4,6-disulfated residues and a corresponding decrease in 4-sulfated residues. Additionally, a decrease in CS terminal 4,6-disulfated residues and an increase in CS terminal 4-sulfated residues has been described for OA cartilage, perhaps due to a lower propensity to the specific 6-sulfotransferase involved in the terminal 4,6 reaction[94-99].

While distinct functional implications of CS sulfation patterns in cartilage have not yet been elucidated, recent work has suggested fundamental biological functions for chondroitin, chondroitin sulfate and dermatan sulfate in other systems. These glycosaminoglycans have been implicated in growth factor and chemokine signaling, play critical roles in the development of the central nervous system, and function as receptors for various pathogens[100-103]. Unsulfated chondroitin has been found to be

integral in the morphogenesis and cell division of C. elegans[104]. These functions are directly related to the sulfation patterns of the glycosaminoglycan chains.

Understanding the degree and level of influence the CS fine structure plays in the biological activity of chondrocytes may provide a more in depth perspective on not only the state of native cartilage (i.e. osteoarthritic, injured, healthy) but also the development of engineered cartilages. A key component of most tissue engineering approaches to regenerating articular cartilage is the choice of a scaffold material. The 3D scaffold provides support for chondrocytes to proliferate and maintain their differentiated function[58,105-107]. In the case of undifferentiated cell populations (*e.g.,* BMSCs, mesenchymal stem cells), the choice of scaffold may influence the differentiation and phenotypic stability of the cell populations. Scaffold materials commonly used for the tissue engineering of cartilage include degradable synthetic polymers (*e.g.,* polyglycolic acid (PGA)[108,109], polylactic acid[110]), fibrillar protein gels (*e.g.,* collagen[111], fibrin[112,113]), and polysaccharide gels (*e.g.,* agarose[114,115], alginate[116,117]). Matrix formation in these systems is typically quantified by measures of gross biochemical composition such as the total sulfated glycosaminoglycan (sGAG) content. While these gross measures are useful, more definitive molecular information is required to fully understand the biochemical characteristics of tissue engineered cartilage matrices.

The study presented in this chapter examined the nature of the proteoglycan / GAG matrices synthesized by chondrocytes seeded in different scaffold materials. In addition to differences in total GAG content, fluorophore-assisted carbohydrate electrophoresis (FACE) revealed differences in CS/DS GAG fine structure among

different scaffold materials. The results of this study were used to choose a scaffold material for use in subsequent studies.

3.2 Materials and Methods

3.2.1 Construct assembly and cell culture

Bovine articular chondrocytes were isolated from the stifle joints of two immature (<5 weeks) donor animals. Tissue was excised from the patellofemoral grooves, minced and digested in DMEM with 0.2% collagenase for 24 h in a 37°C, 5% CO_2 incubator. After centrifugation at 160 x g, cells were washed twice with Ca^{2+}, Mg^{2+} -free PBS and counted with a Coulter counter. Donor cells were kept separate and parallel duplicate experiments were run. Non-digested samples of cartilage were maintained as controls during the course of the experiment. Hydrogel constructs were created by seeding cells at a final density of $15x10^6$ cells/mL in 1.5% low melting point (LMP) agarose, 0.75% sodium alginate, 2 mg/mL type I collagen (rat tail), and 50 mg/mL fibrin. Cells were also seeded on polyglycolic acid (PGA) felt at a target density of $15x10^6$ cells/mL, but a low seeding efficiency resulted in an actual initial cell density of approximately $4x10^6$ cell/mL. It should be noted that seeding density may affect chondrocyte matrix synthesis and viability, perhaps due to diffusional limitations at high cell densities[118,119]. All constructs except PGA were cast in 12mm diameter x 3mm deep cylindrical wells in custom machined polycarbonate molds that were autoclave sterilized prior to gel casting. Agarose constructs were assembled by autoclaving 3% LMP agarose in 1X Ca^{2+}, Mg^{2+} -free PBS and then cooling the solution to 42°C. An equal volume of cells suspended at 30

x10^6 cells/mL in 2X DMEM and 20% FBS was added, and the solution was cooled in the molds. Alginate constructs were similarly assembled by autoclaving 1.5% alginic acid in 1X Ca^{2+}, Mg^{2+} -free PBS to solubilize and sterilize, cooling to 37°C, adding 30x10^6 cells/mL in Ca^{2+}, Mg^{2+} -free PBS and polymerizing the gels in the molds with 102 mM $CaCl_2$. Collagen constructs were assembled by suspending 15x10^6 cell/mL in a solution containing 10% FBS, 0.5x DMEM and 2 mg/mL acid solubilized rat tail collagen type I and titrating the solution to neutral pH with 0.1M NaOH. Constructs were allowed to polymerize in a 37°C, 5% CO_2 incubator for 30 minutes before transfer to 24 well plates with 2ml of media. Fibrin constructs were assembled by suspending cells in a solution of bovine fibrinogen, FBS, 6-aminocaproic acid, and DMEM. Bovine thrombin was dissolved in 40 mM CaCl2 , and 100 µl of the thrombin solution was placed into each well of a polycarbonate mold (12 mm diameter by 3 mm deep), followed by 200 µl of the cell/fibrinogen mixture. Final concentrations in the constructs were 50 mg/mL fibrinogen, 50 U/mL thrombin, 10% FBS, 2 mg/mL 6-aminocaproic acid, and 15x10^6 cells/mL. Constructs were allowed to polymerize in a 37°C, 5% CO2 incubator for 30 min. PGA felts (45 mg/cm^3 polymer density; 12-15 µm fiber thickness; 10 mm diameter by 2 mm thickness) were prewetted overnight in high-glucose DMEM containing 10% FBS. PGA felts were then seeded by repeatedly pipetting 1 mL of cell suspension (1.2x10^6 cells/mL) onto each felt and cultured on a shaker plate at 300 rpm for 24 hours. Additionally, native cartilage samples from the same joints were maintained in identical culture conditions for the comparison of Δ-disaccharide composition.

Constructs and native cartilage samples (n=6 per group per endpoint) were cultured in 24 well plates with 2 mL of DMEM containing 10% FBS, 0.1mM NEAA,

4mM L-glutamine, 5 μg/mL gentamicin sulfate and 50 μg/mL ascorbic acid. For the PGA felts, the culture dish wells had been pre-coated with a thin layer of 1% agarose. As in previous studies on dorsal root ganglia[120], smooth muscle cells[121] and chondrocytes[122,123], 6-aminocaproic acid (2 mg/mL) was added to the media of fibrin constructs to inhibit proteolytic degradation. Media were changed every two days, with samples retained for analysis of the sulfated glycosaminoglycans (sGAG) released from the constructs. After 20 and 40 days, constructs were weighed, lyophilized, reweighed, and digested in 1ml of 100mM ammonium acetate buffer with 250 μg/mL Proteinase K at 60°C for 24 hours. Portions of each digest were assayed for total DNA using the Hoechst 33258 assay with calf thymus DNA as a standard[124] and sGAG using the DMMB assay[125,126] with shark cartilage CS as a standard.

3.2.2 Analytical Techniques

Histological Sample Processing and Characterization

Additional samples were rinsed in PBS, transferred to 10% neutral-buffered formalin for 48 hours, and then stored in 70% ethanol (n=2 per group per endpoint) to reduce the solubility of the GAG sidechains. Samples were subsequently embedded in paraffin and sectioned at five microns. Sections were stained with Safranin-O to visualize sulfated GAG distribution[127].

Δ-Disaccharide Analysis

The chondroitin sulfate and dermatan sulfate (CS/DS) Δ-disaccharide compositions of deposited GAGs were quantified for all 20 and 40 day constructs using

fluorophore assisted carbohydrate electrophoresis (FACE)[128-132]. GAGs were ethanol precipitated (final concentration of 75% v/v) from the Proteinase K digests and aliquots from each construct containing 5 μg of sGAG (as determined by the DMMB dye assay) were further enzymatically processed with 15 mU of chondroitinase ABC and 100 mU hyaluronidase in 100 μL of 50mM ammonium acetate buffer at 37°C for 16 hours. Buffer was evaporated and digestion products were fluorescently labeled for 16 hours at 37°C with 15 μL of 0.1M 2-aminoacridone and 1.0M sodium cyanoborohydride. After fluorescent labeling, 15 μL of glycerol was added to each sample. 5 μL portions of these samples were electrophoretically separated using monosaccharide FACE gels. Fluorescent bands were visualized at 300 nm illumination using a Kodak EDAS 120 gel imaging system. Band intensities were fit with a Gaussian model and converted to pmol amounts using a standard ladder containing a range of concentrations of purified Δ-disaccharides (25-250 pmol) for product identification and quantification (50 pmol of ΔDi-4,6S, 75 pmol hyaluronic acid, 100 pmol of ΔDi-6S, 150 pmol of ΔDi-4S, and 200 pmol of ΔDi-0S). Relative Δ-disaccharide composition was expressed as a percent of total detected internal CS/DS Δ-disaccharides for ΔDi-0S (unsulfated), ΔDi-4S, ΔDi-6S and ΔDi-4,6S, and as the ratio of ΔDi-6S:ΔDi-4S. For comparison, native articular cartilage samples that had been cultured for comparable periods were also analyzed via FACE. For a detailed protocol, see appendix C.

Statistical Analysis

For this chapter, as well as subsequent chapters, the details of the statistical analysis are described in appendix E.

3.3 RESULTS

3.3.1 Histology

For a given construct type, no differences were noted in the organization of cells or sGAG matrix between histological samples from the 20 and 40 day time points. Cells in all scaffolds displayed predominantly a rounded morphology (Figure 3.1b-f) similar to chondrocytes in their native matrix (Figure 3.1a). Agarose constructs (Figure 3.1**Error! Reference source not found.**b) included isolated cells and multiple cell clusters surrounded by a pericellular matrix dense in sGAG, while the other constructs contained primarily isolated cells or small cell clusters. The intensity of pericellular matrix staining in the four other scaffold materials was either considerably less intense (alginate, collagen and PGA) or less extensive (fibrin) than that in agarose. Alginate constructs (Figure 3.1c) also displayed intense pericellular matrix staining, with a relatively high background level of staining due to the negatively charged alginate. Collagen constructs (Figure 3.1d) contained uniformly distributed cells and diffuse matrix staining. In contrast, fibrin constructs (Figure 3.1e) displayed a very immediate staining of sGAG surrounding either single cells or pairs of cells. PGA constructs (Figure 3.1f) contained islands with relatively intense matrix staining and numerous cells surrounded by regions apparently devoid of cells. Articular cartilage, alginate and fibrin constructs were surrounded by a layer with little sGAG staining and cells with a more flattened morphology (images not shown).

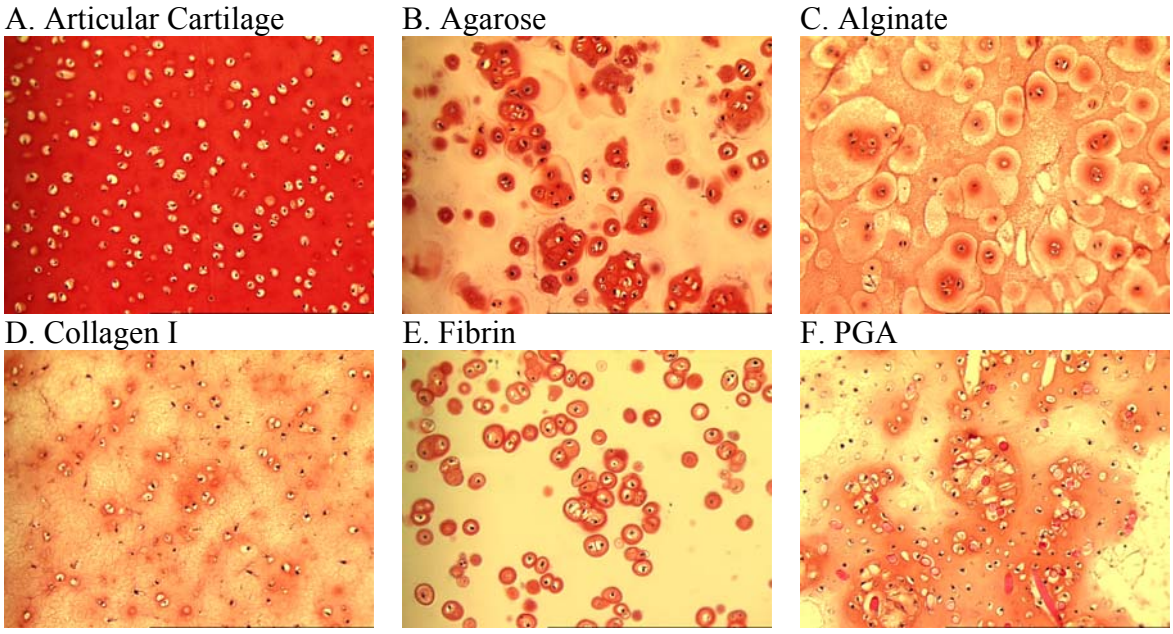

Figure 3.1: Representative interior sections stained with Safranin O from A) articular cartilage and B-F) constructs cultured for 20 days.

3.3.2 DNA Content

The relative changes in DNA content from initial seeding to day 20 or 40 indicated differential increases in the cellular contents among scaffold types (Figure 3.2). The increases in DNA content of agarose and collagen constructs were not significantly different at either time point ($p>0.8$) and reached approximately 3.5 times the initial seeding density. Agarose constructs had significantly greater increases in DNA content than alginate, fibrin or PGA constructs at both day 20 ($p\leq0.0002$) and day 40 ($p\leq0.028$). Collagen constructs had significantly greater increases in DNA content than fibrin and PGA constructs at day 20 ($p\leq0.0016$) and day 40 ($p\leq0.0001$), and significantly greater increases than alginate constructs at day 40 ($p<0.0001$) but not day 20 ($p=0.061$). There were no significant changes in DNA content between 20 and 40 days for any constructs except for PGA ($p<0.0001$). PGA constructs exhibited a small (25%) increase in DNA content by day 20, followed by a substantial (109%, $p<0.0001$) increase in DNA content between days 20 and 40, resulting in a net increase comparable to that seen in the other construct types. At day 40, alginate, fibrin and PGA constructs had reached approximately 2.5 times the original seeding density, with no statistically significant differences among these scaffold materials.

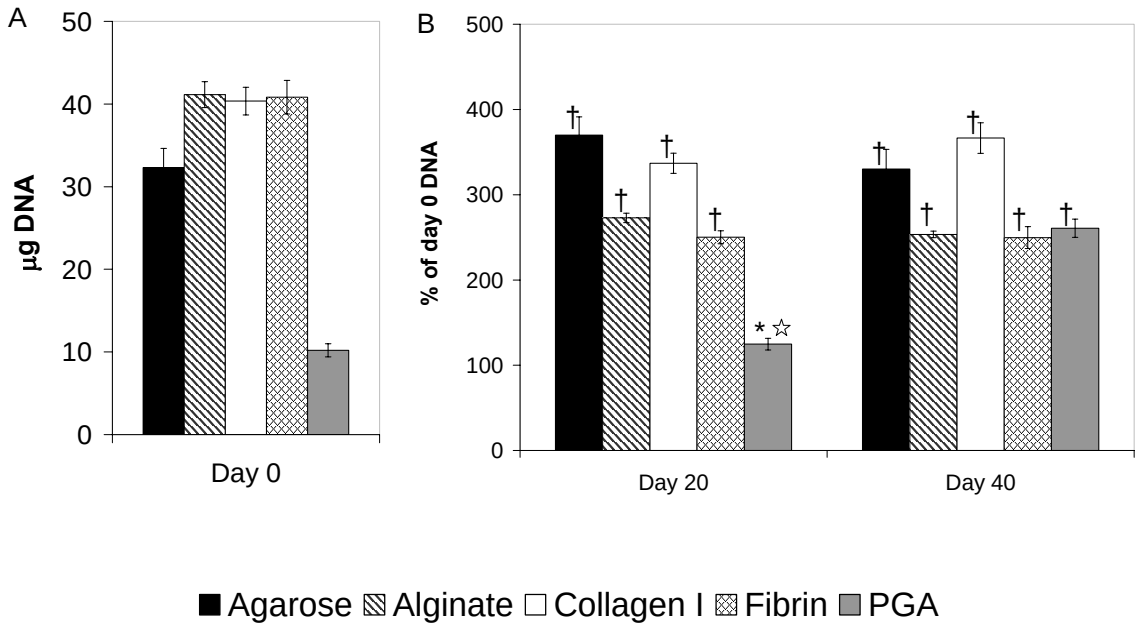

Figure 3.2: Construct DNA contents.

A) DNA contents at day 0. PGA constructs had substantially fewer cells due to a low seeding density. B) DNA contents relative to day 0 levels for each scaffold type after 20 and 40 days of culture. Asterisks indicate $p<0.05$ versus all other scaffolds at the same time point, daggers indicate $p<0.05$ versus some other scaffolds at the same time point, and stars at day 20 indicate $p<0.05$ versus the day 40 value for the same scaffold. Individual differences are discussed in the text. (mean±S.E.M., N=12).

3.3.3 sGAG Production

The sGAG/DNA results indicated that constructs from all scaffold groups accumulated extracellular matrix over the 40 day culture period (Figure 3.3). Between days 20 and 40, agarose constructs exhibited a continued increase in sGAG/DNA ($p<0.0001$) while alginate, collagen, and fibrin constructs exhibited no significant change in sGAG/DNA. PGA constructs had significantly lower sGAG/DNA at day 40 as compared to day 20 ($p<0.0001$), which can be attributed to the dramatic increase in DNA content over that period. The patterns of matrix accumulation and cell content changes resulted in differences in sGAG/DNA among scaffolds at each time point. At day 20, PGA constructs had significantly higher sGAG/DNA than all other groups ($p<0.0001$), while alginate constructs had significantly lower sGAG/DNA than all groups ($p\leq0.0023$) except collagen constructs ($p=0.45$). At day 40, agarose constructs had significantly higher sGAG/DNA than all other groups ($p<0.0001$), while collagen and alginate constructs had significantly lower sGAG/DNA ($p\leq0.0003$ and $p<0.0001$ respectively) than all other groups.

The sGAG detected in the media indicated that sGAG was released from all constructs through the 40 day culture period (Figure 3.4). Overall, the average sGAG release rate was lowest for alginate constructs and comparable for agarose, collagen and PGA constructs. The kinetics of sGAG release were similar for agarose, alginate, collagen and fibrin, with increasing release rates through day 30 followed by a significant (except for agarose) drop in sGAG release on days 31-40. In contrast, the sGAG release rate for PGA constructs was highest on days 1 – 10 and decreased steadily though day 40.

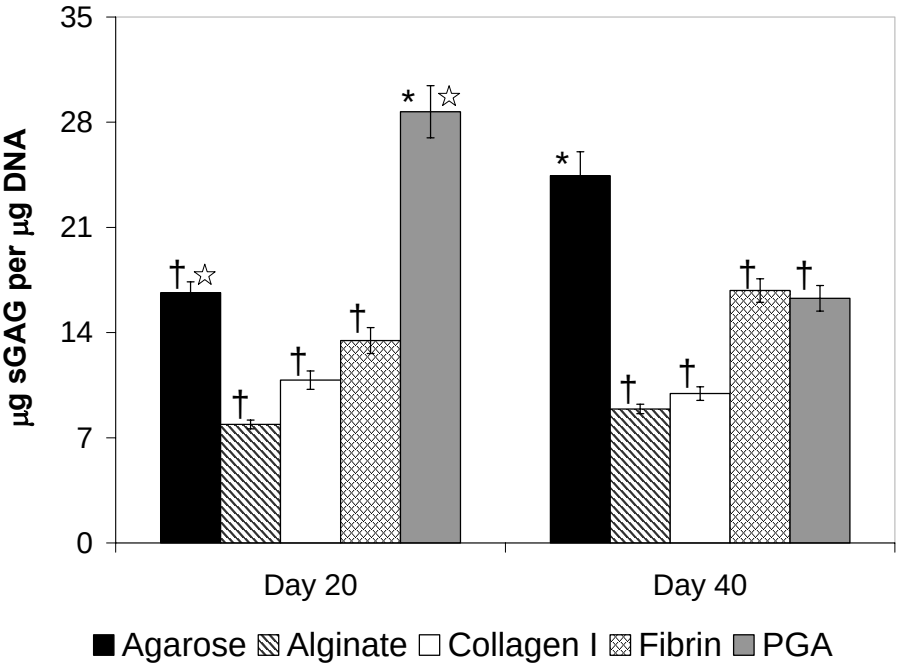

Figure 3.3: Construct sGAG content normalized to DNA content after 20 and 40 days of culture.

Asterisks indicate $p<0.05$ versus all other scaffolds at the same time point, daggers indicate $p<0.05$ versus some other scaffolds at the same time point, and stars at day 20 indicate $p<0.05$ versus the day 40 value for the same scaffold. Individual differences are discussed in the text. (mean±S.E.M., N=12).

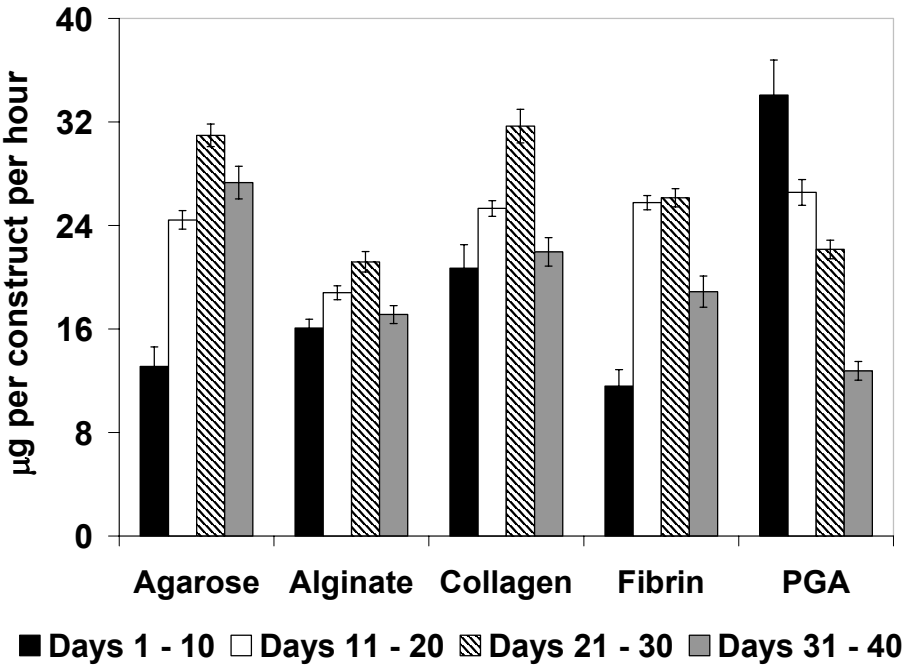

Figure 3.4: Average sGAG release rates during four 10-day intervals. (mean±S.E.M., N=20).

3.3.4 Δ-Disaccharide Composition

As in native articular cartilage, ΔDi-4S and ΔDi-6S comprised the majority (~ 80%) of CS/DS-derived Δ-disaccharides (Table 3-1), although the fraction of each Δ-disaccharide varied somewhat. Overall, the fraction of ΔDi-4S was lower at day 20 than at day 40 ($p=0.0025$), although the pairwise comparisons did not indicate a significant increase for any individual scaffold. The fraction of ΔDi-4S was higher for agarose than for all other scaffolds ($p\leq0.0002$). This pairwise difference was significant at day 20 versus all scaffolds ($p<0.0001$) except collagen ($p=0.053$) and was significant at day 40 versus fibrin ($p=0.031$) and PGA ($p=0.034$) but not collagen ($p=0.055$) or alginate ($p=0.25$). Other than a higher fraction for collagen compared to PGA at day 20 ($p=0.014$), there were no other significant differences in ΔDi-4S among scaffolds at either time point. The fraction of ΔDi-6S was not significantly different between day 20 and day 40 ($p>0.19$), but did vary among scaffolds ($p<0.0001$). Among the construct groups, the fraction of ΔDi-6S was smaller for agarose than for all other scaffolds ($p\leq0.032$) and was smaller for collagen than for alginate ($p=0.0017$) and PGA ($p=0.021$). The ratio of ΔDi-6S: ΔDi-4S in the constructs was generally somewhat higher than that in native tissue explants (Figure 2.5). The ratio of ΔDi-6S: ΔDi-4S was slightly higher at day 20 than at day 40 ($p=0.009$), was lower for agarose than for all other scaffolds ($p\leq0.0019$), and was lower for collagen than for alginate ($p=0.007$) and PGA ($p=0.0075$).

Overall, the fraction of ΔDi-4,6S was significantly higher at day 20 than at day 40 ($p=0.0017$), but other than a slightly higher level for fibrin constructs at day 40 ($p=0.078$) there were no significant differences in the fraction of ΔDi-0S between days 20 and 40. There were significant differences among scaffold types in the fractions of both

unsulfated ΔDi-0S and disulfated ΔDi-4,6S. Alginate constructs had a lower fraction of ΔDi-0S than all other scaffold groups ($p<0.0001$) and a higher fraction of ΔDi-4,6S than all other scaffold groups ($p<0.0001$). In contrast, collagen constructs had a higher fraction of ΔDi-0S than all other scaffold groups ($p\leq0.023$) and a lower fraction of ΔDi-4,6S than alginate, fibrin or PGA ($p\leq0.0001$) constructs. Other than a significantly higher level of ΔDi-0S for agarose than for fibrin at day 20 ($p=0.0084$), there were no other significant differences among scaffold groups in the fractions of ΔDi-0S or ΔDi-4,6S.

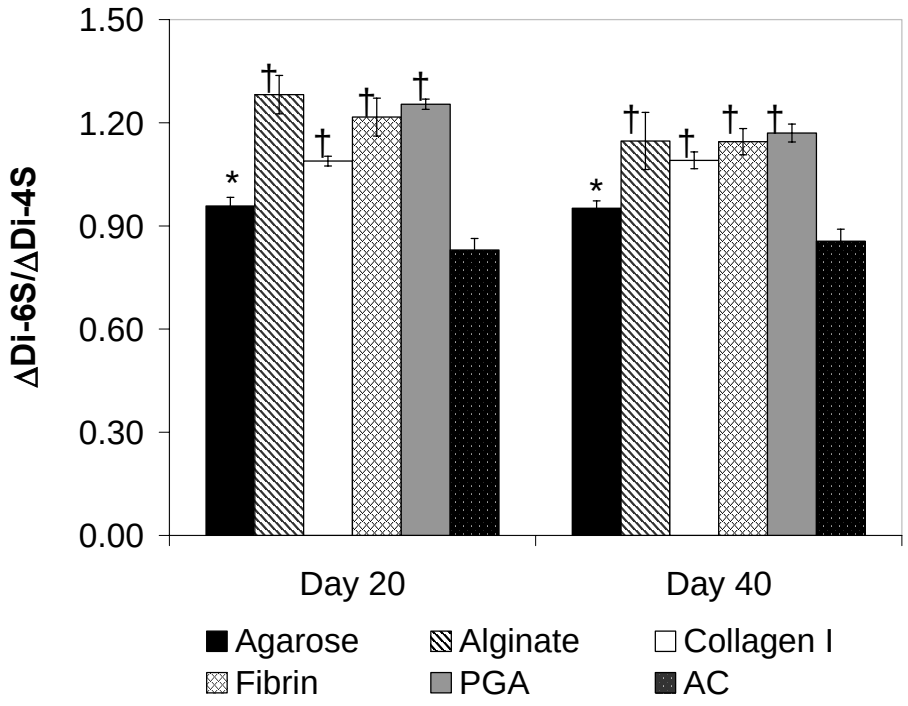

Figure 3.5: Construct ΔDi-6S/ΔDi-4S ratios after 20 and 40 days of culture.

Levels for articular cartilage (AC) cultured for comparable periods are included for visual comparison. Asterisks indicate $p<0.05$ versus all other scaffolds at the same time point and daggers indicate $p<0.05$ versus some other scaffolds at the same time point. Individual differences are discussed in the text. (mean±S.E.M., N=12).

Table 3-1: GAG Δ-disaccharide contents derived from CS and DS after 20 and 40 days of culture.

Levels for articular cartilage cultured for comparable periods are included for comparison. Values are expressed as percentages of total Δ-disaccharide measured. Asterisks indicate $p < 0.05$ versus all other scaffolds at the same time point and daggers indicate $p<0.05$ versus some other scaffolds at the same time point. (mean±S.E.M., N=12).

	ΔDi-0S	ΔDi-6S	ΔDi-4S	ΔDi-4,6S
20 days				
Agarose	14.27 ± 0.31 †	38.65 ± 0.46 *	40.62 ± 0.61 †	6.46 ± 0.12 †
Alginate	7.43 ± 0.19 *	44.49 ± 0.83 †	34.99 ± 0.89 †	13.08 ± 0.29 *
Collagen I	16.89 ± 0.30 *	40.82 ± 0.32 †	37.51 ± 0.33 †	4.78 ± 0.17 †
Fibrin	11.86 ± 0.52 †	42.93 ± 1.18 †	35.46 ± 0.93 †	9.75 ± 1.51 †
PGA	13.51 ± 0.42 †	42.59 ± 0.46 †	33.99 ± 0.29 †	9.91 ± 0.41 †
Articular Cartilage	*12.56 ± 0.87*	*37.12 ± 0.51*	*45.10 ± 1.32*	*5.21 ± 0.26*
40 days				
Agarose	14.91 ± 0.35 †	38.20 ± 0.65 *	40.26 ± 0.39 †	6.63 ± 0.43 †
Alginate	8.09 ± 0.31 *	42.50 ± 1.60 †	37.78 ± 1.70	11.63 ± 0.54 *
Collagen I	17.69 ± 0.39 *	40.41 ± 0.38 †	37.17 ± 0.58	4.73 ± 0.23 †
Fibrin	14.27 ± 0.70 †	42.02 ± 0.94 †	36.97 ± 0.97 †	6.73 ± 1.65 †
PGA	12.90 ± 0.50 †	43.25 ± 0.48 †	37.02 ± 0.49 †	6.82 ± 0.26 †
Articular Cartilage	*14.69 ± 0.76*	*36.53 ± 0.66*	*42.91 ± 0.99*	*5.87 ± 0.24*

3.4 DISCUSSION

While a wide variety of biomaterials have been proposed for use in cartilage tissue engineering, few studies have quantitatively compared details of chondrocyte activity and extracellular matrix production in different scaffold materials. This study found significant differences in cell proliferation and extracellular matrix accumulation among five scaffolds commonly used for chondrocyte *in vitro* culture studies and cartilage tissue engineering. Over the first 20 days, PGA constructs had the lowest increase in cell content but the greatest accumulation of sGAG per cell and the greatest rate of sGAG release to the media. Between day 20 and day 40, the sGAG/DNA of the other constructs was fairly stable while that of PGA constructs decreased substantially due to the substantial increase in cell proliferation in PGA scaffolds. Chondrocytes in agarose synthesized the most sGAG throughout the study, resulting in a substantially higher sGAG/DNA than all other scaffolds at day 40. Distinct differences between scaffolds were also noted in the distributions of cells and matrix. The differences in the distribution of the chondrocytes in the various scaffolds may be due to inherent differences in the preparation required for the various scaffolds or in how the cells interact with particular scaffolds after seeding. Other possible reasons for the cell clustering include the migration of cells into colonies or localized cell death.

Furthermore, this study revealed substantial quantitative differences in the Δ-disaccharide composition of the proteoglycans accumulated in the different scaffolds. Overall, the internal Δ-disaccharide profiles of glycosaminoglycans in alginate constructs least resembled that of native articular cartilage, whereas the profile of agarose constructs most closely resembled that of articular cartilage. The primary notable difference in the

levels of the monosulfated ΔDi-4S and ΔDi-6S was for agarose constructs, which had a higher fraction of ΔDi-4S, lower fraction of ΔDi-6S, and lower ΔDi-6S: ΔDi-4S than all other scaffold groups. More striking differences were seen in the levels of unsulfated ΔDi-0S and disulfated ΔDi-4,6S. Alginate constructs had a lower fraction of unsulfated residues and a higher fraction of disulfated residues than other groups. Conversely, collagen constructs had the highest fraction of unsulfated residues and the lowest fraction of disulfated residues. These patterns suggest that some aspects of the construct environment influence a tradeoff between incorporation of unsulfated ΔDi-0S and disulfated ΔDi-4,6S into newly synthesized proteoglycans. Further studies would be necessary to identify the causes of the observed differences in sulfation patterns (*e.g.*, altered sulfotransferase activity, altered ratios of proteoglycan species, *etc.*). Interestingly, the influence of mechanical stimulation on GAG disaccharide composition also appears to depend on the cellular environment. Cyclic compression of cartilage tissue explants had no effect on the internal disaccharide composition of newly synthesized GAGs[133], while cyclic compression of chondrocytes in fibrin constructs significantly decreased the proportion of unsulfated ΔDi-0S[134]. Further exploration of variations between scaffolds in the response to mechanical stimulation will be important in the development of mechanically functional engineered cartilage constructs.

The similarities and differences among scaffolds in proteoglycan accumulation and glycosaminoglycan composition were consistent for both donor animals at both time points, suggesting that the scaffold material directly or indirectly influences chondrocyte proteoglycan metabolism. Prior to the deposition of any extracellular matrix, chondrocyte interactions with the scaffold would vary substantially depending on the type of scaffold.

Direct chondrocyte binding to protein scaffolds such as collagen or fibrin via integrins or other cell surface receptors may influence a variety of cellular functions[135-137]. In contrast, chondrocytes would initially be isolated from interactions with the scaffold material when suspended in the agarose and alginate hydrogels. In PGA scaffolds, chondrocytes initially adhere to and spread on serum proteins absorbed onto the polymer mesh, resulting in an initial state somewhat similar to monolayer culture[138,139].

In each of these systems, chondrocytes would eventually interact primarily with the new extracellular matrix produced by the cells, but the accumulation of that matrix could be influenced by the physical properties of the scaffold[140]. For example, the highly permeable, macroscopically porous PGA scaffolds initially provide little resistance to diffusion of secreted proteins and proteoglycans, allowing much of the newly synthesized material to escape the construct[141,142]. Conversely, scaffolds such as alginate and agarose provide substantial resistance to diffusion of large molecules, resulting in more concentrated pericellular accumulation of secreted matrix components[143]. Additionally, the biophysical environment of the cell may vary between scaffolds. For example, the agarose gel provides an electrochemically neutral environment, while the negatively charged alginate may affect both the ionic environment and the interstitial pH, potentially influencing cell behavior and the ability of the local environment to sequester important growth factors, cytokines and chemokines.

While the functional implications of altered Δ-disaccharide sulfation patterns in native or engineered cartilage are unknown, there is evidence of structure-function relationships in other tissues and with other sulfated GAGs. Oversulfation of CS/DS chains containing GlcAβ1-3GalNAc(4,6-O-disulfate) or IdoAα1-3GalNAc(4,6-O-

disulfate) in the large aggregating proteoglycan versican affects its ability to bind to L- and P-selectin and chemokines[144]. Additionally, any amount of sulfation has been shown to inhibit the ability of versican to interact with CD44[145]. It has been shown that oversulfated CS chains play a role in the development of the brain. Specifically, CS chains with oversulfated structures are involved in neuronal adhesion, migration and neuritogenesis [146]. Thus, the possibility exists that variations in the sulfation of the CS chains in cartilage may alter the binding of nutrients, chemokines and growth factors, thereby influencing chondrocyte migration, differentiation, and matrix production.

With advances in tissue engineering, it has become apparent that more sophisticated methods of evaluating engineered cartilage constructs need to be employed. In this study, articular chondrocytes seeded into different scaffolds exhibited differences in proliferation, the quantity of matrix accumulated and the fine structure of the newly synthesized glycosaminoglycans. It should be noted that many evolving approaches to cartilage tissue engineering rely on either passage expanded chondrocytes or chemically manipulated progenitor cells, either of which would be expected to continue differentiating towards a chondrocytic phenotype within the construct environment. In such cases where relatively rapid changes in phenotype are expected, the influence of the scaffold environment on cell behavior and matrix composition may be more pronounced. An appreciation of the details of the extracellular matrix structure in engineered tissues may be important in understanding the relative maturity and health of the engineered tissue and the degree to which engineered implants may differ from and integrate with the surrounding native tissues.

CHAPTER 4 INFLUENCE OF VARIOUS ION-CHANNEL MECHANOTRANSDUCTION PATHWAYS ON THE BIOSYNTHESIS OF BOVINE ARTICULAR CHONDROCYTES

4.1 INTRODUCTION

The biomechanical environment contributes to the regulation of cartilage development, maturation and maintenance[147]. Experimental studies have indicated that moderate exercise leads to increased proteoglycan content, while joint immobilization leads to loss of proteoglycan content[45,46]. *In vitro* studies have provided important information regarding how mechanical loading influences articular chondrocyte metabolism[8,148]. In previous *in vitro* investigations using cartilage tissue explants or chondrocytes in hydrogel culture, static compression decreased both aggrecan and type II collagen gene expression and synthesis, whereas dynamic compression at appropriate frequencies increased anabolic activity[52,149-152]. While tissue culture experiments have demonstrated the sensitivity of articular chondrocytes to mechanical stimuli, the cellular-level physical signals that chondrocytes sense, and to which they respond in their biophysical environment, remain unclear.

In vivo compression of cartilage results in a variety of physical effects at the tissue and cell levels, including electrokinetic effects, hydrostatic fluid pressurization, direct cellular deformation and interstitial fluid flow[153]. Any or all of these effects may be important mechanical stimuli. In cartilage, chondrocytes are completely surrounded by extracellular matrix networks, thus receiving physical signals from a 3D environment. In

contrast, most studies of the mechanisms involved in chondrocyte mechanotransduction have been performed in the absence of a 3D matrix via monolayer experiments.

Studies with articular chondrocytes in monolayer suggest that mechanosensitive ion-channels may participate in chondrocyte mechanotransduction. Fluid flow-induced shear, which chondrocytes may experience *in vivo* due to load-induced convective flow, results in a variety of morphological and metabolic changes in cultured articular chondrocytes. Flow-induced shear can stimulate a rise in intracellular calcium concentration due to both G-protein modulation and the release of Ca2+ stores, possibly through an inositol 1,4,5-trisphosphate (IP3)-dependent mechanism[154]. It has also been suggested that transient increases in intracellular Ca2+ concentrations may be one of the earliest events involved in the response of chondrocytes to mechanical stress through deformation-induced Ca2+ waves initiated via mechanosensitive ion-channels[54]. Stretch-activated channels have been suggested to participate in the control of chondrocyte proliferation. Also, blocking the Ca2+-senstitive K+ have been demonstrated to have an effect on both proliferation and mRNA levels of certain proteins[55].

However, important differences exist between chondrocyte behavior in monolayer and 3D cultures, and the extent to which these same ion-channels are involved in the transduction of mechanical stimuli in 3D culture is unclear. In one of the few studies to examine similar issues in 3D culture, the upregulation of aggrecan gene expression in bovine articular cartilage explants subjected to a compressive stress of 0.1MPa for 1 hour was reversed in the presence of thapsigargin, which depletes Ca^{2+} stores, with no significant effect on the aggrecan expression in the tare-loaded explants[155].

The objectives of the studies presented in this chapter were to investigate the dose-dependent inhibition of protein and sGAG synthesis by inhibitors of four ion-channel inhibitors in articular cartilage explants, to investigate the recovery of protein and sGAG synthesis by the four ion-channel inhibitors in articular cartilage explants and to investigate the response of chondrocytes seeded in agarose to dynamic compression when cultured with each of these inhibitors. Four ion-channel inhibitors that have been implicated in chondrocyte mechanotransduction in monolayer studies were examined: 4-Aminopyridine (4AP), a voltage-dependent K+ channel blocker, Nifedipine (Nf), an L-type voltage sensitive calcium channel blocker, Gadolinium (Gd), an inhibitor of cation-selective stretch-activated ion-channels, and Thapsigargin (Tg), a natural plant product which depletes the Ca2+ store in the sarcoplasmic and endoplasmic reticula by inhibiting ATP-dependent Ca2+ pumps.

4.2 Materials and Methods

4.2.1 Explant and construct culture

In a preliminary experiment examining effects of the inhibitors on proteoglycan and protein synthesis as well as gross viability, cartilage explants 3 days post-explantation and chondrocytes seeded into agarose gels and cultured for 5 weeks responded similarly to varying doses of the inhibitors (data not shown). Due to the short duration of preculture required for the explants, they were used to examine the dose-response of chondrocytes to the inhibitors, as well as the recovery after exposure to the

inhibitors. To eliminate zonal variations in cartilage explant stiffnesses which might be influential when loading, chondrocytes were enzymatically released from the cartilage and cast into agarose gels to examine the response of chondrocytes to static and dynamic compression.

Full thickness cartilage explants were excised with a 4mm biopsy punch from immature bovine femoral condyles and femoropatellar grooves. After removing the superficial and deep zone layers, the cartilage was sliced into multiple 3mm thick disks using a custom cutting block. Explants from different locations were randomly dispersed across groups. Prior to any exposure to inhibitors, explants were precultured for 3 days in basal media consisting of DMEM plus 10% FBS, non-essential amino acids, Antibiotic-Antimycotic, 50μg/mL ascorbate and 0.4mM proline.

To enzymatically isolate chondrocytes, tissue was excised from the femoral-patellar grooves, minced and digested in DMEM with 0.2% collagenase for 24 hours in a 37°C, 5% CO_2 incubator. After centrifugation at 160 x g, cells were washed twice with Ca2+, Mg^{2+} -free PBS and counted with a Coulter counter. Cells were seeded at a final density of $10x10^6$ cells/mL in 2% LMP agarose. Constructs were cast in 4mm diameter x 3mm deep cylindrical wells in custom machined polycarbonate molds that were autoclave sterilized prior to gel casting. Agarose constructs were assembled by autoclaving 4% LMP agarose in 1X Ca2+, Mg2+ -free PBS and then cooling the solution to 42°C. An equal volume of cells suspended at $20x10^6$ cells/mL in 2X DMEM and 20% FBS was added, and the solution was cooled in the molds at room temperature for 10 minutes. Gels were removed from molds and precultured for 4 weeks in basal medium prior to the addition of any ion-channel inhibitors. Medium was changed every two days.

Ion-channel inhibitors

Four ion-channel inhibitors that have been implicated in chondrocyte mechanotransduction in monolayer studies were examined. 4-Aminopyridine (4AP), a voltage-dependent K+ channel blocker, has been shown to temporally affect chondrocyte proliferation[156,157]. Nifedipine (Nf), an L-type voltage sensitive calcium channel blocker, has been shown to inhibit dynamic mechanical strain induced upregulation of parathyroid-hormone-related protein expression[158], as well as prostaglandin E2 upregulation of insulin-like growth factor binding protein-3 expression and synthesis in chondrocytes.[159]. Gadolinium (Gd), an inhibitor of cation-selective stretch-activated ion-channels, has been shown to increase sGAG synthesis at 4mM and inhibit proliferation in a dose-dependent manner[160]. Thapsigargin (Tg), a natural plant product which depletes the Ca2+ store in the sarcoplasmic and endoplasmic reticula by inhibiting ATP-dependent Ca2+ pumps, has been shown to inhibit protein production and secretion, as well as sGAG synthesis (but not GAG synthesis)[161]. 4AP was solubilized in water, Nf in DMSO, Gd in 1M HCl, and Tg in DMSO. The range of doses examined for the inhibitors is shown in Table 4-1, as well as the dose chosen for the recovery and compression experiments.

4.2.2 Experimental Design

As the effects of sustained exposure to the toxins and appropriate doses for 3D culture were unknown, dose-response and recovery experiments were first performed for each of the inhibitors. For the dose-response experiment, tissue explants (n=4-6/condition) were cultured for 24 hours in basal medium alone or supplemented with

various levels of the four ion-channel inhibitors (Table 4-1), followed by 20 hours in media containing both inhibitors and radiolabeled precursors. For the recovery experiment, tissue explants (n=8/condition) were cultured for 24 hours in basal medium alone or supplemented with one level of the four ion-channel inhibitors. After exposure to the inhibitors, explants were rinsed three times for 10 minutes each time in PBS and then transferred into basal medium without inhibitors. Explants were cultured for 20 hours in radiolabeled precursors beginning 4, 24 or 48 hours after return to basal medium to evaluate their ability to recover both protein and sGAG synthesis rates.

For the static and dynamic compression studies, gels (n=8-10/condition) were cultured in basal medium with or without a single level of each ion-channel inhibitor for 24 hours prior to loading. Gels were cultured for an additional 20 hours in the same media supplemented with radiolabeled precursors under the following conditions: static compression (10%), 1Hz oscillatory compression (10%±3%) and free swelling (FS). Control samples were also cultured at 0%, providing similar nutrient diffusion limitations due to the platens. Dynamic compression was applied using a custom designed mechanical loading system (see appendix D).

Table 4-1: Ion-channel inhibitors and levels used in dose-response, recovery and compression experiments.

Dose-response levels spanned five orders of magnitude. 4-Aminopyridine (4AP) is a voltage-dependent potassium channel blocker. Nifedipine (Nf) is an L-type voltage sensitive calcium channel blocker. Gadolinium (Gd) blocks cation-selective stretch-activated ion-channels. Thapsigargin (Tg) is a natural plant product which depletes the Ca2+ store in the sarcoplasmic and endoplasmic reticula by inhibiting ATP-dependent Ca2+ pumps.

Toxin	Dose Response Low – High	Recovery & Compression Values
4AP (*4-Aminopyridine*)	10mM – 100mM	10mM
Gd (*Gadolinium*)	1mM – 10mM	1mM
Nf (*Nifedipine*)	1mM – 10mM	1mM
Tg (*Thapsigargin*)	1nM – 10mM	10nM

4.2.3 Analytical Techniques

Radiolabel incorporation

Media were supplemented with 20μCi/mL L-5-^{3}H-proline and 10μCi/mL ^{35}S-sodium sulfate for the final 20 hours of each culture period to measure protein and sGAG synthesis, respectively. At the end of the specified period, the samples were removed from the radiolabeled media and washed four times for 30 minutes each time in PBS supplemented with 0.8 mM sodium sulfate and 1 mM L-proline at 4°C to allow unincorporated radiolabeled precursors to diffuse out of the samples. Samples were then weighed, lyophilized, reweighed, digested in 1ml of 100mM ammonium acetate buffer with 250 μg/mL Proteinase K at 60°C for 24 hours and assayed for radiolabel content with an LS5000TD liquid scintillation counter (Beckman Coulter, Fullerton, CA). Portions of each digest were assayed for total DNA using the Hoechst 33258 assay with calf thymus DNA as a standard[162] and sGAG using the 1,9-dimethyl-methylene blue assay[125,163] with shark cartilage chondroitin sulfate as a standard.

Viability Staining

Gel constructs were imaged for cell viability using the Molecular Probes Live/Dead kit (n=3/group/timepoint). Constructs were imaged directly after 24 hours in the inhibitors (levels as indicated for the recovery portion of the experiment), and then 24, 48, and 60 hours after being returned to basal media. After rinsing samples in three 10-minute PBS washes with gentle agitation, they were incubated for 1 hour in 4μM calcein and 4μM ethidium in PBS. To remove any unincorporated calcein and ethidium,

samples were rinsed in three 10-minute PBS washes. Samples were then imaged with a confocal microscope at the requisite excitation and emission wavelengths.

4.3 RESULTS

4.3.1 Dose Response

Each inhibitor induced a dose-dependent inhibition of sGAG synthesis, but inhibition of protein synthesis was less consistent. The voltage-dependent K+ channel inhibitor 4AP inhibited both protein and sGAG synthesis at levels equal to or above 10mM ($p \leq 0.01$) (Figure 4.1A). The cation-selective stretch-activated channel inhibitor Gd had no significant effect on protein synthesis, but inhibited sGAG synthesis at 10mM ($p=0.0001$) (Figure 4.1B). The L-type voltage sensitive calcium channel inhibitor Nf had no significant effect on protein synthesis, and only the highest level (10mM) inhibited sGAG synthesis ($p=0.0011$) (Figure 4.1C). The ATP-dependent Ca2+ pumps inhibitor Tg inhibited sGAG synthesis at 100nM ($p<0.0001$), 1μM ($p<0.0001$) and 10μM ($p<0.0001$); protein synthesis was significantly inhibited at 100nM ($p=0.0094$) and 1μM ($p=0.034$) (Figure 4.1D).

Inhibitor levels for subsequent studies were determined based on the dose-response results and practical concerns including the precipitation of high concentrations of certain inhibitors out of solution. Table 4-1 shows the values chosen for the subsequent studies.

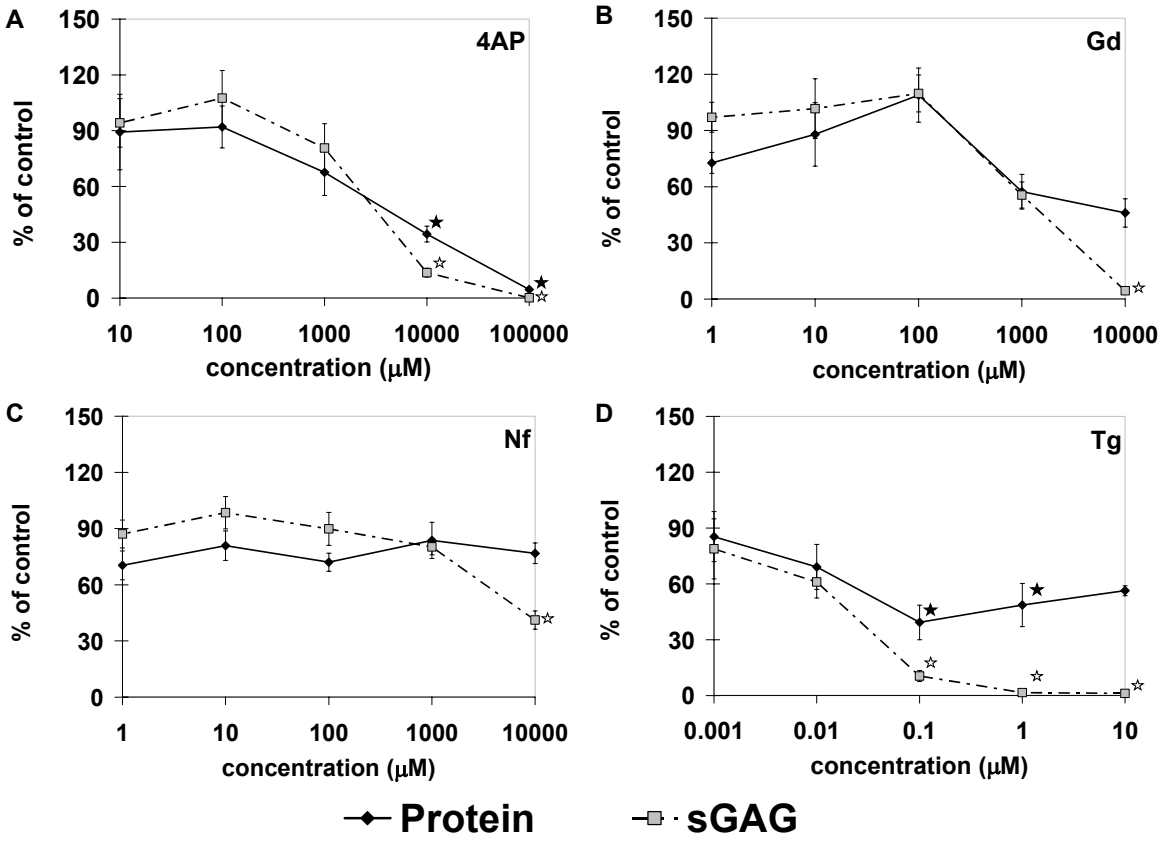

Figure 4.1: Dose-dependent inhibition of cartilage explant protein (L-5-^{3}H-proline incorporation) and sGAG (^{35}S-sodium sulfate incorporation) synthesis rates for each of the ion-channel inhibitors.

4.3.2 Recovery

There were no qualitative differences in explant cell viability either immediately after exposure to the inhibitors (Figure 4.2) or 24, 48 or 60 hours after being returned to basal medium. Both the protein and sGAG synthesis rates of the explants exposed to each of the inhibitors fully recovered by three days after removal of the inhibitors (Figure 4.3**Error! Reference source not found.**). After one recovery day, protein synthesis of the explants exposed to 4AP was not statistically different from that of the control explants ($p=0.086$), with increasing recovery by day 2 ($p=0.94$) (Figure 4.3A). SGAG synthesis of samples exposed to 4AP had recovered by day 2 ($p=0.89$). Protein synthesis by samples exposed to Gd and Nf had recovered after one day ($p=1.0$ and $p=0.97$ respectively) (Figure 4.3B, C). sGAG synthesis by samples exposed to Gd and Nf had recovered after one day ($p=1.0$ and $p=0.99$ respectively). Protein and sGAG synthesis rates by samples exposed to Tg had recovered after three days ($p=1.0$) (Figure 4.3D).

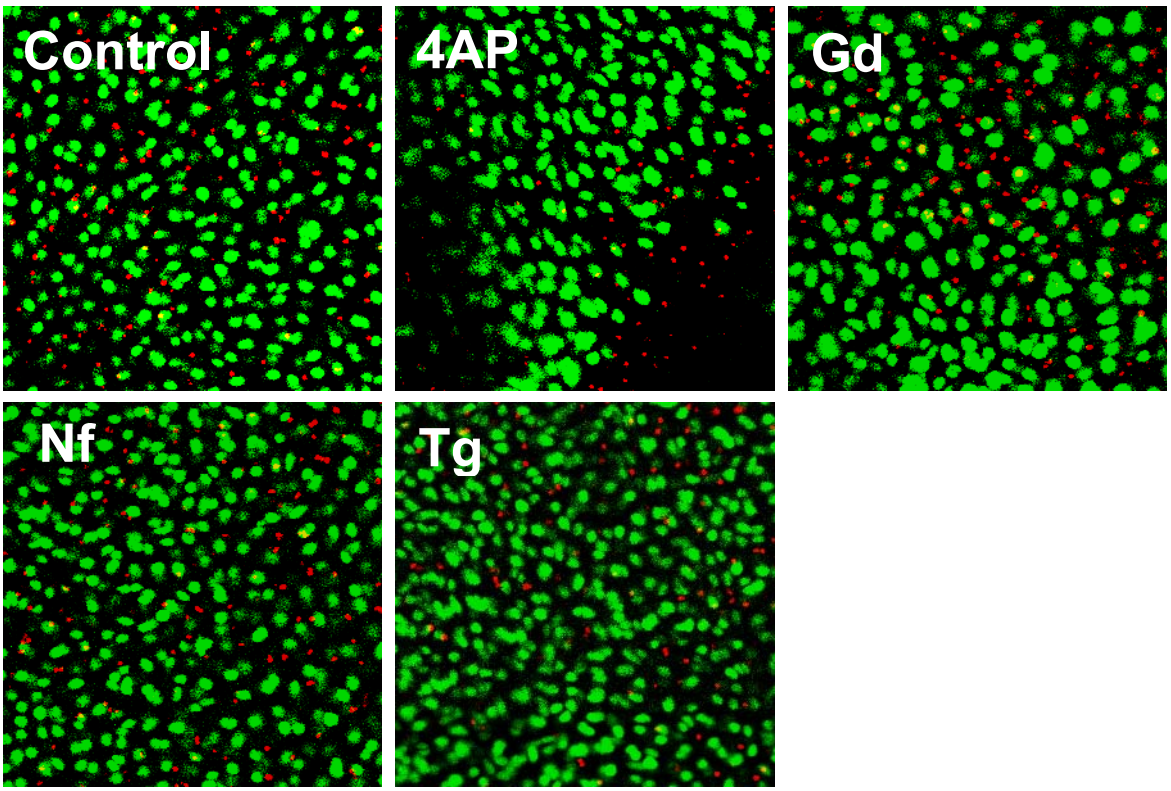

Figure 4.2: Representative Live/Dead images of cartilage explants exposed to the ion-channel inhibitors for 24 hours.

Viability was similar to controls for all inhibitors, and no decrease in viability was observed for up to three days after removal from the inhibitors (not shown).

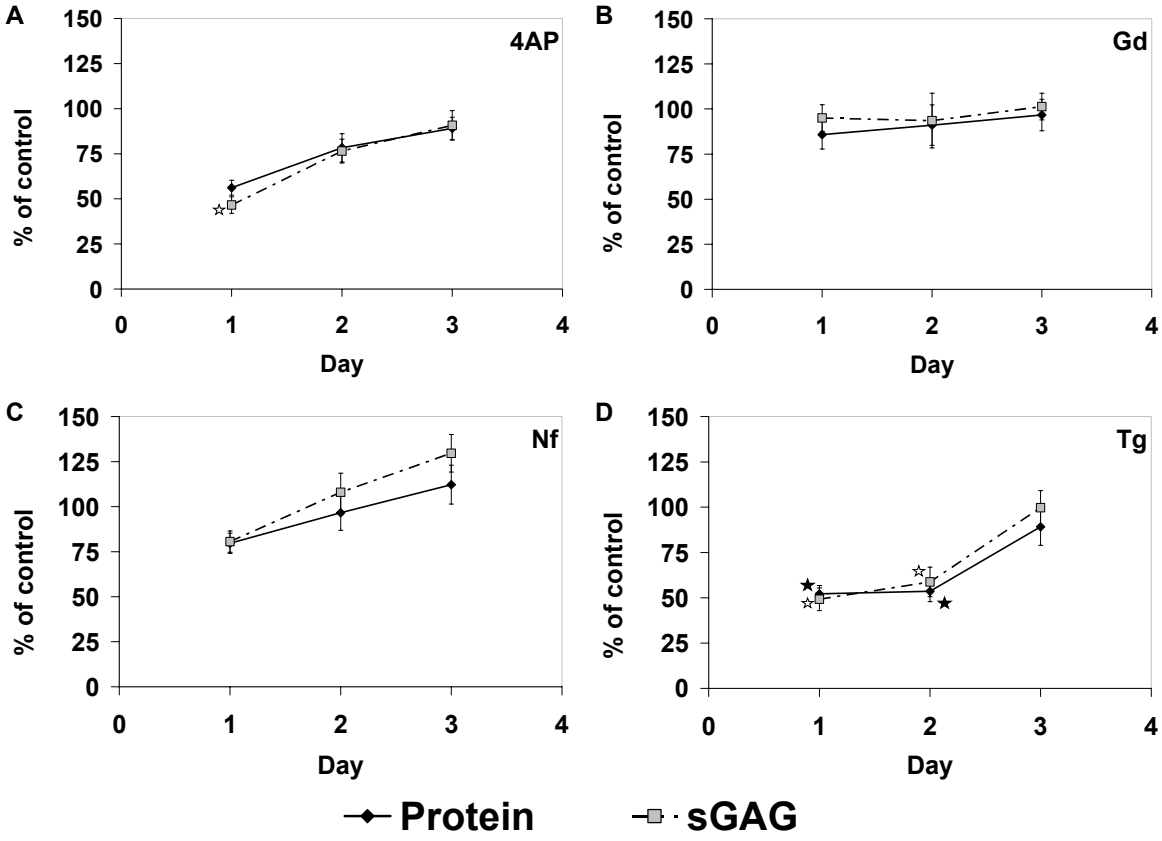

Figure 4.3: Protein and sGAG synthesis rates of cartilage explants during recovery from 24 hours of exposure to the ion-channel inhibitors.

Data are normalized by synthesis rates of untreated control explants cultured for comparable periods. ★ indicates $P < 0.05$ vs. control for protein synthesis and ☆ indicates $P < 0.05$ vs. control for sGAG synthesis. (mean ± S.E.M., $N = 8$)

4.3.3 Gel Response

For the static and dynamic compression experiments, free-swelling gels in all media conditions were run in parallel to account for baseline effects of the inhibitors (Figure 4.4). The addition of 4AP, Nf, and Tg significantly inhibited both protein and sGAG synthesis rates ($p<0.0001$). The addition of Gd inhibited sGAG synthesis, but not protein synthesis ($P<0.0001$ and $P=0.94$ respectively).

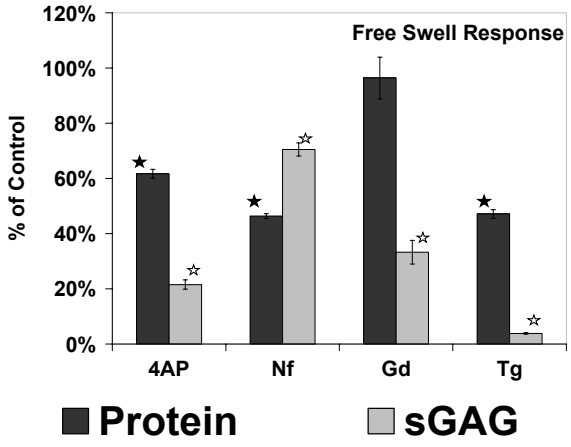

Figure 4.4: Protein and sGAG synthesis rates of free-swelling gels after 44 hours of exposure to the ion-channel inhibitors.

Data are normalized by synthesis rates of untreated controls. ★ indicates $P < 0.05$ vs. control for protein synthesis and ☆ indicates $P < 0.05$ vs. control for sGAG synthesis. (mean ± S.E.M., N = 8-10)

4.3.4 Static Compression

While static compression significantly inhibited protein synthesis in all treatment groups, the effects on sGAG synthesis were more variable (Figure 4.5). For the control and 4AP groups, 50% static compression inhibited protein synthesis over the 0% and 10% groups ($p \leq 0.0067$), with no significant effect on sGAG synthesis. For the Gd groups, all levels of static compression significantly affected protein synthesis (0%>10%>50%) ($p \leq 0.0056$); 10% static compression inhibited sGAG synthesis over the 0% group ($p = 0.0077$). For the Nf groups, 50% static compression inhibited both protein and sGAG synthesis over the 0% and 10% groups ($p \leq 0.017$). For the Tg groups, all levels of static compression significantly affected protein synthesis (0%>10%>50%) $p \leq 0.015$); 50% static compression inhibited sGAG synthesis over the 0% group ($p = 0.034$).

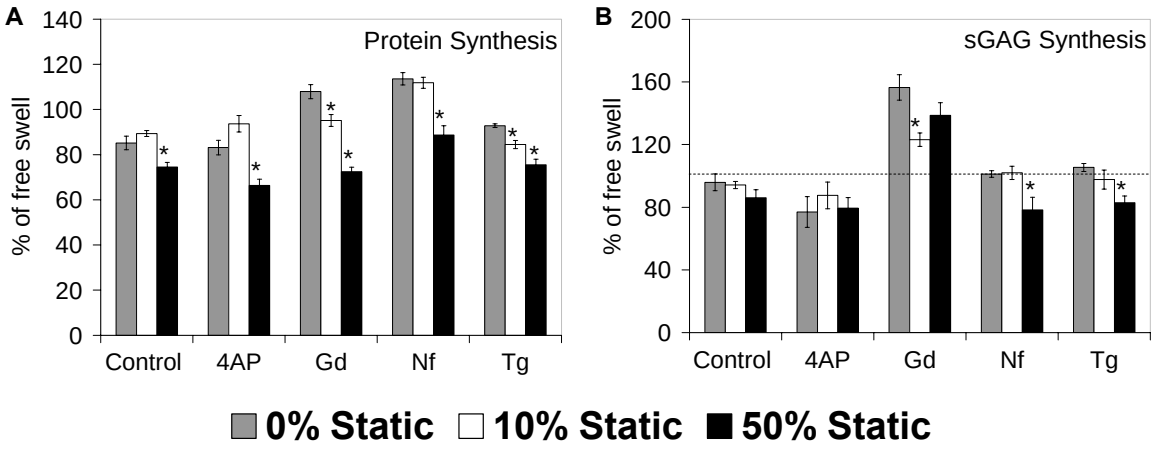

Figure 4.5: Protein (A) and sGAG (B) synthesis rates for gels subjected to varying grades of static compression for 20 hours in the presence of ion-channel inhibitors.

Data are normalized by respective free-swelling synthesis rates. * indicates $P < 0.05$ vs. respective 0% static group. (mean ± S.E.M., N = 8-10)

4.3.5 Dynamic Compression

As with the static compression, the effects of dynamic compression on protein synthesis were more consistent than the effects on sGAG synthesis (Figure 4.6). For all groups except 4AP, dynamic compression significantly stimulated protein synthesis over static controls ($p \leq 0.001$). For only the control and Gd groups, dynamic compression significantly stimulated sGAG synthesis ($p < 0.0001$).

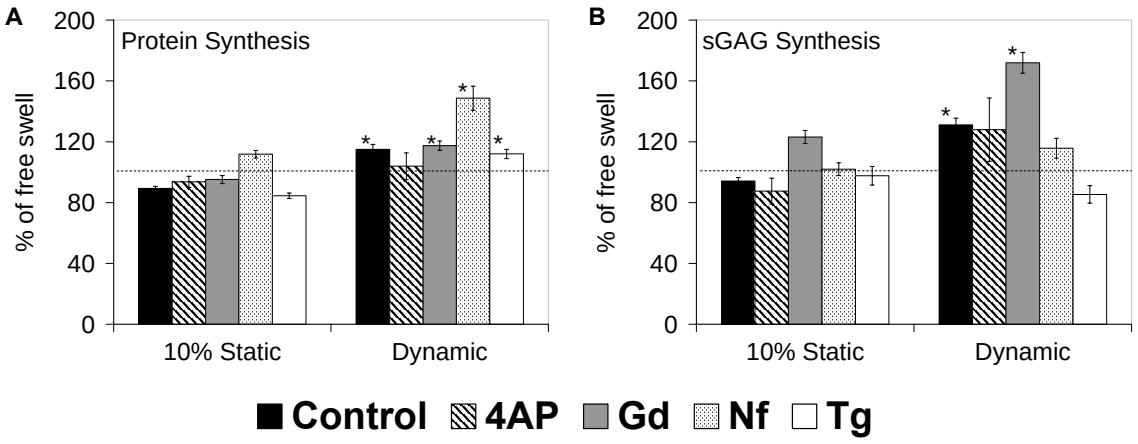

Figure 4.6: Protein (A) and sGAG (B) synthesis rates for gels subjected to static and dynamic compression for 20 hours in the presence of ion-channel inhibitors.

Data are normalized by respective free-swelling synthesis rates. * indicates $P < 0.05$ vs. respective 10% static group. (mean ± S.E.M., N = 8-10)

4.4 DISCUSSION

While chondrocytes respond to mechanical stimuli in both 3D culture and monolayer, the mechanisms linking these alterations in the cellular environment to specific changes in cell behavior are not well understood. This study examined whether blocking specific ion-channels, a technique demonstrated with cells in monolayer, modifies the cellular response to compression in 3D culture.

As appropriate doses for 3D culture were unknown, the treatment levels in this study included inhibitor levels above and below those typically used in previous monolayer studies. Compression-independent changes in matrix synthesis were observed for at least one level of all inhibitors, with a generally greater impact on sGAG synthesis than on protein synthesis. Although cytotoxicity could explain some of these effects, Live/Dead staining of tissue samples incubated with each of the inhibitors revealed no substantial changes in cell viability. Additionally, the results of the recovery experiment indicated that samples exposed to all inhibitors recovered both protein and sGAG synthesis rates. Sustained protein synthesis at levels down-regulating sGAG synthesis suggests a selective inhibition of cellular functions. Chondrocytes in agarose generally retained the capacity to increase protein synthesis rates in response to oscillatory compression, suggesting that inhibition of the specific channels did not block any non-redundant pathways or that the inhibition produced was transient and found to be similar to that of controls.

Overall, treatment with the inhibitors more significantly affected sGAG synthesis suggesting that these ion-channels influence proteoglycan production or processing. Inhibition of Ca2+ channels by Nf affected protein synthesis, with little effect on sGAG

synthesis, a unique response of the four inhibitors examined. In contrast to the compression independent selective inhibition of protein synthesis by Nf, the upregulation of protein synthesis due to dynamic stimulation was unaffected, while the upregulation of sGAG synthesis was blocked. A potential reason for the inhibition of mechanically-stimulated upregulation of sGAG synthesis may be due to a critical role in the mechanoregulation of proteoglycan production by Ca2+ channel signaling. There was no significant stimulation of either protein or sGAG synthesis rates by dynamic compression in the presence of 4AP, the voltage-dependent Ca2+ channel inhibitor, which could suggest a role for K+ signaling in mechanotransduction. Alternatively K+ channels may play such a dominant role in overall matrix synthesis such that any upregulation of matrix components may be overwhelmed. Treatment with Tg significantly impaired both overall protein and sGAG synthesis rates, with a substantial decrease in sGAG synthesis. There was a significant upregulation of protein synthesis by dynamic compression with Tg treatment, but there was no effect on sGAG synthesis. With the overall levels of sGAG synthesis being so low, it is difficult to discern whether this trend is valid, although the effect on sGAG synthesis is consistent with previous reports[155].

Very little is known about how mechanical signals are transduced from extracellular matrix to inside of the cell to activate biosynthesis and cellular activity. One group of the membrane molecules that can potentially transmit matrix deformation signals to inside of the cell are cation-channels[164]. Some of these channels that transmit Ca2+ have been shown to play an important role in regulating chondrocyte proliferation and maturation in monolayer[55,165]. Sensing the dynamic polarization of the cell membrane may be required to mechanotransduce the differential forces involved in static

and dynamic compression, portions of which are affected by the addition of the voltage-dependent channel inhibitors, 4AP and Nf.

Recent evidence from C. elegans suggests that mechanosensitive ion-channels are part of the mechanotransducing complex that connects the extracellular matrix to the cytoskeleton. It has been postulated that the deformation of the collagen matrix may mechanically affect the opening and closing of ion-channels, which are linked to the matrix by direct binding of the collagenous molecules[166-168]. The results of this study found that interruption of Ca2+ signaling pathways abolished the upregulation of sGAG synthesis by dynamic mechanical compression. It remains to be determined whether direct binding of the matrix is the mechanism that is responsible for the involvement of ion-channels in mechanotransduction of chondrocytes. Future directions to investigate this possibility might include disrupting the collagenous extracellular matrix prior to loading with enzymatic digestion or mechanically loading freshly seeded gels, where there is no matrix for the cells to interact with. Overall, this study suggests that different ion-channels play distinct, yet cooperative, roles to convert the same mechanical signals into different cellular responses, but that the roles of these ion channels in 3D are less distinct than in 2D culture experiments.

CHAPTER 5 INFLUENCE OF THE TGF-β SIGNALING PATHWAY ON THE CHONDROCYTE RESPONSE TO DYNAMIC COMPRESSIVE LOADING

5.1 INTRODUCTION

In addition to using mechanical stimulation to control chondrocyte behavior, biochemical factors have been found to influence chondrocyte proliferation and metabolism. Different biochemical factors have been used to expand chondrocyte cell populations, to increase cartilage-specific ECM production and to influence chondrocyte differentiation state. Members of the TGF-β superfamily, as well as Insulin Growth Factor I (IGF-I), have been found to positively influence gene expression and matrix synthesis. Specifically, TGF-β has been found to maintain chondrocyte phenotype *in vitro*. Isoforms of TGF-β, including, but not limited to, TGF-β1 and TGF-β3, have been found to promote chondrogenesis in undifferentiated cell populations such as BMSCs, periosteally-derived cells and adipose-derived cells.

The overall objective of the studies presented in this chapter was to investigate the role of the TGF-β signaling pathway in the BACs under dynamic compressive loading. Specifically the effects of dynamic and static compressive loading on BAC gene expression and matrix synthesis in the presence of the TGF-β signaling inhibitor SB431542 were examined. Investigation of the influence of transforming growth factor β1 (TGF-β1) signaling in the response of chondrocytes to dynamic compressive loading may provide clues to the mechanisms involved in chondrocyte maintenance through mechanical stimulation. The mechanisms through which mechanotransduction occurs in

chondrocytes remain largely elusive. This work addresses a potential mechanism for mechanotransduction in BAC cells.

5.2 Materials and Methods

5.2.1 Construct culture

To enzymatically isolate chondrocytes, tissue was excised from the femoral-patellar grooves, minced and digested in DMEM with 0.2% collagenase for 24 hours in a 37°C, 5% CO_2 incubator. After centrifugation at 160 x g, cells were washed twice with Ca2+, Mg^{2+} -free PBS and counted with a Vi-Cell Cell Viability Analyzer. Cells were seeded at a final density of $20x10^6$ cells/mL in 3% LMP agarose. Constructs were cast in 4mm diameter x 3mm deep cylindrical wells in custom machined polycarbonate molds that were autoclave sterilized prior to gel casting. Agarose constructs were assembled by autoclaving 3% LMP agarose in 1X Ca2+, Mg2+ -free PBS and then cooling the solution to 42°C. Cells were centrifugally pelleted and resuspended in the agarose to yield a final concentration of $20x10^6$ cells/mL, and the solution was cooled in the molds at room temperature for 10 minutes. Gels were removed from molds and precultured for 24 hours in basal medium prior to the addition of the inhibitor. Medium was changed every two days.

5.2.2 TGF-β Inhibitor

SB431542 is a small molecule ATP-mimetic inhibitor of the kinase activity associated with members of the activin receptor-like kinase (ALK) family, specifically

ALK5 (TGF-β type I receptor, TGF-βRI), ALK4 (activin type I receptor) and ALK7 (nodal type I receptor)[169-171]. The hypothesized mechanism for TGF-β signaling inhibition due to SB431542 is competition for the ATP-binding site on the type I receptor[169-171]. Upon phosphorylation by the type II receptor and ATP binding, the type I receptor (ALK5) phosphorylates Smad 2 and Smad 3 proteins[172,173]. Without ATP binding, the kinase activity of ALK5 is inhibited[172,173]. Therefore, the phosphorylation of the target substrates, Smad 2 and Smad 3 (Smad2/3), is inhibited[169-171].

5.2.3 Experimental Design

Dose and Recovery Responses

As the effects of sustained exposure to the inhibitor and appropriate doses for 3D culture were unknown, dose-response and recovery experiments were first performed. The dose response of SB431542 on protein and sGAG synthesis rates was investigated. BAC constructs (n=6-8/condition) were cultured for two hours in basal media alone or supplemented with 0.1, 1, 10 or 100 μM of the inhibitor, followed by 20 hours in media containing both inhibitors and radiolabeled precursors. The concentration of the inhibitor to be used in both the recovery and mechanical stimulation studies was determined by the first dose exhibiting a repression of either proteoglycan or protein synthesis rates.

To investigate the recovery from the inhibitor, BAC constructs (n=8/condition) were cultured for 24 hours in basal medium alone or supplemented with 1 μM of the inhibitor. The 1 μM concentration of SB431542 was the first dose level to display inhibition of protein synthesis. 1 μM of SB431542 has also been used in previous monolayer experiments investigating the inhibitory effects of the molecule[169,170]. After

exposure to the inhibitor, constructs were rinsed three times for 10 minutes each time in PBS and then transferred into basal medium without inhibitors. Constructs were cultured for 20 hours in radiolabeled precursors beginning 4, 24 or 48 hours after return to basal medium to evaluate their ability to recover both protein and sGAG synthesis rates. The recovery study was used to evaluate whether there were any sustained effects of BAC matrix synthesis rates by exposure to SB431542.

Mechanical Stimulation

Dynamic compression was applied using a custom designed mechanical loading system (see appendix D). For the static and dynamic compression studies, constructs were cultured in basal medium with or without 1 μM of SB431542 for 2 hours prior to loading (BASAL and BASAL+SB respectively). One subset of the constructs (n=6/condition) were cultured for an additional 20 hours in the same media supplemented with radiolabeled precursors under the following conditions: static compression (10%), 1Hz oscillatory compression (10%±3%) and free swelling (FS). The other subset of constructs (n=8/condition) were cultured for an additional 20 hours under the following conditions: static compression (10%), 1Hz oscillatory compression (10%±3%) and free swelling (FS) before being analyzed for mRNA expressions.

5.2.4 Analytical techniques

Radiolabel incorporation

Media were supplemented with 20μCi/mL L-5-^{3}H-proline and 10μCi/mL ^{35}S-sodium sulfate for the final 20 hours of each culture period to measure protein and sGAG

synthesis rates, respectively. At the end of the specified period, the samples were removed from the radiolabeled media and washed four times for 30 minutes each time in PBS supplemented with 0.8 mM sodium sulfate and 1 mM L-proline at 4°C to allow unincorporated radiolabeled precursors to diffuse out of the samples. Samples were then weighed, lyophilized, reweighed, digested in 1ml of 100mM ammonium acetate buffer with 250 μg/mL Proteinase K at 60°C for 24 hours and assayed for radiolabel content with an LS5000TD liquid scintillation counter (Beckman Coulter, Fullerton, CA). Portions of each digest were assayed for total DNA using the Hoechst 33258 assay with calf thymus DNA as a standard[162].

Real-Time RT-PCR

Agarose gels were immediately dissociated in Qiagen Lysis Buffer with 1% beta-mercaptoethanol. The RNeasy Total RNA Kit (Qiagen, Chatsworth, CA) was then used according to manufacturer's protocol to purify RNA from the samples. The yield of the purified isolate was read at 260 nm and 280 nm on a UV-1601 Spectrophotometer (Shimadzu, Columbia, MD).

1μg of mRNA was transcribed to cDNA using the Promega RT System (Promega, Madison, WI) and manufacturer's protocol. The SYBR Green PCR Master Mix (Applied Biosystems, Foster City, CA) was mixed with primers and cDNA for real time detection of amplification. Real time, quantitative RT-PCR was performed with an ABI PRISM 7700 Sequence Detector System (PE Biosystems, Foster City, CA).

For primer information, see Table 5-1.

Table 5-1: Primer sequences for real-time RT-PCR for bovine β-actin, aggrecan, biglycan, collagen type I, collagen type II, collagen type X, decorin, GAPDH, TGF- β1 and TGF- β receptor type I (TβRI).

Bovine Gene	**Forward Primer 5'-3'**	**Reverse Primer 5'-3'**
β-actin	CGA GCA TTC CCA AAG TTC TAC	TTC CTG TAA CAA TGC ATT TCG
aggrecan	CCT CAG GGT TTC CTG ACA TTA	TAA GCT CAG TCA CGC CAG ATA
biglycan	GGT CCT CGT GAA CAA CAA GAT	GGA TCT CAC ACA GGT GGT TCT
collagen type I	AAG AAC CCA GCT CGC ACA TG	GGT TAG GGT CAA TCC AGT AGT AAC CA
collagen type II	GCA TTG CCT ACC TGG ACG AA	CGT TGG AGC CCT GGA TGA
collagen type X	TCT CCA AAG CTT ACC CAG CTA	CAG GTG AAG ATT CCA GTT CTT G
decorin	ACT GAA GGA ATT GCC AGA GAA	CTA CGA CGA TCA TCT GGT TCA
GAPDH	CCT TCA TTG ACC TTC CTA CAT GGT CTA	TGG AAG ATG GTG ATG GCC TTT CCA TTG
TGF- β1	GGC AAC AAA ATC TAT GAC	CTT CAA GTG GAC ATT AAC GG
TβRI	TCG AAA GCA TGA AGG ACA AC	CCA GCA CTC AGT CAA CGT CT

5.3 RESULTS

5.3.1 Dose Response

Protein synthesis was inhibited in a dose-dependent manner by SB431542, while significant inhibition of sGAG synthesis only occurred at the highest dose (Figure 5.1). At 0.1 μM of the inhibitor, neither protein nor sGAG synthesis rates were inhibited. At 1 and 10 μM, only protein synthesis was inhibited (68% of control, $p<0.001$ and 46% of control, $p<0.001$). At 100 μM, both protein and sGAG synthesis rates were inhibited to approximately 20% of control synthesis rates ($p<0.001$). Consistent with previous work using the TGF-β inhibitor SB431542[171], 1 μM of the inhibitor was chosen to investigate the recovery of matrix synthesis after inhibitor exposure and the response to mechanical stimulation in the presence of the inhibitor.

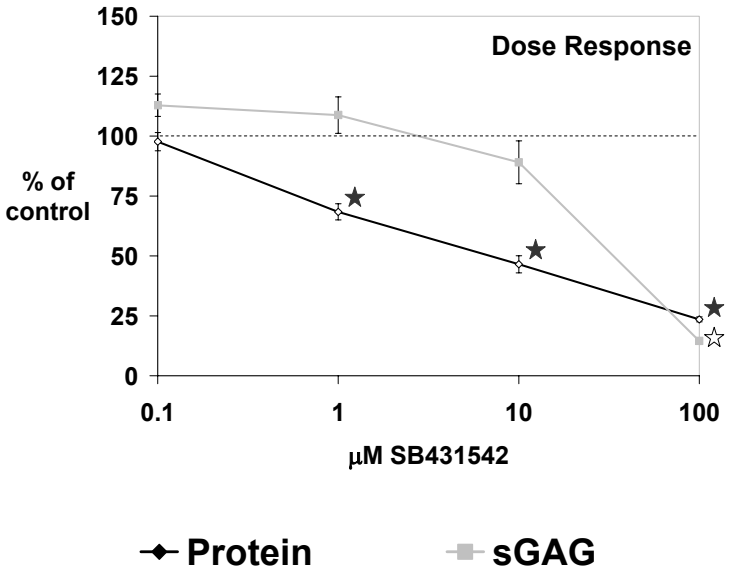

Figure 5.1: Dose-dependent inhibition of BAC construct protein (L-5-^{3}H-proline incorporation) and sGAG (^{35}S-sodium sulfate incorporation) synthesis rates for the inhibitor SB431542.

Data are normalized by synthesis rates of untreated control constructs (dashed line indicates 100% of control). ★ indicates $P < 0.05$ vs. control for protein synthesis and ☆ indicates $P < 0.05$ vs. control for sGAG synthesis. (mean ± S.E.M., N = 6)

5.3.2 Recovery Response

There was no inhibition of sGAG synthesis during or after exposure to 1 μM SB431542 (Figure 5.2). SGAG synthesis was not significantly different from unexposed samples during the first 48 hours after inhibitor exposure. After 3 days post-exposure to the inhibitor, sGAG synthesis was stimulated in the samples previously exposed to the inhibitor compared to unexposed samples (121% of control, $p=0.027$).

Protein synthesis was still inhibited during the 24 hour period after exposure to SB431542 ($p=0.008$). By the second day post-exposure, protein synthesis was stimulated in the samples previously exposed to the inhibitor compared to unexposed samples ($p=0.005$). By the third day post-exposure, protein synthesis was not significantly different from control samples.

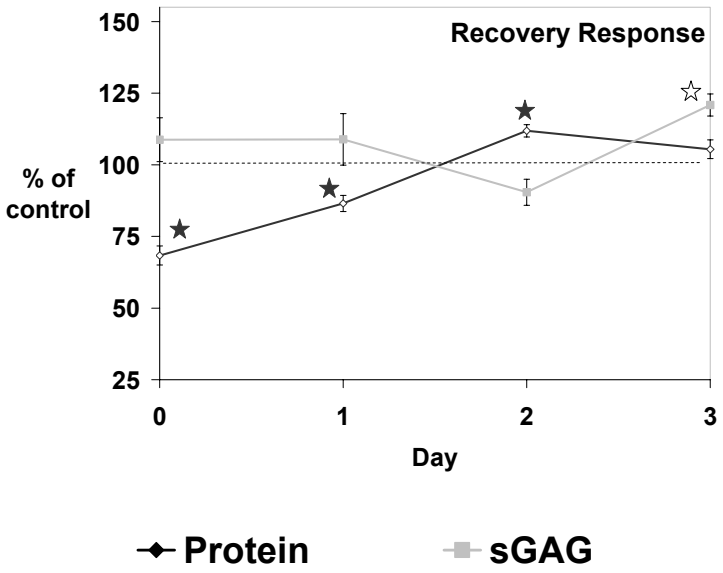

Figure 5.2: Recovery response of BAC construct protein (L-5-^{3}H-proline incorporation) and sGAG (^{35}S-sodium sulfate incorporation) synthesis rates for the inhibitor SB431542.

Day indicates days post-exposure to inhibitor. Data are normalized by synthesis rates of untreated control constructs cultured in parallel (dashed line indicates 100% of control). ★ indicates $P < 0.05$ vs. control for protein synthesis and ☆ indicates $P < 0.05$ vs. control for sGAG synthesis. . (mean ± S.E.M., N = 5-6)

5.3.3 Mechanical Stimulation: Gene Expression

There was no significant regulation of aggrecan or the housekeeping gene GAPDH by either dynamic compression or the inhibitor SB431542. (Figure 5.3E,F)

In the absence of the inhibitor, collagen II gene expression was stimulated 1.6-fold and collagen I gene expression was stimulated 2.2-fold by dynamic compression ($p=0.031$ and $p=0.037$ respectively) (Figure 5.3A,B). While there was no significant stimulation by dynamic compression of TGF-β1 gene expression, there was a stimulation of TGF-β Receptor I (ALK5) gene expression in the absence of the inhibitor ($p=0.042$) (Figure 5.3C,D). Exposure to the inhibitor SB431542 inhibited the regulation of collagen II, collagen I, and TGF-β Receptor I gene expressions, without significantly affecting the expressions of the exposed static samples compared to the unexposed static samples.

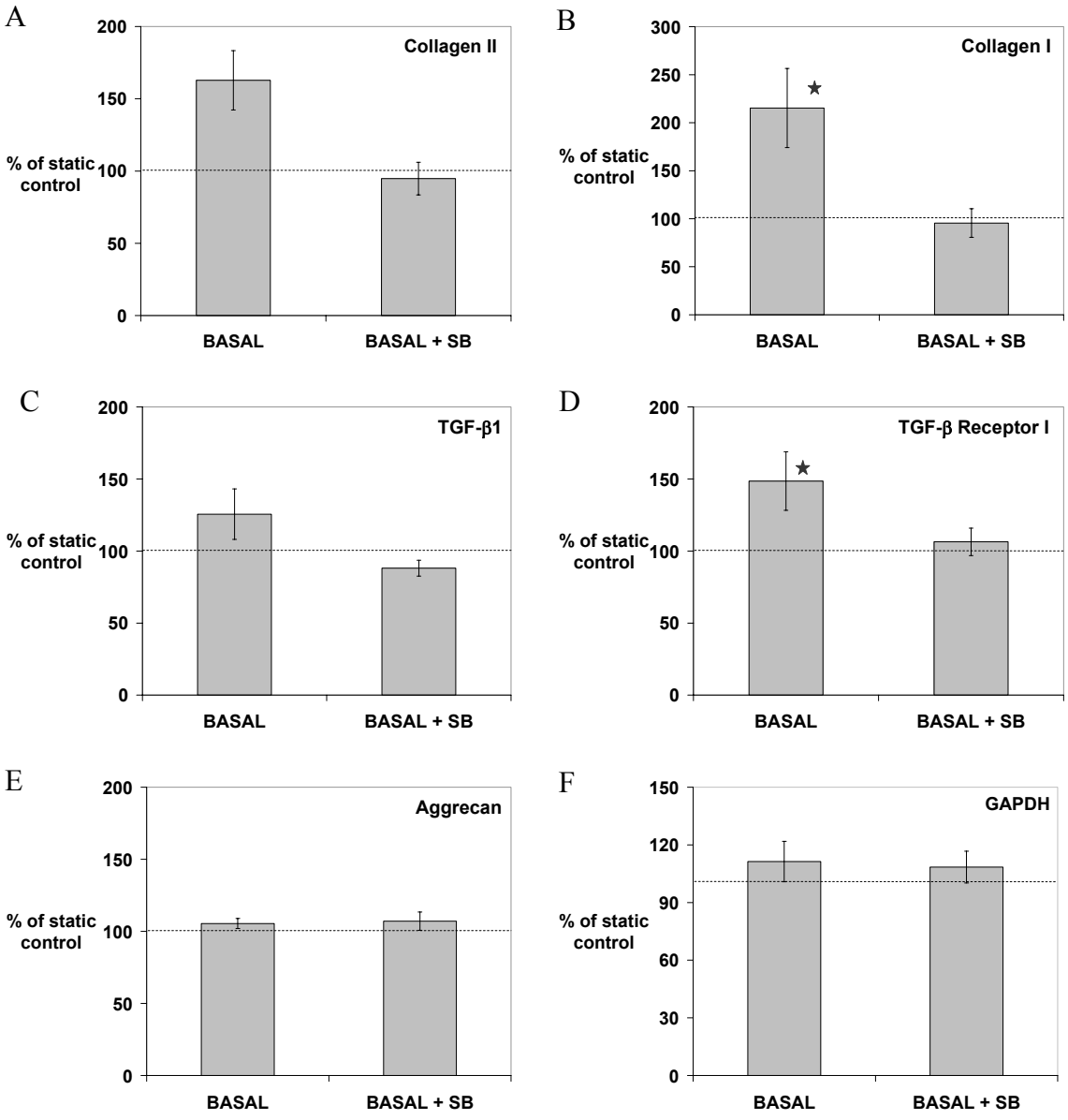

Figure 5.3: Gene expression for BAC constructs dynamically compressed for 20 hours in the absence (BASAL) or presence of the inhibitor SB431542 (BASAL+SB).

Data are normalized by respective static group (dashed line indicates 100% of static for that condition). No significant differences were found in gene expression between static groups. ★ indicates $P < 0.05$ vs. respective static group. (mean ± S.E.M., N = 6-8)

5.3.4 Mechanical Stimulation: Matrix Synthesis Rates

For the unexposed samples, dynamic compression stimulated protein synthesis 1.3-fold and slightly stimulated sGAG synthesis 1.1-fold over static compression in BASAL samples ($p<0.001$ and $p=0.005$ respectively) (Figure 5.4). There was no stimulation of either protein or sGAG synthesis rates by dynamic compression in the samples exposed to 1μM SB431542. For the statically compressed samples, there were no significant differences in either protein or sGAG synthesis rates between media conditions.

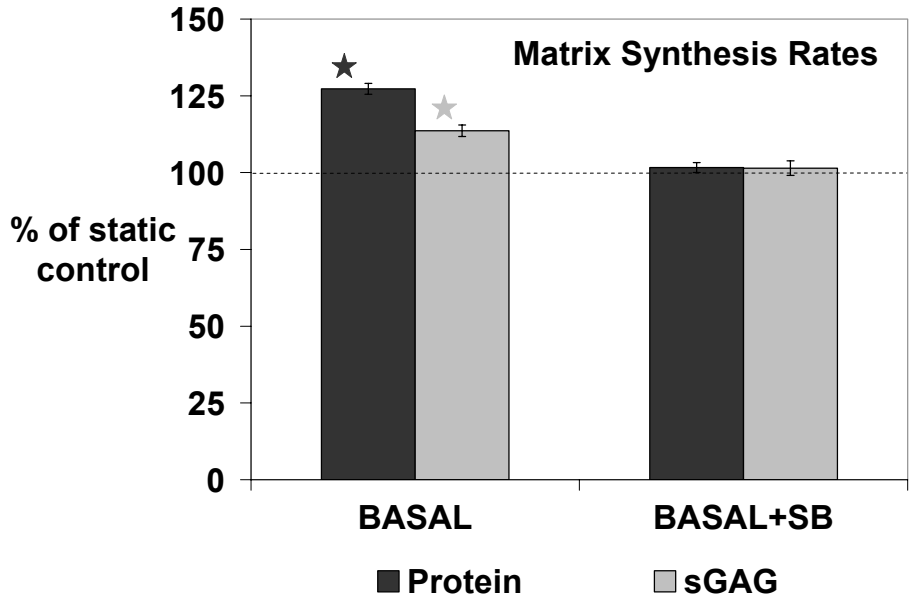

Figure 5.4: Matrix synthesis rates for BAC constructs dynamically compressed for 20 hours in the absence or presence of the inhibitor SB431542.

Data are normalized by respective static group (dashed line indicates 100% of static for that condition). ★ indicates $P < 0.05$ vs. control for protein synthesis and ★ indicates $P < 0.05$ vs. control for sGAG synthesis. (mean ± S.E.M., N = 5-6)

5.4 DISCUSSION

Both biomechanical and biochemical stimuli have been shown to influence cartilage maintenance and metabolism. Dynamic compression and exogenous TGF-β have been found to maintain chondrocyte phenotypic expression *in vitro*. Buschmann *et al.* have hypothesized that there is a synergistic relationship between the growth factor and compressive loading of chondrocytes[174]. In rabbit BMSCs cultured in agarose, Huang *et al.* found that sustained dynamic compression stimulated TGF-β1 gene expression, as well as TGF-β receptors I and II gene and protein expressions[175,176]. Huang *et al.* also found was that dynamic compression stimulated the expression of chondrocytic genes and proteins such as aggrecan and collagen II at a similar level as treatment with TGF-β1 only, although the overall level of chondrogenesis in any group was fairly modest. The combination of TGF-β1 and dynamic compression had no greater effect than treatment with TGF-β1 alone. While the signaling pathway through which TGF-β acts has been thoroughly explored, the mechanisms through which cells respond to mechanical stimulation are far less clear. This objective of this study was to explore the possible interaction between TGF-β signaling and mechanical regulation of BAC biosynthesis. The effects of dynamic and static compressive loading on BAC gene expression and matrix synthesis in the presence of the TGF-β signaling inhibitor SB431542 were examined.

TGF-β signaling has been shown to be dependent on both ALK5 and the TGF-β type II receptor. Signaling is mediated via phosphorylation of the cytoplasmic proteins Smad 2 and Smad 3 (Smad2/3). Upon phosphorylation by ALK5, Smad2/3 are released

from the receptor. The auto-inhibitory 3D folding is relieved. Smad4 is bound and the complex translocates to the nucleus where transcriptional regulation occurs[72,177].

The small molecule SB431542 was chosen to inhibit TGF-β signaling due to its nanomolar inhibition of ALK5 kinase abilities with greater than 100-fold selectivity against p38 MAPK and 25 other kinases[171]. Inman *et al.* found SB431542 preferentially inhibited ALK5 kinase activity in cells transfected with constitutively active type I receptors (ALK2 through ALK7)[170]. SB431542 is a small molecule ATP-mimetic inhibitor of the kinase activity. The hypothesized mechanism for TGF-β signaling inhibition due to SB431542 is competition for the ATP-binding site on the type I receptor[169,171]. Upon phosphorylation by the type II receptor and ATP binding, the type I receptor (ALK5) phosphorylates Smad2/3 proteins. Without ATP binding to ALK5, the kinase activity of ALK5 in inhibited. Therefore the phosphorylation of the target substrates, Smad2/3, is inhibited.

The present study found that SB431542 selectively inhibited protein synthesis over sGAG synthesis in BAC agarose constructs. Protein synthesis was inhibited linearly in a dose dependent manner. Inhibition was found to be recoverable after removal from the inhibitor. The inhibition of protein synthesis by 22 hours of exposure to 1 μM of SB431542 had recovered to 87% of basal levels by 24 hour after removal from the inhibitor. By 2 days post-exposure, protein synthesis had recovered to 112% of basal synthesis rates. SGAG synthesis was only significantly affected at the highest inhibitor level of 100 μM.

Exposure to 1 μM of SB431542 had no significant effect on either gene expression or matrix synthesis rates for BAC samples statically compressed compared to

statically compressed BASAL samples. In addition, the addition of the inhibitor also abrogated the stimulation of protein and sGAG synthesis by dynamic compression seen in the BASAL samples.

With no effect on aggrecan gene expression and a low level of stimulation of sGAG synthesis by dynamic compression in the basal samples, the effect, if any, of inhibiting the TGF-β signaling pathway on proteoglycan gene expression is unclear. Conversely, there was a substantial and significant upregulation of collagen I and II gene expressions, as well as protein synthesis, in basal samples by dynamic stimulation. The effect of inhibiting TGF-β signaling seems to occur at the transcriptional level, with no stimulation occurring due to dynamic stimulation in the presence of the inhibitor. These results demonstrate that the TGF-β signaling pathway potentially plays a profound role in the mechanotransduction of BACs subjected to dynamic compression.

Tschumperlin *et al.* postulate that mechanotransduction in epithelial cells potentially occurs via growth factor shedding from the extracellular matrix, inducing autocrine binding of epidermal growth factor ligands to the epidermal growth factor receptor, requiring no direct conformational alteration by any protein by mechanical stress[178]. Since there is little to no extracellular matrix in these 1-day old BAC agarose constructs, a mechanism involving growth factor shedding is unlikely. Most likely, the majority of TGF-β accessible to the BACs is in solution in the medium, either produced by the BACS or introduced with the FBS.

While speculative, there are multiple potential regulatory mechanisms through which TGF-β1 signaling and mechanical stimulation interact. The mechanisms fall into one of two categories, either TGF-β1 signaling influencing mechanotransduction or

mechanotransduction influencing TGF-β1 signaling. One potential mechanism for mechanical stimulation modulation of TGF-β1 signaling involves the production and activation of endogenous TGF-β, as well as the activation of latent TGF-β introduced into the system by the FBS. Increased proteolytic cleavage of the latent complex could result from either an upregulation in plasmin or stromelysin-1 concentrations in the pericellular and extracellular matrix[179,180]. In either system, stimulation of TβR1 is one potential mechanism for the modulation of dynamic loading via TGF-β signaling. An increase in the available supply of TβR1 could potentially lead to a greater level of Smad2/3 activation, amplifying the signaling occurring as a result of TGF-β1 exogenous stimulation. Another possible mechanism for regulation of chondrogenesis by mechanical stimulation is an increase in the phosphorylation of the Smad2/3 proteins and/or its translocation to the nucleus.

Another Smad-related possibility involves an increase in Smad activation of mechanosensitive proteins by TGF-β signaling, such as focal adhesion kinase (FAK) and paxillin thus increasing the mechanosensitivity of the cells[181-183]. There are other potential regulatory mechanisms through which TGF-β1 signaling and mechanical stimulation may interact including regulation by mechanical stimulation of proteolytic moieties such as plasmin, leading to the activation of latent TGF-β1, either endogenously produced (both BACs and BMSCs) or introduced into the culture system by the FBS (BACs only). Both chondrocytes and BMSCs have been found to be affected by TGF-β concentrations in the media[77,184,185].

In differentiating cells, TGF-β1 and TGF-β3 have been shown to upregulate Sox9 gene expression. This upregulation of Sox9 expression is indicative of chondrogenesis in

MPC populations. Sox9 has been shown to bind to the promoter region of type II collagen, enhancing transcription and collagen II mRNA expression. Smad3 has been found to enhance the transcriptional activity of Sox9 and the expression of the α1 (II) collagen (COL2A1) gene by forming a transcriptional complex with Sox9 and binding to the promoter region of COL2A1[186]. While Sox9 levels parallel COL2A1 in differentiating cells, Aigner *et al.* found no positive correlation between Sox9 and COL2A1 expression levels in adult articular chondrocytes[187]. For this reason, Sox9 expression was not analyzed in the current study. Possibly, dynamic compression may upregulate chondrocytic gene expression and production through mechanisms similar to those utilized in cells undergoing chondrogenic differentiation including upregulation of Sox9 levels. If this was the case, inhibiting TGF-β signaling during mechanical stimulation would be analogous to depriving a differentiating cell of the growth factor.

Future studies are needed to investigate the interactions between TGF-β signaling and mechanical stimulation. The efficacy and efficiency of the inhibition of Smad2/3 phosphorylation by incubation with SB431542 should be determined. Both western blotting and IHC could be used to determine the levels of total Smad and phosphorylated Smad, as well as localization in the presence and absence of both the inhibitor and mechanical stimulation. A more thorough analysis of protein expression is needed to complement the gene expression data presented in this study, including looking at TβRI protein expression. Overall this study established an interaction between TGF-β signaling and dynamic compression in BACs in agarose culture. TGF-β signaling was found to be critical in the upregulation of chondrocyte gene and protein expressions by dynamic compression.

CHAPTER 6 INFLUENCE OF PASSAGING, MEDIA SUPPLEMENTS AND SCAFFOLD ENVIRONMENT ON CHONDROGENESIS OF BMSCs

6.1 INTRODUCTION

Osteogenesis and chondrogenesis have been demonstrated in BMSCs from multiple species including human[188,189], bovine[190-192], canine[193] and rat[194]. The *in vitro* chondrogenesis of bone marrow derived MPCs has been described using the aggregate culture (i.e. pellet[195]) and gel culture (agarose[196], alginate[197]) of MPCs in media supplemented with transforming growth factor-beta 1 (TGF-β1)[63]. Fibroblast growth factor 2 (FGF-2) has been found to maintain cells in a more proliferative state, allowing *in vitro* expansion of BMSCs[64]. BMSCs have been shown to retain some level of chondrogenic potential through 20 or more passages[198].

While numerous studies have investigated chondrogenesis in a variety of animal models and culture systems, the conditions of culture have varied including passage number, cell seeding density in hydrogels, and media conditions. The studies presented in this chapter investigate whether these factors can significantly impact BMSC differentiation and should be considered when developing cell-based therapies for cartilage repair.

6.2 Material and Methods

6.2.1 Cell Isolation

BMSCs were isolated from both the femoral and tibial diaphyses of 2-4 week old calves within 24 hours of slaughter. After removal of all fascia and muscle, the bones were cut at the mid-diaphysis with a sterile bone saw. Marrow was removed from the medullary canal and transferred to a 50mL conical with sterile PBS plus 1% antibiotic/antimycotic (A/A: 100U/mL penicillin, 100ug/mL streptomycin, 250 ng/mL Amphotericin). Marrow was sequentially passed through large bore (25mL) and small bore (5mL) pipets to disrupt large pieces. Marrow was then sequentially passed through 16- and 18-gauge needles. Marrow suspension was centrifuged at 300 x g for 15 minutes. The separated fatty layer was removed and discarded. The cell pellet was resuspended in PBS and passed through a 20-gauge needle. Mononuclear cells were counted with a Vi-Cell Cell Viability Analyzer using the Trypan Blue exclusion method.

Cells were plated in T-flasks at 5 x 10^3 mononuclear cells per cm^2 in passaging medium (consisting of low glucose DMEM, 10% FBS, 1% antibiotic/antimycotic, ± 1ng/mL bFGF). Nonadherent cells were removed during media change three days later. Cells were cultured until confluent (~ 2 weeks, P1), detached with 0.05% trypsin/1mM EDTA, and replated at 5 x 10^3 cells per cm^2. Cells were passaged up to a total of four times and seeded into either 2% alginate or 3% agarose gels.

Gels were cultured in basal media consisting of high glucose DMEM plus antibiotic/antimycotic, non-essential amino acids, 1% ITS+ and 50μg/mL ascorbate (BASAL), basal media plus 10ng/mL TGF-β1 (TGF-β1), or basal media plus 10ng/mL TGF-β1 and 100nM dexamethasone (TGF-β1+DEX). Dexamethasone only was ran in a

preliminary study and found to not be statistically different from BASAL media (data not shown). Media were changed every two days for 16 days.

6.2.2 Experimental Design

Passaging Study

Bovine BMSCs were plated at $1x10^6$ cells per T-150 flask and expanded to confluence (3 doublings) in monolayer for 2, 3 or 4 passages (P2, P3, P4 respectively). After each passage, BMSCs were seeded at $25x10^6$ cells/mL in 2% LVG Pronova alginate and cultured as stated above. Samples were after 7 days in culture (n=4-6/group).

Seeding Density Study

Passage 3 BMSCs were seeded at $12.5x10^6$ (LOW), $25x10^6$ (MID) and $50x10^6$ (HIGH) cells/mL in 2% LVG Pronova alginate and cultured as stated above. Samples were after 7 days in culture (n=4-6/group).

Alginate Time Course

Passage 3 BMSCs were seeded at $25x10^6$ cells/mL and cultured in 2% LVG Pronova alginate and cultured as stated above for 2, 4, 7 or 14 days (n=6/group).

Agarose Time Course

Passage 3 BMSCs were seeded at $20x10^6$ cells/mL and cultured in 3% agarose and cultured in basal media consisting of high glucose DMEM plus

antibiotic/antimycotic, non-essential amino acids, 1% ITS+, 50μg/mL ascorbate and 0.4mM proline (BASAL), basal media plus 10ng/mL TGF-β1 (TGF-β1), or basal media plus 10ng/mL TGF-β1 and 100nM dexamethasone (TGF-β1+DEX) for 8 or 16 days. Media were changed every two days (n=6/group).

6.2.3 Analytical techniques

Quantitative RT-PCR

Alginate gels were dissociated in 100mM EDTA and the cells were pelleted down and resuspended in Qiagen Lysis Buffer with 1% beta-mercaptoethanol. Agarose gels were immediately dissociated in Qiagen Lysis Buffer with 1% beta-mercaptoethanol. The RNeasy Total RNA Kit (Qiagen, Chatsworth, CA) was then used according to manufacturer's protocol to purify RNA from the samples. The yield of the purified isolate was read at 260 nm and 280 nm on a UV-1601 Spectrophotometer (Shimadzu, Columbia, MD).

1μg of mRNA was transcribed to cDNA using the Promega RT System (Promega, Madison, WI) and the manufacturer's protocol. The SYBR Green PCR Master Mix (Applied Biosystems, Foster City, CA) was mixed with primers and cDNA for real time detection of amplification. Real time, quantitative RT-PCR was performed with an ABI PRISM 7700 Sequence Detector System (PE Biosystems, Foster City, CA).

Radiolabel Incorporation

Media were supplemented with 20μCi/mL L-5-^{3}H-proline and 10μCi/mL ^{35}S-sodium sulfate for the final 20 hours of each culture period to measure protein and sGAG

syntheses, respectively. At the end of the specified period, the samples were removed from the radiolabeled media and washed four times for 30 minutes each time in PBS supplemented with 0.8 mM sodium sulfate and 1 mM L-proline at 4°C to allow unincorporated radiolabeled precursors to diffuse out of the samples. Samples were then weighed, lyophilized, reweighed, digested in 1ml of 100mM ammonium acetate buffer with 250 μg/mL Proteinase K at 60°C for 24 hours and assayed for radiolabel content with a Perkin Elmer Tri-Carb 2900TR liquid scintillation counter. Portions of each digest were assayed for total DNA using the Hoechst 33258 assay with calf thymus DNA as a standard[162] and sGAG using the 1,9-dimethyl-methylene blue assay[125,199] with shark cartilage chondroitin sulfate as a standard.

Viability Staining

Gel constructs were imaged for cell viability using the Molecular Probes Live/Dead kit (n=3/group/timepoint). Constructs were imaged directly after 24 hours in the inhibitors (levels as indicated for the recovery portion of the experiment), and then 24, 48, and 60 hours after being returned to basal media. Samples were rinsed in three 10-minute PBS washes with gentle agitation, followed by incubation for 1 hour in 4μM calcein and 4μM ethidium in PBS. To remove any unincorporated calcein and ethidium, samples were rinsed in three 10-minute PBS washes. Samples were then imaged with a confocal microscope at the requisite excitation and emission wavelengths.

Histology

For histology, additional samples were rinsed in PBS, transferred to 10% neutral-buffered formalin for 48 hours, and then stored in 70% ethanol (n=2 per group per endpoint) to reduce the solubility of the GAG sidechains. Samples were subsequently embedded in paraffin and sectioned at five microns. Sections were stained with safranin-O to visualize the sGAG distribution[200].

6.3 RESULTS

6.3.1 Passaging Study

Gene Expression

Collagen II expression varied with both passage and media supplementation. Overall, collagen II expression was highest in the samples treated with both TGF-β1 and dexamethasone (TGF+DEX) ($p \leq 0.016$) (Figure 6.1). Collagen II expression was highest in the passage 3 (P3) samples treated with both TGF-β1 and dexamethasone (TGF+DEX) and decreased with passage number for all groups except for the group treated with both TGF-β1 and dexamethasone (TGF+DEX) ($p < 0.001$) (Figure 6.1A).

Aggrecan expression varied with passage number. Expression was higher in the passage 2 samples compared to either passage 3 or 4 ($p \leq 0.012$) (Figure 6.1B). There were no significant differences found between media conditions for any passage.

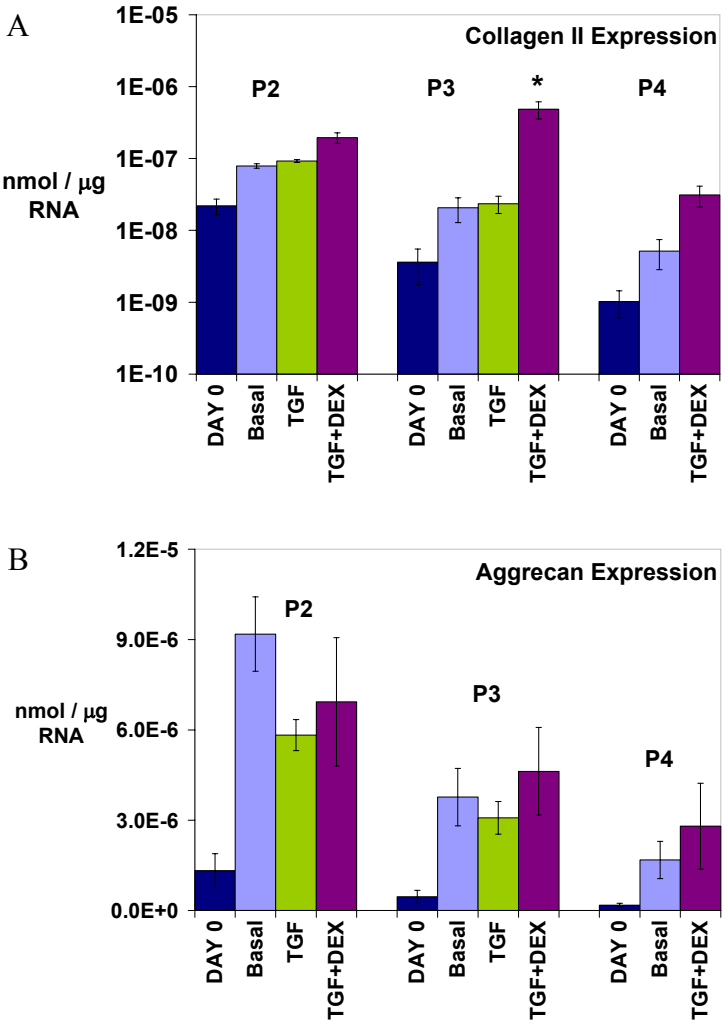

Figure 6.1: Gene expression results for BMSCs passaged 2, 3 and 4 times and seeded in 2% alginate.

* indicates $p<0.05$ vs.all. (mean±S.E.M., N=4-6)

sGAG per DNA

sGAG accumulation varied with both passage number and media supplementation. Overall, sGAG per DNA accumulation was highest in the samples treated with both TGF-β1 and dexamethasone (TGF+DEX) ($p \leq 0.044$) and lowest in the samples not supplemented with TGF-β1 (BASAL) ($p \leq 0.013$) (Figure 6.2). sGAG per DNA accumulation was dropped off at the 4th passage for the samples treated with both TGF-β1 and dexamethasone (TGF+DEX) with no significant changes in the samples not supplemented with TGF-β1 (BASAL) ($p \leq 0.003$). Due to the upregulation of both collagen II expression and sGAG/DNA accumulation, subsequent studies were performed using passage 3 cells.

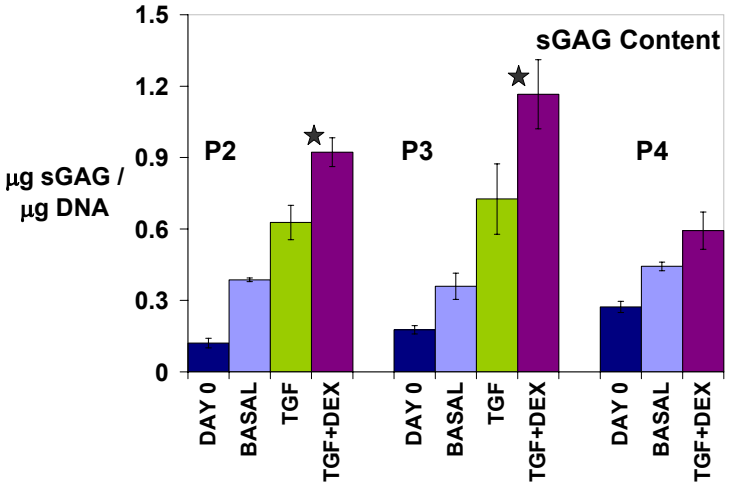

Figure 6.2: sGAG per DNA accumulation for BMSCs passaged 2, 3 and 4 times and seeded in 2% alginate.

★ indicates $p<0.05$ vs. passage's respective BASAL group. (mean±S.E.M., N=4-6)

6.3.2 Seeding Density Study

Gene Expression

Aggrecan expression was lowest in the samples not treated with TGF-β1 (BASAL) ($p \leq 0.001$) (Figure 6.3A). For the groups treated with both TGF-β1 and dexamethasone (TGF+DEX), expression was higher in the samples seeded at $25x10^6$ cells/mL (MID) compared to those seeded at $12.5x10^6$ cells/mL (LOW) ($p<0.001$).

Collagen II expression varied with both seeding density and media supplementation. Expression was highest in the samples treated with both TGF-β1 and dexamethasone (TGF+DEX) ($p \leq 0.010$) and lowest in the samples not supplemented with TGF-β1 (BASAL) ($p \leq 0.002$) (Figure 6.3B). Collagen II expression was lower in the samples seeded at $12x10^6$ cells/mL (LOW) compared to the samples seeded at $25x10^6$ cells/mL (MID) ($p=0.010$). For the groups treated with TGF-β1 only (TGF) and both TGF-β1 and dexamethasone (TGF+DEX), collagen II expression was highest in the samples seeded at $25x10^6$ cells/mL (MID) ($p \leq 0.001$) (Figure 6.3B).

Collagen I expression varied with media supplementation, but not significantly with seeding density (Figure 6.3C). Expression was highest in the samples treated with only TGF-β1 (TGF) ($p \leq 0.003$) and lowest in the samples not treated with TGF-β1 (BASAL) ($p \leq 0.001$).

Collagen X gene expression was the highest in the samples seeded at $12.5x10^6$ cells/mL (LOW) ($p \leq 0.004$) (Figure 6.3D).

Sox9 expression was lowest in the samples not treated with TGF-β1 (BASAL) ($p \leq 0.026$) (Figure 6.3E). Expression was higher in the samples treated with $50x10^6$ cells/mL (HIGH) compared to those seeded at $12.5x10^6$ cells/mL (LOW) ($p=0.002$). For

the samples treated with TGF-β1 only (TGF), Sox9 expression was the highest in the samples seeded at $50x10^6$ cells/mL (HIGH) ($p<0.006$) (Figure 6.3E). For the groups treated with both TGF-β1 and dexamethasone (TGF+DEX), Sox9 expression was the highest in the samples seeded at $50x10^6$ cells/mL (HIGH) ($p<0.021$) and the lowest in the samples seeded at $12.5x\ 10^6$ cells/mL (LOW) ($p<0.001$).

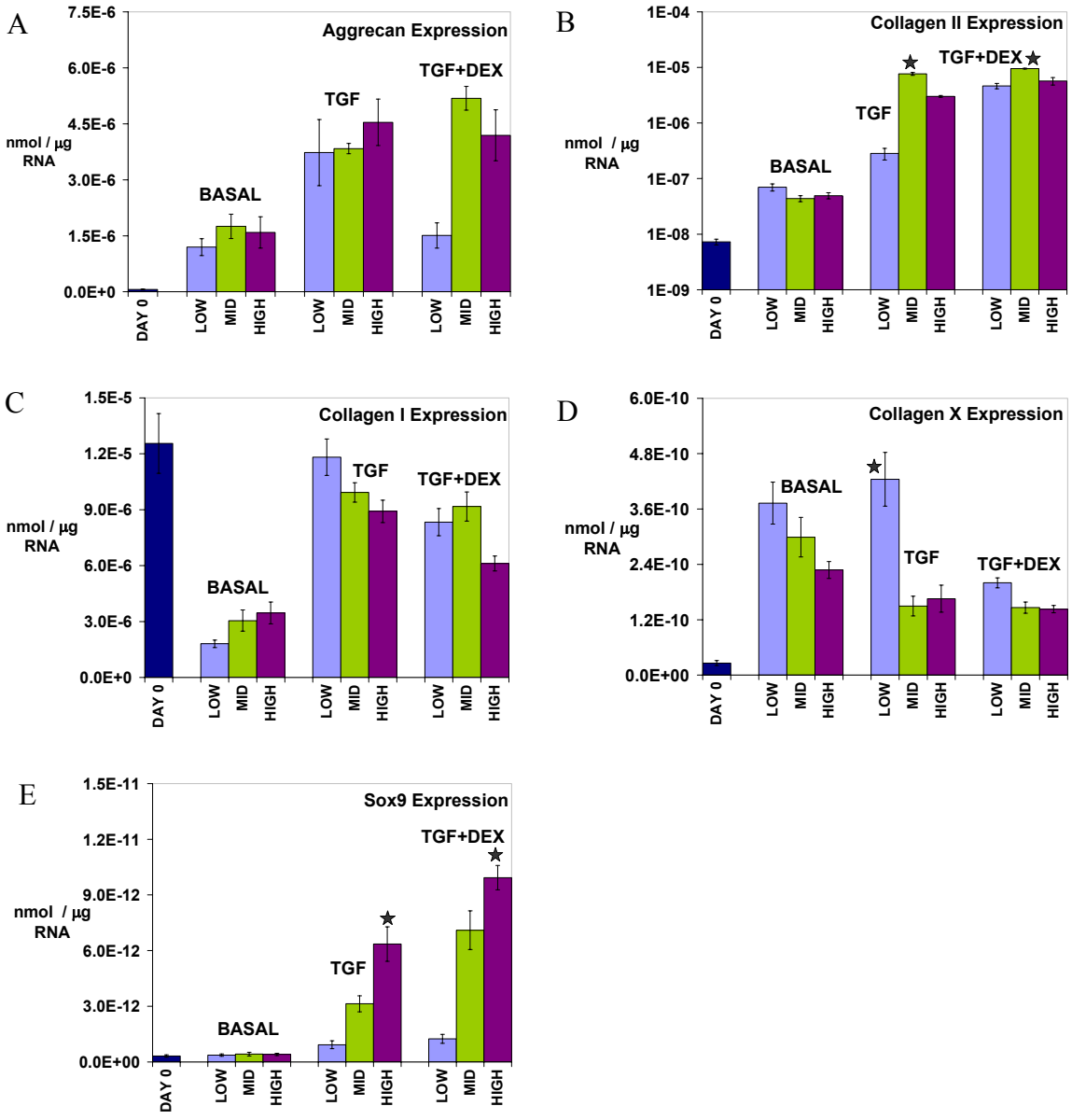

Figure 6.3: Gene expression for BMSCs seeded at three different cellular densities in 2% alginate (LOW=12.5x10^6, MID=25x10^6 and HIGH=50x10^6 cells/mL).

★ indicates $p<0.05$ vs. other densities within respective media condition.
(mean±S.E.M., N=4)

sGAG per DNA

Overall, samples treated with both TGF-β1 and dexamethasone (TGF+DEX) had the highest amount of sGAG per DNA ($p<0.001$) and samples not treated with TGF-β1 (BASAL) had the lowest amount ($p<0.001$) (Figure 6.4). Groups seeded at $25x10^6$ cells/mL (MID) had a greater amount of sGAG per DNA compared to those seeded at $12.5x10^6$ cells/mL (LOW) ($p=0.003$). Compared to the other groups treated with TGF-β1 only (TGF), samples seeded at $25x10^6$ cells/mL had a greater amount of sGAG per DNA accumulation compared to the other two seeding densities ($p\leq0.016$).Overall, the group seeded at $25x10^6$ cells/mL (MID) and supplemented with both TGF-β1 and dexamethasone (TGF+DEX) had the highest sGAG per DNA compared to all other groups ($p<0.001$). Due to the upregulation of sGAG/DNA accumulation, subsequent studies were performed using a seeding density of approximately $15x10^6$ cells/mL.

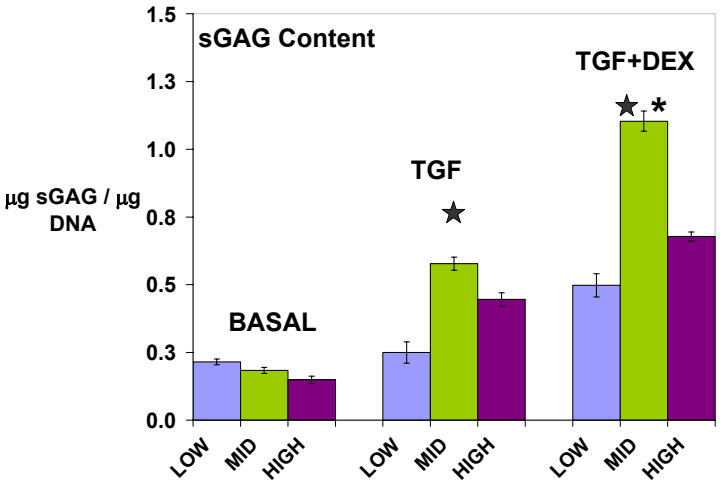

Figure 6.4: sGAG per DNA accumulated for BMSCs seeded at three different cellular densities in 2% alginate.

LOW=12.5x10^6, MID=25x10^6 and HIGH=50x10^6 cells/mL. ★ indicates $p<0.05$ vs. other densities within respective media condition. * indicates $p<0.05$ vs. all. (mean±S.E.M., N=5-7)

6.3.3 Alginate Time Course

Gene Expression

Only two media conditions were evaluated for the time course: no TGF-β1 added (BASAL) and both TGF-β1 and dexamethasone added (TGF+DEX). Overall, aggrecan and collagen II gene expressions were higher in the samples treated with both TGF-β1 and dexamethasone (TGF+DEX) ($p<0.042$) (Figure 6.5A,B). Aggrecan and Sox9 gene expressions were highest in the day 4 samples treated with both TGF-β1 and dexamethasone (TGF+DEX) ($p<0.001$ and $p<0.001$ respectively) (Figure 6.5A,C). Collagen II expression was the highest in the day 14 samples treated with both TGF-β1 and dexamethasone (TGF+DEX) ($p<0.001$) (Figure 6.5B).

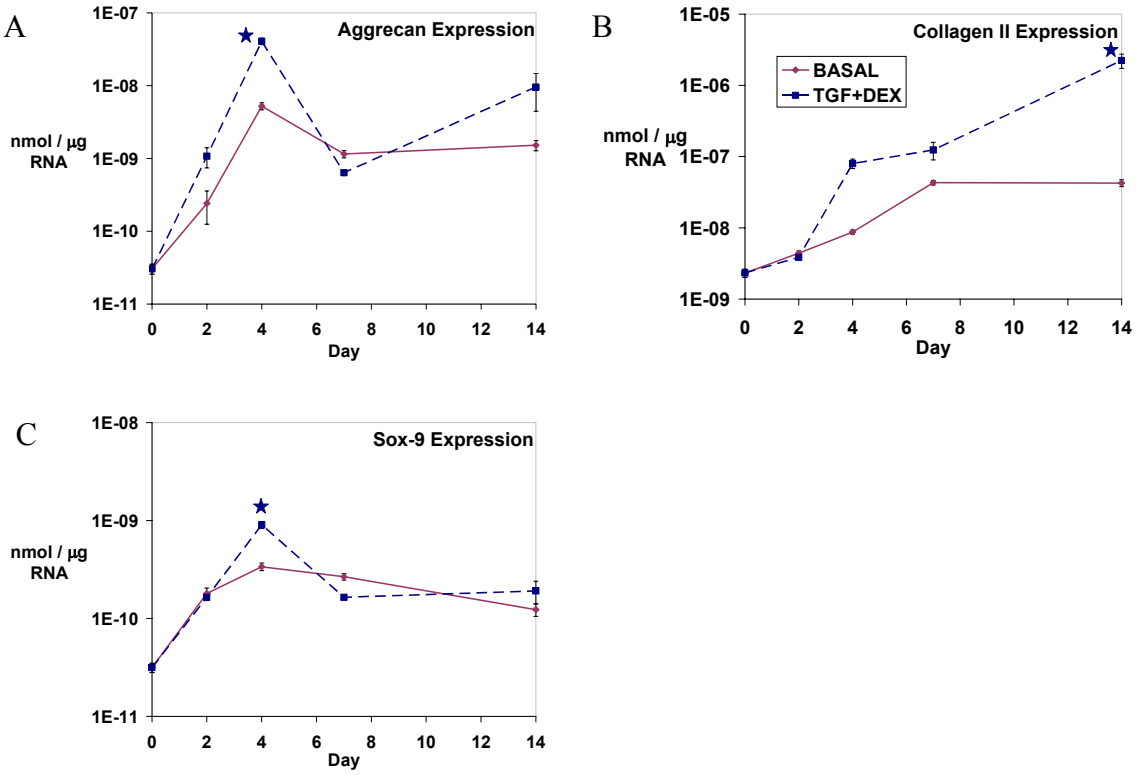

Figure 6.5: Gene expression time course for passage 3 BMSCs seeded $25x10^6$ cells/mL in 2% alginate.

★ indicates $p<0.05$ vs. all. (mean±S.E.M., N=4)

sGAG per DNA

Overall, sGAG per DNA values were higher in the samples treated with both TGF-β1 and dexamethasone (TGF+DEX) (p=0.003) (Figure 6.6). The day 14 sGAG per DNA levels in the samples treated with both TGF-β1 and dexamethasone (TGF+DEX) were higher than all other timepoints for both media conditions (p<0.001).

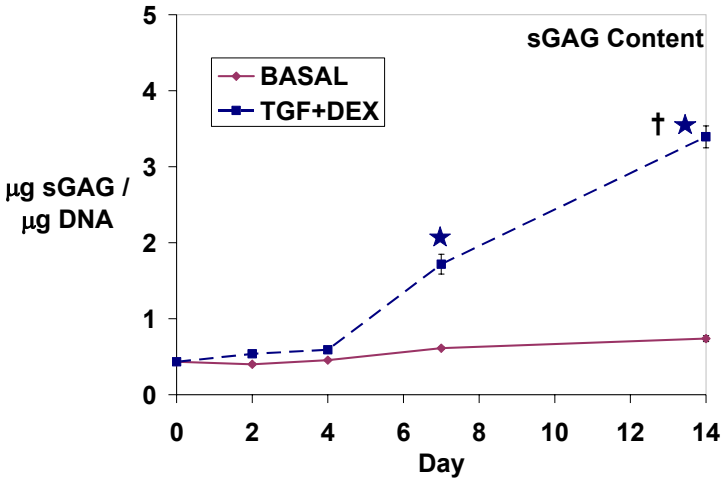

Figure 6.6: sGAG per DNA time course for passage 3 BMSCs seeded $25x10^6$ cells/mL in 2% alginate.

★ indicates p<0.05 vs. respective BASAL timepoint. † indicated p<0.05 vs. all. (mean±S.E.M., N=4)

6.3.4 Agarose Time Course

Viability

There were no overall differences in cellular viability between the gels imaged on day 8 and on day 16, therefore only images from day 8 samples are shown (Figure 6.7). Qualitatively, there was a dramatic difference in viability between the samples treated with basal media and those treated with TGF-β1, with a much higher proportion of dead cells found in the samples treated with basal media only. Samples treated with basal media had substantially more dead cells. There were no drastic differences between the two groups treated with TGF-β1. Viability was also less in the interior of the constructs compared to the edges for all groups.

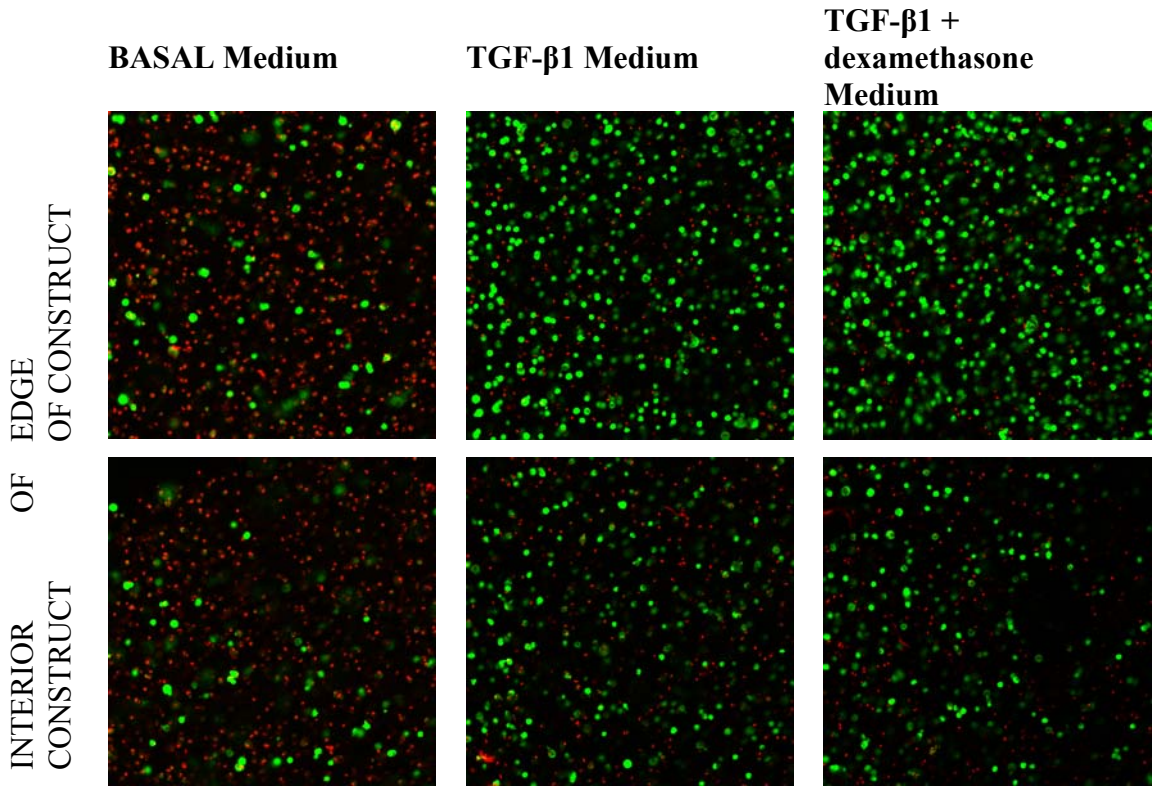

Figure 6.7: Viability staining for BMSCs in agarose cultured for 16 days. Green indicates live cells; red indicates dead cells. (N=4)

Gene Expression

Overall, aggrecan, collagen II and collagen I gene expressions were higher in the samples treated with TGF-β1+DEX and lower in BASAL samples ($p<0.001$) (Figure 6.8).

Aggrecan, collagen II and collagen I expressions were upregulated over day 0 levels at both timepoints for BASAL samples ($p<0.001$). There was an upregulation from day 8 to 16 for both collagen II and I expressions ($p<0.005$) (Figure 6.8B,C). There was a downregulation in expression from day 8 to 16 for aggrecan ($p=0.008$) (Figure 6.8A).

Aggrecan, collagen II and collagen I expressions were upregulated over day 0 levels at both timepoints for TGF samples ($p<0.001$). There was a upregulation from day 8 to 16 for collagen II expression ($p=0.004$) (Figure 6.8B,C). There was a downregulation in expression from day 8 to 16 for both aggrecan and collagen I expressions ($p=0.008$) (Figure 6.8B,C).

Aggrecan, collagen II and collagen I expressions were upregulated over day 0 levels at both timepoints for TGF+DEX samples ($p<0.005$). There was a upregulation from day 8 to 16 for both aggrecan and collagen II expressions ($p<0.008$) (Figure 6.8A,B). There was a downregulation in expression from day 8 to 16 for collagen I expression ($p<0.001$) (Figure 6.8B,C).

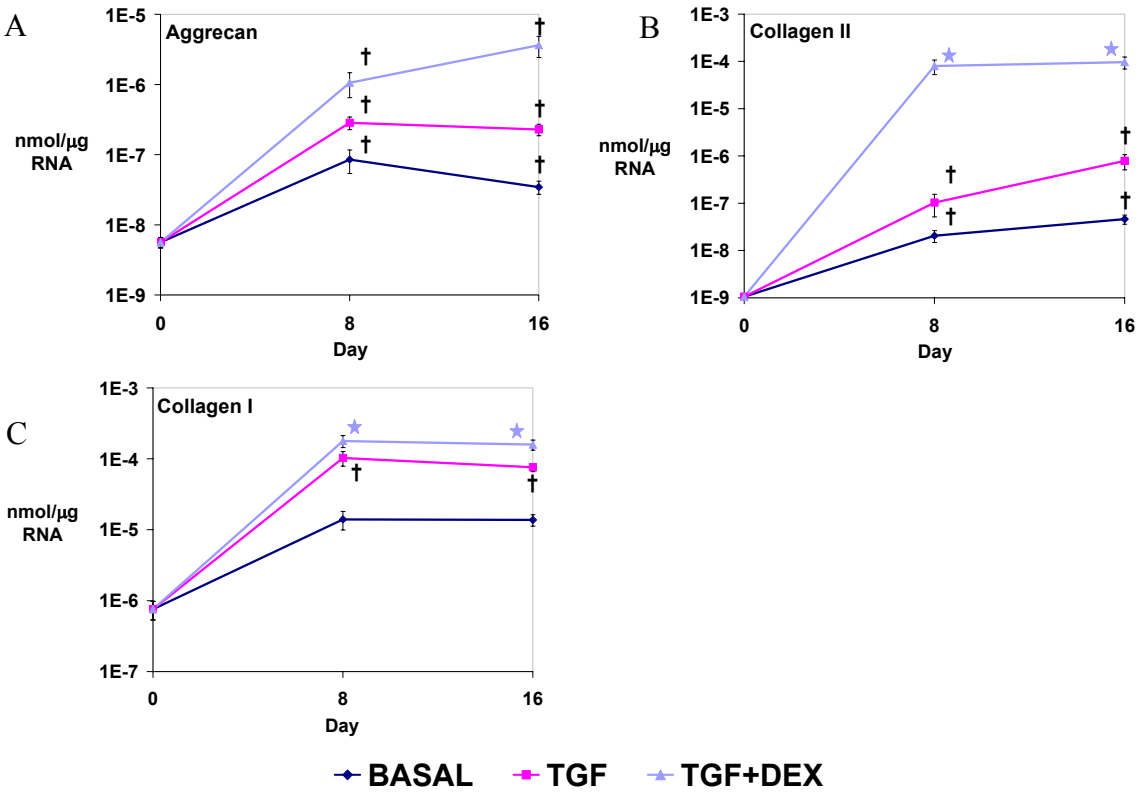

Figure 6.8: Gene expression for BMSCs in agarose cultured for 8 and 16 days.

★ indicates $P < 0.05$ vs. day 0 levels and † indicates $P < 0.05$ vs. all other in the respective media condition. (mean±S.E.M., N=6)

Matrix Synthesis Rates

Consistent with the gene expression results, both protein and sGAG synthesis rates increased with the addition of TGF-β1 and furthermore with the addition of dexamethasone ($p<0.001$) (Figure 6.9). Both protein and sGAG synthesis rates increased significantly with time for samples treated with TGF+DEX ($p\leq0.002$).

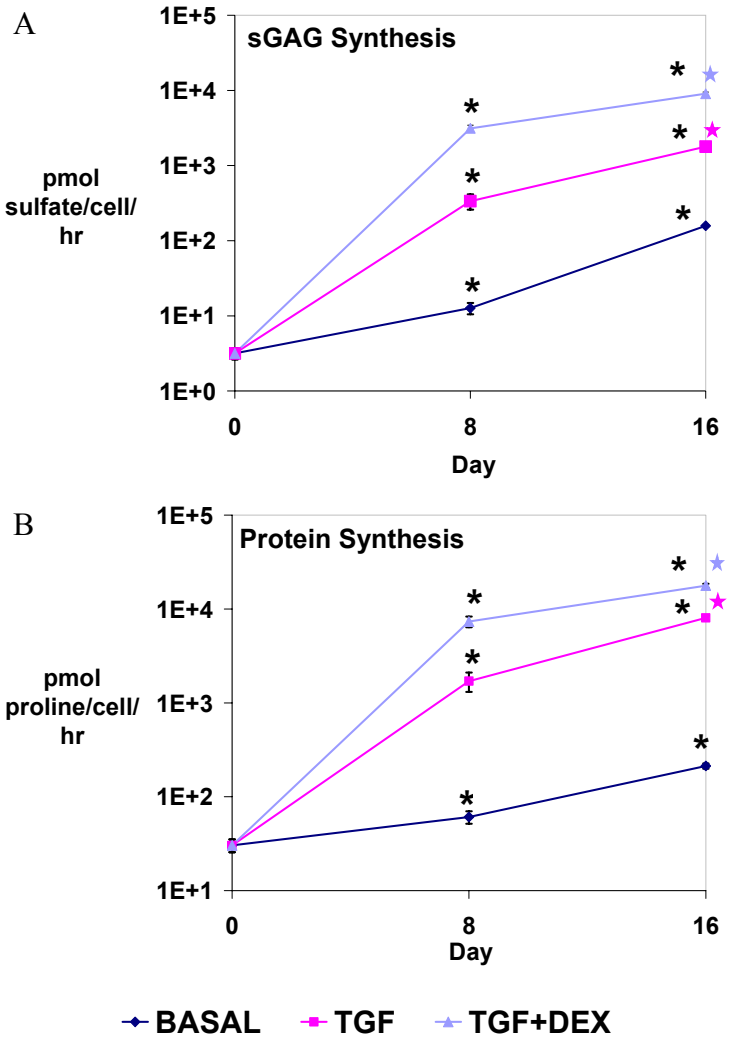

Figure 6.9: Matrix synthesis rates for BMSCs in agarose cultured for 8 and 16 days.

* indicates $P < 0.05$ vs. day 0 levels and ★ indicates $P < 0.05$ vs. respective group's day 8 levels synthesis. (mean±S.E.M., N=6)

sGAG

Consistent with both the gene expression and matrix synthesis rates, at both days 8 and 16, sGAG accumulation was the highest in the gels treated with TGF-β1+DEX and lowest in the gels treated with basal medium ($p<0.001$ for all) (Figure 6.10). There were no changes in sGAG content for the gels treated with basal media over time. sGAG content increased over time for the samples treated with TGF-β1 only ($p\leq0.0085$) and for the TGF-β1+DEX samples ($p<0.001$).

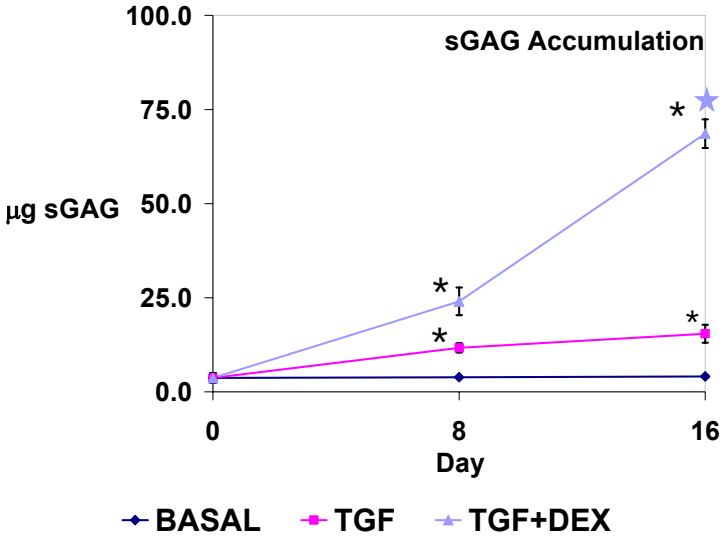

Figure 6.10: sGAG accumulation for BMSCs in agarose cultured for 8 and 16 days.

* indicates $P < 0.05$ vs. day 0 levels and ★ indicates $P < 0.05$ for day 16 vs. respective group's day 8 levels. (mean±S.E.M., N=6)

Histology

There were drastic differences in sGAG deposition between the three media groups and two timepoints (Figures 6.11, 6.12). Samples treated with basal media showed no observable sGAG staining after 16 days of culture. TGF-β1 samples had limited sGAG staining in the interiors of the scaffolds even after 16 days, with a marked increase in sGAG deposition between days 8 and 16 near the edges of the constructs. sGAG deposition was limited to the pericellular area of individual cells. Samples treated with TGF-β1 and dexamethasone showed no significant sGAG deposition in the interior of the construct after 8 days of culture, with more deposition seen near the edges (Figure 6.**Error! Reference source not found.**12). After 16 days of culture, samples treated with TGF-β1 and dexamethasone showed significantly more sGAG deposition both internally and in the edge regions compared to other timepoints and media conditions. There was diffuse staining with an increased intensity pericellularly.

Overall, the addition of TGF-β1 and furthermore dexamethasone increased both chondrogenic gene expression and sGAG per DNA accumulation compared to BASAL supplementation. There was a marked increased in sGAG accumulation from days 8 to 16 for both the samples treated with TGF-β1 only and both TGF-β1 and dexamethasone. Samples treated with both TGF-β1 and dexamethasone accumulated a substantially greater amount of sGAG after 16 days of culture.

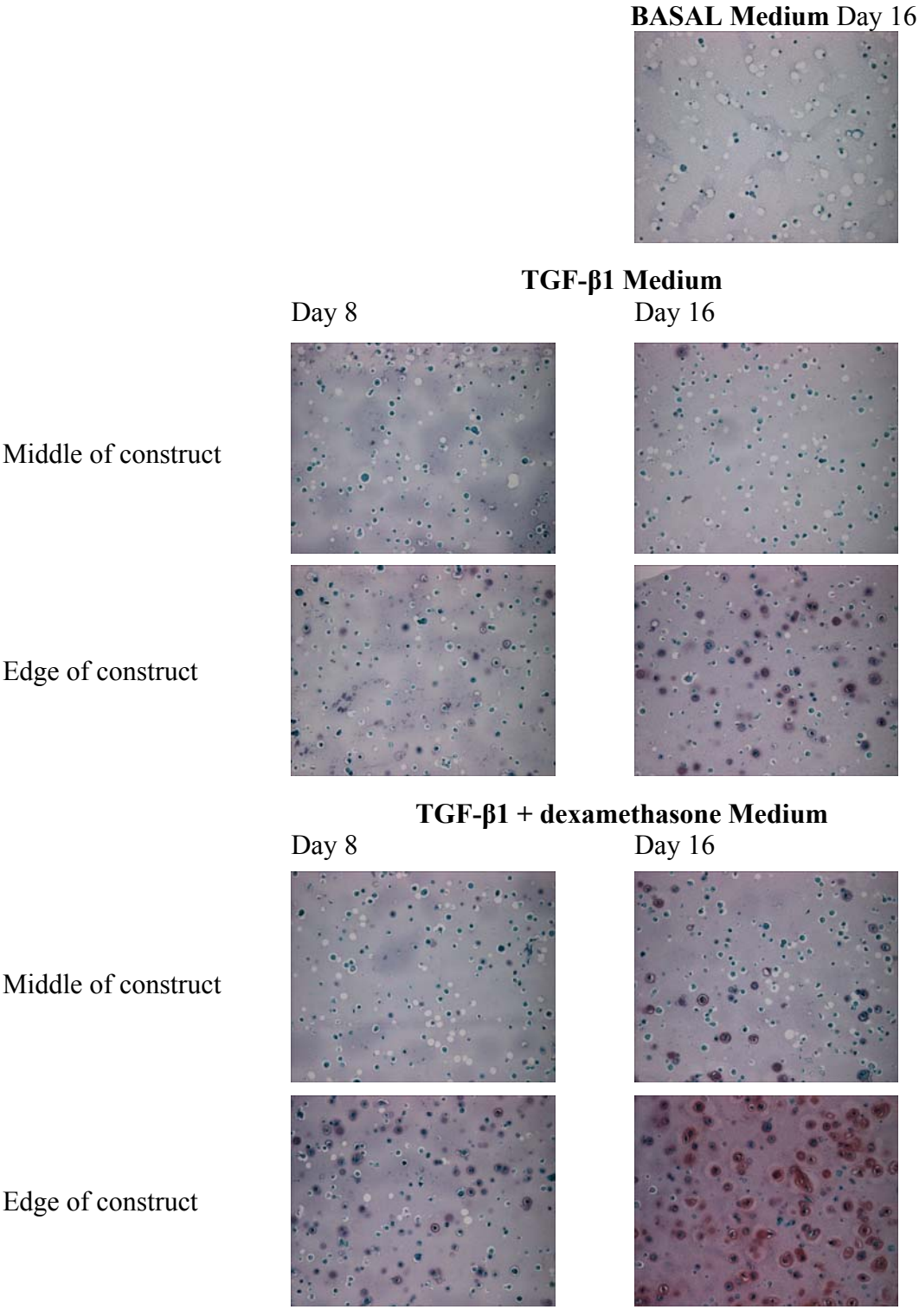

Figure 6.11: Safranin O staining for BMSCs in agarose cultured for 8 and 16 days (20X objective). (N=4)

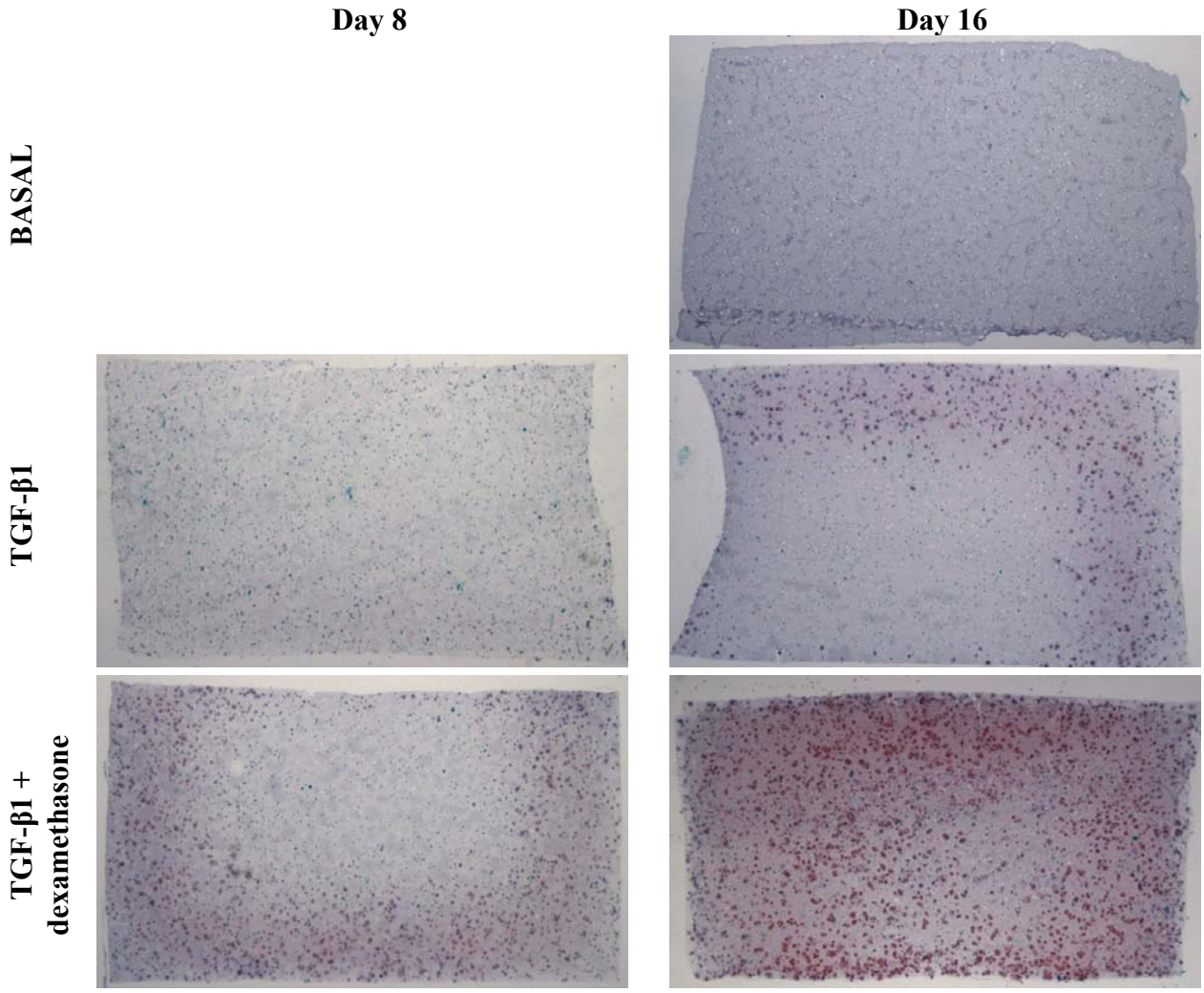

Figure 6.12: Representative Safranin O stained sections for BMSCs in agarose cultured for 8 and 16 days (10X objective).

6.4 DISCUSSION

It has been well established that the parameters of culturing progenitor cell populations affect the differentiation capacity of these cells[201,202]. For human MPCs, the constituents of the basal medium including the quality of FBS, glucose concentration, and stable glutamine, as well as culture conditions such as passaging and seeding densities affect the final outcome[201]. For this reason, it was important to characterize the bovine BMSC culture variables.

Of the critical genes of interest, Sox9, aggrecan and collagen II, results were not always self-consistent within a given perturbed parameter. Differences between parameters in aggrecan results, in particular, were often unclear and insignificant. In general, collagen II gene expression was consistent with the sGAG accumulation for the TGF-β1 groups for all parameters investigated. While gene expression provided useful information on the effects of varying culture parameters, sGAG accumulation data were generally the easiest to understand and interpret, therefore more emphasis was placed on that variable in putting various parameters into perspective.

While there were no discernable differences in either the BASAL or TGF-β1 groups between passage numbers, passage 3 had the most positive response in the TGF-β1+DEX group. Collagen II expression was significantly higher in the P3 TGF-β1+DEX group compared to all other groups. sGAG per DNA accumulation was significantly higher in the P3 TGF-β1+DEX group compared to the other P3 groups. While not significant, the P3 levels of sGAG accumulation were qualitatively higher than the other two passages for the P3 TGF-β1+DEX group.

While there were no discernable differences in either the BASAL group by seeding density, the MID density ($25x10^6$ cells/mL) had the most positive response in the TGF-β1and TGF-β1+DEX groups for both collagen II gene expression and sGAG per DNA accumulation. When compared within themselves, the gene expression results were not entirely consistent. There were little observable differences in aggrecan and collagen I expressions between seeding densities, or between the two media conditions containing TGF-β1. Collagen X expression, an indicator of chondrocyte hypertrophy, was highest in the LOW density ($12.5x10^6$ cells/mL) samples and Sox9 expression was highest in the HIGH density ($50x10^6$ cells/mL) samples.

For both the passaging and seeding density comparisons, the TGF-β1+DEX samples stimulated both chondrogenic gene expression and matrix synthesis, compared to the BASAL and TGF-β1 groups. In the chondrogenesis of the bovine BMSCs, the addition of dexamethasone had an overwhelmingly positive effect on the parameters examined, including upregulating sGAG accumulation, aggrecan and collagen II expressions, while downregulating collagen X expression. The response to the addition of dexamethasone in different culture systems is varied. Awad *et al.* found that the addition of dexamethasone appeared to amplify protein synthesis but had suppressive effects on sGAG synthesis and accumulation on human adipose-derived stromal cells supplemented with TGF-β1[203]. Dexamethasone has been found to suppress proliferation and chondrogenesis in the chondrogenic ATDC5 cells[204,205]. Conversely, scrapie-responsive protein 1 precursor (SCRG-1) expression has been found to be dexamethasone-dependent during chondrogenesis. SCRG1 in human MPCs suppressed their proliferation, and stimulated chondrogenesis in C3H10T1/2 cells, confirmed by

reduced collagen type I and elevated collagen type IIB expression. While the mechanism (or mechanisms) though which dexamethasone works in the culture system presented in this dissertation is not known, the addition of dexamethasone to TGF-β1 supplementation had a positive effect on the gene expressions and matrix syntheses outcomes measured.

The overall level of chondrogenesis was higher in the agarose hydrogel culture compared to the alginate hydrogel culture for the samples treated with TGF-β1+DEX. After 2 weeks of culture, collagen II gene expression was 3 orders of magnitude higher in the agarose samples treated with TGF-β1 and dexamethasone, compared to the alginate samples treated with both TGF-β1 and dexamethasome, with no differences between the untreated samples for either scaffold. There was also a 2-fold difference in sGAG per DNA accumulation between agarose and alginate after two weeks, approximately 3.4 μg sGAG per μg DNA in alginate at day 14 compared to 8.5 μg sGAG per μg DNA at day 16 (data not shown). In each system, the cellular content was similar both initially and after two weeks. Differences in the chondrogenic response of BMSCs between the scaffold types may be due to differences in the material properties including charge and diffusional restrictions. While agarose is relatively inert, alginate carries a negative charge. Also, as the study presented in chapter 3 demonstrated, chondrocytes produce a matrix more similar to articular cartilage in agarose compared to alginate. In addition to preserving the phenotype of BACs, agarose may also support chondrogenesis in BMSCs preferentially than in alginate.

Numerous studies have investigated chondrogenesis in a variety of animal models and culture systems using different passages, cell densities, and media conditions. The present study demonstrates that these factors can significantly impact BMSC

differentiation and should be considered when developing cell-based therapies for cartilage repair. Passage 3 cells were chosen to be utilized for future studies due to the increase in collagen II expression and sGAG accumulation in the samples treated with TGF+DEX. Practical concerns, such as expanding the BMSC population adequately for 3D culture also made passage 3 an attractive option. The mid-range seeding density of $25x10^6$ cells/mL was chosen to be utilized for future studies due to the increased collagen II expression and sGAG accumulation in the samples treated with TGF and TGF+DEX. Due to the increase in chondrogenic markers in agarose compared to alginate, agarose was chosen for downstream studies. Another potential benefit in using agarose as a 3D hydrogel is that it is relatively easy to get a series of uniform samples with a set geometry. Casting of alginate makes it somewhat more labor intensive to achieve similar results in uniformity. For the purpose of this dissertation, further studies utilized passage 3 BMSCs seeded at approximately $20x10^6$ cells/mL of 3% agarose.

CHAPTER 7 INTERACTION BETWEEN THE TGF-β SIGNALING PATHWAY AND DYNAMIC COMPRESSIVE LOADING IN THE CHONDROGENESIS OF BONE MARROW STROMAL CELLS

7.1 INTRODUCTION

Both biochemical and biomechanical stimulation have been shown to influence the growth and differentiation of BMSCs. Much effort investigating the effect of growth factor and cytokine supplementation on the chondrogenesis of BMSCs has focused around members of the transforming growth factor β (TGF-β) superfamily (TGF-βs, BMPs, activins) which have been found to play roles in chondrocyte growth, differentiation and commitment[66]. TGF-β family members have also been shown to participate in the control of proliferation, extracellular matrix synthesis, migration and apoptosis in many different cell types, including chondrocytes and chondrogenic progenitor cells[19,66,77,206]. Multiple members of the TGF-β family, including TGF-β1, have been shown to induce *in vitro* chondrogenesis of BMSCs[68,207].

The transforming growth factor β (TGFβ) superfamily is involved in the regulation of multiple cellular processes, including cell proliferation, differentiation and apoptosis[208]. TGF-β transmits its signal from the cell surface via a transmembrane serine/threonine kinase receptor complex[209,210]. Upon ligand binding, the type II receptor subunit engages and transphosphorylates a type I receptor subunit (TβRI), which in turn phosphorylates the receptor-activated Smad proteins (R-Smads) Smad2 and Smad3 (Figure 1). A protein complex with Smad4 is formed with the activated R-Smads and translocated into the nucleus where they interact with additional transcription factors,

binding to the promoters of responsive genes and regulate their expression by cooperating with other activators or repressors[72]. In addition to the Smad pathway, TGF-β has been shown to activate other signaling pathways including p38 MAPK[73] and protein kinase C (PKC)[74]. TGF-β signaling has been demonstrated through the p38 MAPK pathway through activation of mitogen-activated protein kinase 1 (MEK1) and subsequent ERK/ELK signaling[75,211]. It has also been shown that G-protein-dependent activation of PKC results from TGF-β stimulation of growth plate chondrocytes[74]. It has been suggested that TGF-β responsiveness requires the activation of the R-Smad2/4 complexes as well as other signaling pathways.

Mechanical stimulation has been shown to be important in the development of certain tissues and may influence differentiation of BMSCs[78]. It has been suggested that the combination of chondrogenic media and dynamic compressive loading may enhance chondrogenesis of BMSCs over the addition of exogenous factors alone[79]. Dynamic compressive loading has been shown to increase the expression of chondrogenic markers, aggrecan and collagen II, in rabbit BMSCs in agarose culture[79]. Dynamic compressive loading has also been shown to induce chondrogenesis in chick-bud mesenchymal cells[212,213]. Studies on human BMSCs cultured under conditions promoting chondrogenesis found that the application of cyclic hydrostatic pressure for multiple days increased proteoglycan and collagen contents after 14 days in culture[82]. Mechanical loading has been found to be critical in the differentiation of other tissue types, including bone. BMSCs cultured on partially demineralized bone subjected to four-point bending loading experienced elevated osteogenic differentiation, compared to unloaded controls[83]. Combined with the substantial knowledge base that mechanical stimulation can affect the

maintenance of cartilage, these studies suggest that controlled mechanical stimulation may direct differentiation and subsequent matrix assembly in engineered cartilage derived from mesenchymal progenitor cells.

The overall objective of the studies presented in this chapter was to investigate the mechanotransduction of BMSCs through the interactions between TGF-β1, dexamethasone and dynamic compressive loading. Specifically, the effects of dynamic and static compressive loading on BMSC gene expression, matrix synthesis and TGF-β signaling though Smad effector molecules were examined. Investigation of the influence of transforming growth factor β1 (TGF-β1) signaling on the response of chondrocytes and BMSCs to dynamic compressive loading may provide clues to the mechanisms involved in chondrocyte differentiation and define other potential targets to regulate this process. The mechanisms through which mechanotransduction occurs in chondrocytes and chondroprogenitor cells remain largely elusive. This work addresses a potential mechanism for mechanotransduction in these cells.

7.2 Materials and Methods

7.2.1 Cell Isolation

BMSCs were isolated from both the femoral and tibial diaphyses of 2-4 week old calves within 24 hours of slaughter. After removal of all fascia and muscle from the bones, the bones were cut at the mid-diaphysis with a sterile bone saw. Marrow was removed from the medullary canal and transferred to a 50ml conical with sterile PBS plus 1% antibiotic/antimycotic (A/A: 100U/mL penicillin, 100ug/mL streptomycin, 250

ng/mL Amphotericin). Marrow was sequentially passed through large bore (25mL) and small bore (5mL) pipets to disrupt large pieces. Marrow was then sequentially passed through 16- and 18-gauge needles. Marrow suspension was centrifuged at 300 x g for 15 minutes. The separated fatty layer was removed and discarded. The cell pellet was resuspended in PBS, passed through a 20-gauge needle and filtered through a 100μm nylon filter. Mononuclear cells were counted with a Vi-Cell Cell Viability Analyzer using the Trypan Blue exclusion method.

Cells were plated in T-flasks at 5 x 10^3 mononuclear cells per cm^2 in passaging medium (consisting of low glucose DMEM, 10% FBS, 1% antibiotic/antimycotic, ± 1ng/mLbFGF). Nonadherent cells were removed during the first media change three days later. Cells were cultured until confluent (~ 2 weeks, P1), detached with 0.05% trypsin/1mM EDTA, and replated at 5 x 10^3 cells per cm^2. Cells were again cultured until confluence and seeded into 3% agarose gels. Agarose gels were assembled by autoclaving 6% LMP agarose in 1X Ca^{2+}, Mg^{2+} -free PBS and then cooling the solution to 42°C. An equal volume of cells suspended at 40 x10^6 cells/mL in 1X Ca^{2+}, Mg^{2+} -free PBS was combined with the agarose for a final concentration of 20 x10^6 cells/mL in 3% agarose. The agarose was cast in 3mm sheets between two electrophoresis plates and cooled until polymerized (approximately 10 minutes). Biopsy punches were used to extract gels 4mm in diameter.

Gels were cultured in basal medium consisting of high glucose DMEM plus antibiotic/antimycotic, non-essential amino acids, 1% ITS+, 50μg/mL ascorbate and 0.4mM proline (BASAL), basal medium plus 10ng/mL TGF-β1 (TGF-β1), or basal medium plus 10ng/mL TGF-β1 and 100nM dexamethasone (TGF-β1+DEX). In a

preliminary study, dexamethasone alone did not significantly increase sGAG accumulation over 8 days relative to BASAL media (data not shown). As the focus of these studies was on the interactions between TGF-β and compression, the non-chondrogenic dexamethasone-alone condition was excluded from further studies. Media were changed every two days.

7.2.2 Experimental Design

Short Term Loading

Dynamic compression was applied using a custom designed mechanical loading system (see appendix D). Samples were cultured in either BASAL, TGF-β1 or TGF-β1+DEX media for either 8 or 16 days before the application of loading. Mechanical stimulation groups included static compression (10%), 1Hz dynamic compression (10% ± 3%) and free swelling (FS). Samples were mechanically stimulated for 3 hours to evaluate gene expression and 20 hours to evaluate matrix synthesis rates. For immunohistochemistry and Western blotting, cells were mechanical stimulated for 1 hour. See appendix E for the Western blotting protocol.

Long Term Loading

Dynamic compression was applied using a custom designed mechanical loading system (see appendix D). Samples were cultured in either BASAL, TGF-β1 or TGF-β1+DEX media for either 8 days before the application of loading. Samples were mechanically stimulated for 12 hours each day for 8 days. In the 12 hours of the day, constructs were maintained at the 10% static offset. Mechanical stimulation groups included static

compression (10%), 1Hz dynamic compression (10% ± 3%) and free swelling (FS). Samples were either analyzed using immunohistochemistry for collagen I and collagen II localization (see appendix D) or general biochemistry methods.

7.2.3 Analytical Techniques

Quantitative RT-PCR

Agarose gels were immediately dissociated in Qiagen Lysis Buffer with 1% beta-mercaptoethanol. The RNeasy Total RNA Kit (Qiagen, Chatsworth, CA) was then used according to manufacturer's protocol to purify RNA from the samples. The yield of the purified isolate was read at 260 nm and 280 nm on a UV-1601 Spectrophotometer (Shimadzu, Columbia, MD).

1μg of total RNA was transcribed to cDNA using the Promega RT System (Promega, Madison, WI) and manufacturer's protocol. The SYBR Green PCR Master Mix (Applied Biosystems, Foster City, CA) was mixed with primers and cDNA for real time detection of amplification. Real time, quantitative RT-PCR was performed with an ABI PRISM 7700 Sequence Detector System (PE Biosystems, Foster City, CA).

7.3 RESULTS

7.3.1 Day 8 Short Term Loading

Gene Expression

The effects of dynamic compression varied greatly between media conditions and genes for the samples cultured for 8 days prior to loading (Figure 7.1). Dynamic

compression downregulated aggrecan gene expression for the samples treated with TGF-β1 (5-fold, p=0.0053) and TGF-β1 and dexamethasone (3-fold, p=0.035), with no effect on the BASAL samples (Figure 7.1A). Dynamic compression upregulated collagen II expression in BASAL samples (3-fold, p=0.0006) and samples treated with TGF-β1 and dexamethasone (2-fold, p=0.021), with no effect on TGF-β1 samples (Figure 7.1B). Dynamic compression upregulated collagen I expression for BASAL samples (3-fold, p=0.0012), with no effect on the samples treated with TGF-β1 or TGF-β1 and dexamethasone (Figure 7.1C).

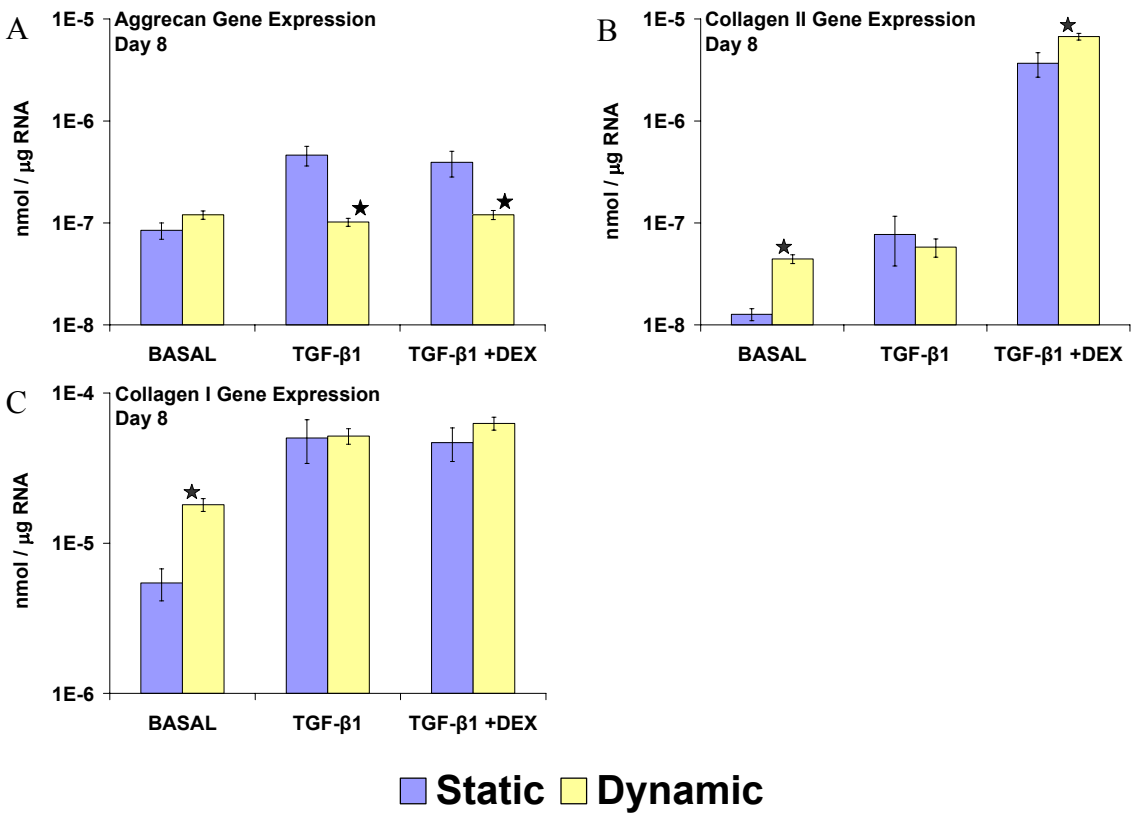

Figure 7.1: Gene expression for BMSCs seeded in agarose and subjected to 3 hours of mechanical stimulation on day 8.

★ indicates $P < 0.05$ vs. respective media static group. (mean±S.E.M., N=6)

Matrix Synthesis

There were no differences in the pairwise comparisons for any of the media conditions for either protein or sGAG synthesis rates for the samples cultured for 8 days prior to loading (Figure 7.2). Overall, basal samples had the lowest sGAG synthesis rates ($p<0.001$) and samples treated with TGF-β1 and dexamethasone had the highest ($p<0.001$). Basal samples had the lowest protein synthesis rates ($p<0.001$).

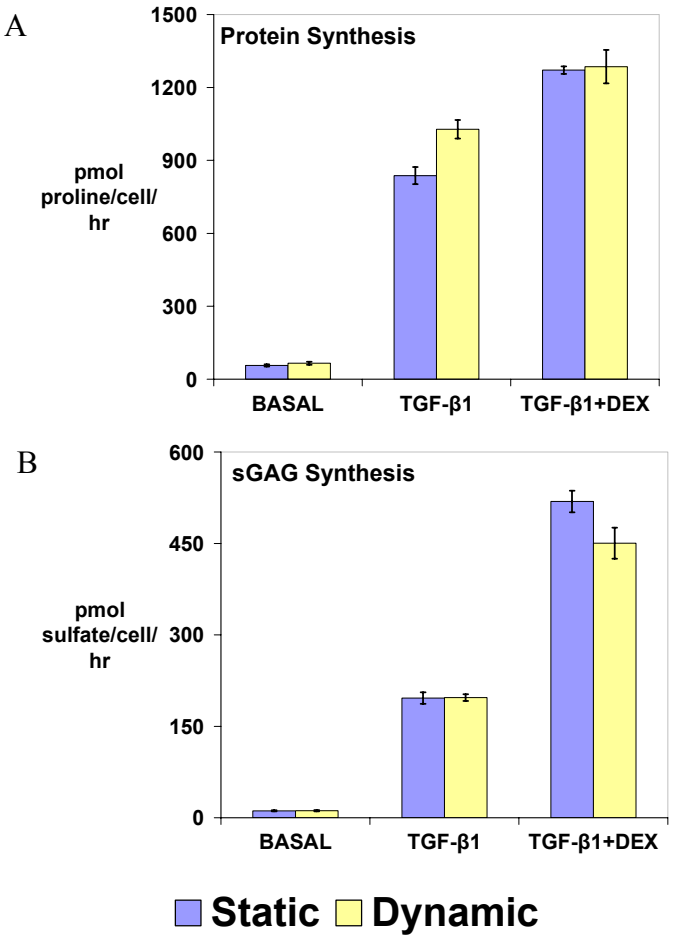

Figure 7.2: Matrix synthesis rates for BMSCs seeded in agarose and subjected to 20 hours of mechanical stimulation on day 8.

No significant effect of dynamic compression was found for any group. (mean±S.E.M., N=6)

7.3.2 Day 16 Short Term Loading

Gene Expression

The effects of dynamic compression varied greatly between media conditions and genes for the samples cultured for 16 days prior to loading but were strikingly different from effects of loading on day 8 (Figure 7.3). Dynamic compression upregulated aggrecan gene expression for both basal samples (2-fold, $p=0.017$) and samples treated with TGF-β1 and dexamethasone (3-fold, $p<0.001$), with no effect on the TGF-β1 samples (Figure 7.3A). Dynamic compression upregulated collagen II expression for samples treated with TGF-β1 (5-fold, $p=0.002$) or TGF-β1 and dexamethasone (60-fold, $p=0.000$), with no effect on the basal samples (Figure 7.3B). Dynamic compression upregulated collagen I expression for samples treated with TGF-β1 (30-fold, $p<0.001$) or TGF-β1 and dexamethasone (100-fold, $p<0.001$), with no effect on the basal samples (Figure 7.3C).

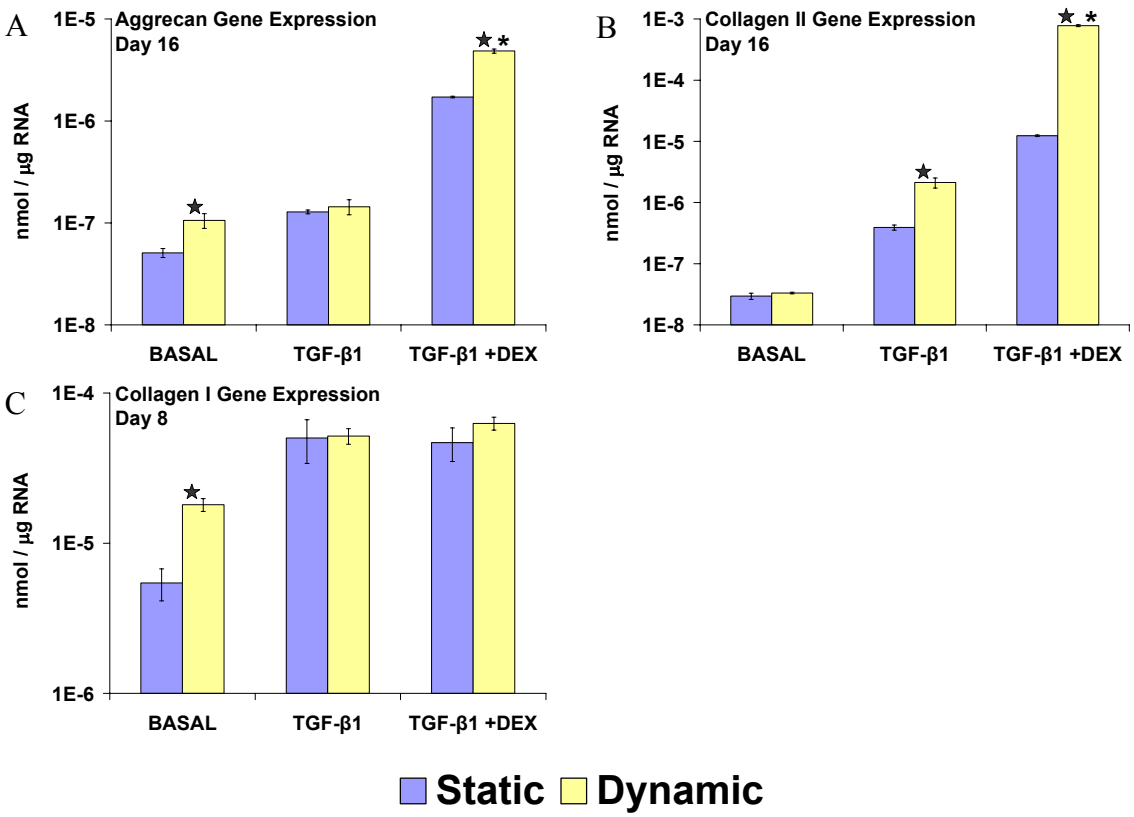

Figure 7.3: Day 16 gene expression for BMSCs seeded in agarose and subjected to 3 hours of mechanical stimulation.

★ indicates $P < 0.05$ vs. respective media static group. * $P < 0.05$ vs. all other groups. (mean±S.E.M., N=6)

Matrix Synthesis

Matrix synthesis rates were fairly consistent with the gene expression results for 16 days prior to loading. Overall, both protein and sGAG synthesis rates were lowest in the basal samples ($p<0.001$) and highest in the samples treated with TGF-β1 and dexamethasone ($p<0.001$) (Figure 7.4). Dynamic compression had no significant effect on either protein or sGAG synthesis rates for basal samples. Dynamic compression stimulated protein synthesis rates for TGF-β1 samples (2-fold, $p<0.001$), but not sGAG synthesis rates. Dynamic compression stimulated both protein (2-fold, $p<0.001$) and proteoglycan (2-fold, $p<0.001$) synthesis rates for samples treated with TGF-β1 and dexamethasone.

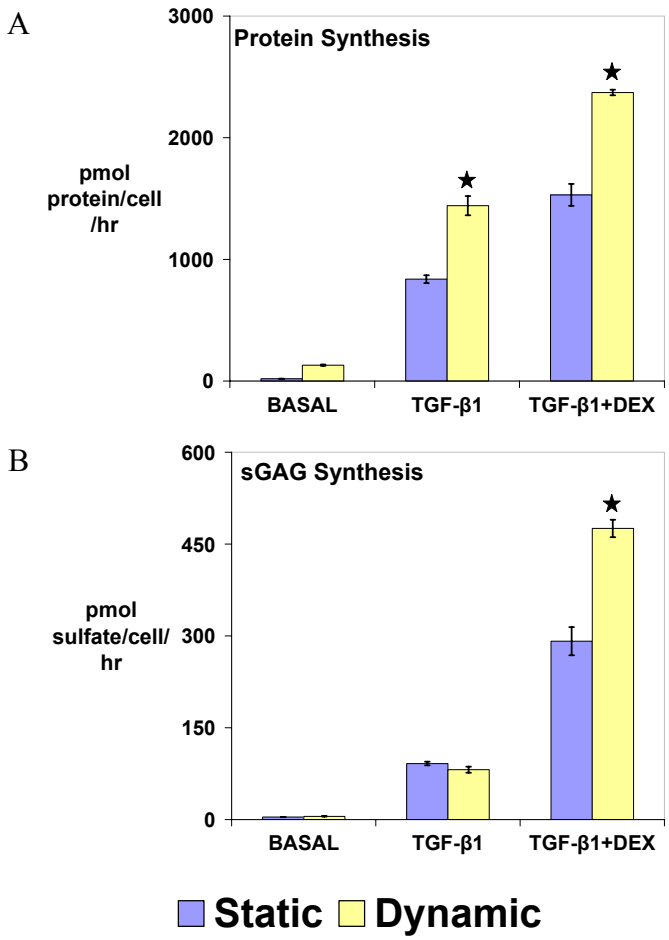

Figure 7.4: Day 16 matrix synthesis rates for BMSCs seeded in agarose and subjected to 20 hours of mechanical stimulation.

★ indicates $P < 0.05$ vs. respective media static group. (mean±S.E.M., N=6)

Total Smad 2/3

The results of IHC indicated qualitative differences not elucidated via Western blotting. In all media and mechanical stimulation conditions, there was diffuse Smad2/3 cytoplasmic staining for total Smad2/3 throughout the cells, with no noticeable differences in the level of staining or the numbers of cells stained (Figure 7.6, 7.6). In constructs treated with BASAL media, nuclear localization of Smad2/3 was low, with no qualitative differences between the different modes of mechanical stimulation.

In the constructs treated with TGF-β1, there was a marked increase in Smad2/3 nuclear localization compared to BASAL conditions, with both a greater number of cells displaying localization and more intense staining. There was also a qualitative increase in the number of cells with pronounced Smad2/3 nuclear localization in the dynamically compressed samples compared to the statically compressed samples. In constructs treated with TGF-β1+dexamethasone, there were more cells with pronounced nuclear localization of Smad2/3 than in either the BASAL or TGF-β1 samples, regardless of mechanical stimulation. A greater number of cells in the samples dynamically stimulated seemed to have pronounced nuclear localization than in either the statically compressed or unloaded samples. While preliminary, these observations suggest that dynamic compression increases the percentage of total Smad2/3 localized to the nucleus.

Between media conditions, there were no significant differences in the levels of Smad2/3 detected by Western blotting (Figure 7.7). In a pair-wise comparison, dynamic compression increased Smad2/3 protein levels over static compression for the samples treated with TGF-β1+dexamethasone ($p<0.001$). There were no differences detected in either the BASAL or TGF-β1 groups with dynamic compression.

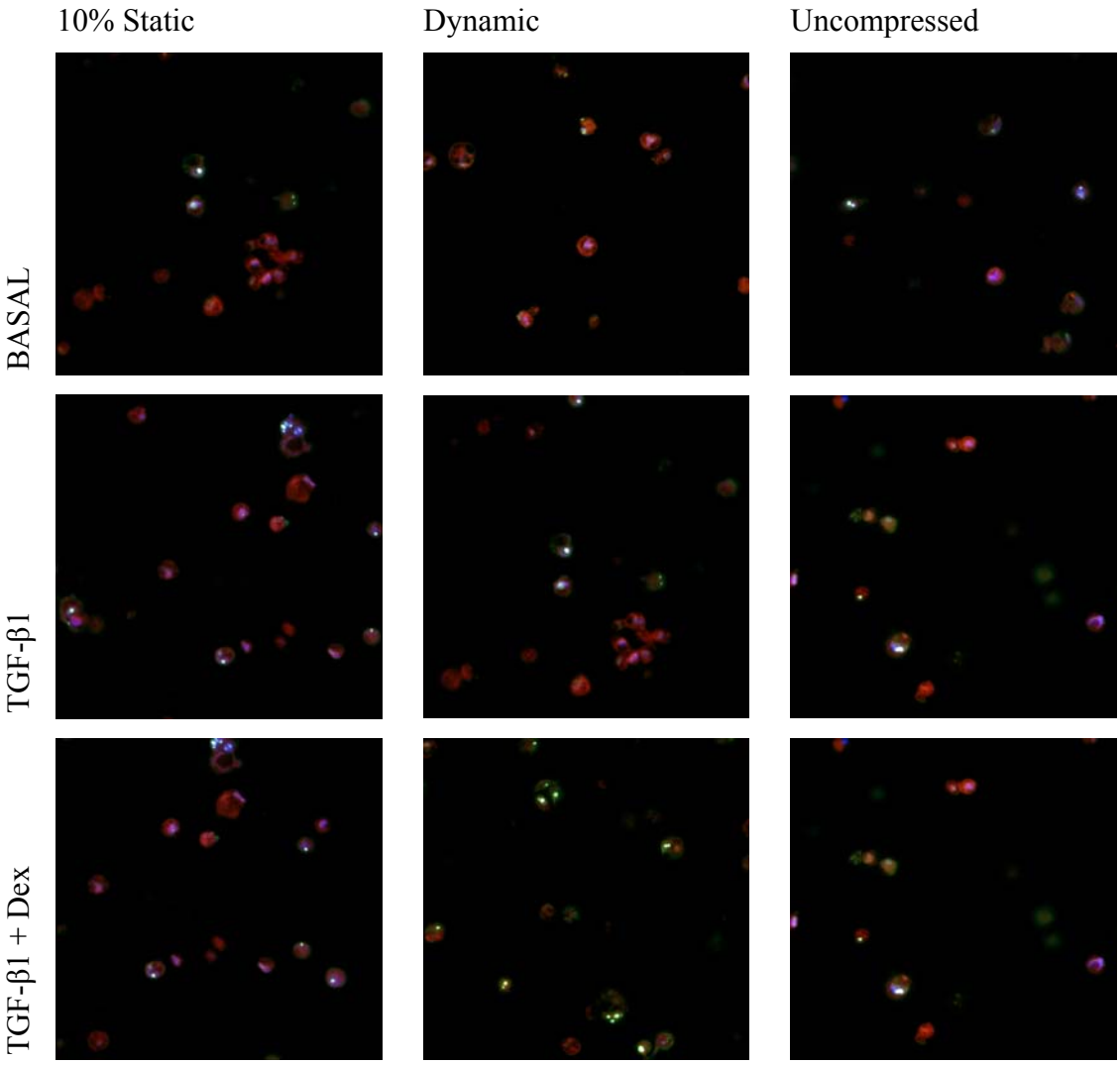

Figure 7.5: Total Smad2/3 immunohistochemical staining after 1 hour of mechanical stimulation.

Constructs were cultured for 16 days prior to mechanical stimulation. Representative sections shown. Images taken at 20X magnification via fluorescence microscopy. (n=4)

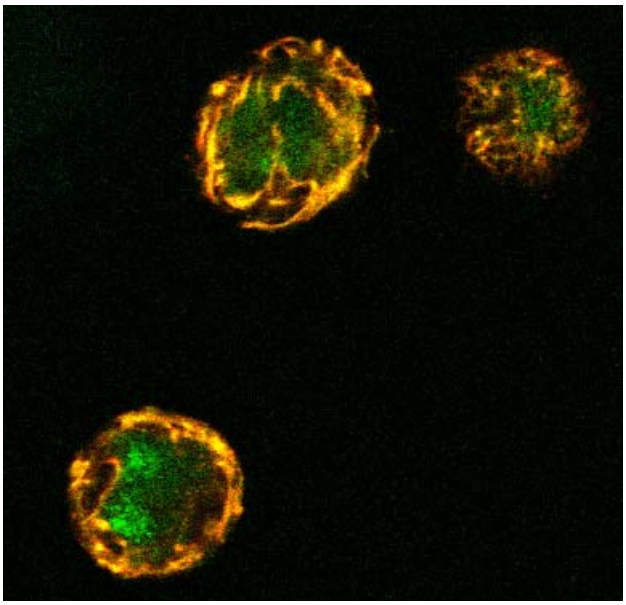

Figure 7.6: Total Smad 2/3 (Smad 2/3) immunohistochemical staining.

Smad 2/3 localization was both cytoplasmic as well as nuclear. Constructs were cultured for 16 days prior to mechanical stimulation. Unloaded construct stimulated with TGF-β1 shown and representative of positive pSmad 2/3 staining. Image taken at 100X magnification via confocal microscopy. (n=4)

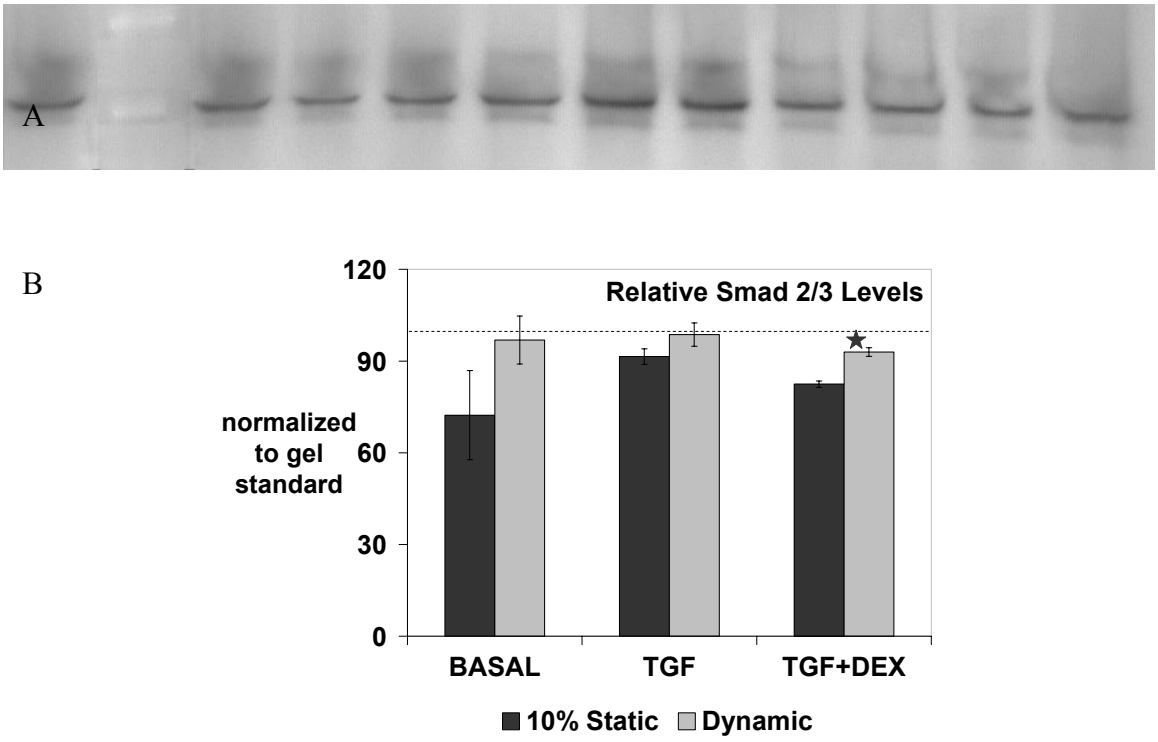

Figure 7.7: Smad 2/3 levels.

Smad 2/3 levels were measured by Western blotting and normalized by gel background and a standard on each gel. Constructs were cultured for 16 days prior to mechanical stimulation. (A) Representative blot for the TGF samples with the normalizing standard in the lane 1 (discussed in appendix E), static samples in lanes 3-7, and dynamic samples in lanes 8-12. (B) Dashed line indicates 100% of gel standard. ★ indicates $P < 0.05$ vs. respective static group for relative Smad 2/3 levels. (mean±S.E.M, n=5)

Phospho-Smad2/3

In all media and mechanical stimulation conditions, diffuse Phospho-Smad2/3 (pSmad2/3) cytoplasmic staining throughout the cells was comparable to background staining using fluorescent microscopy (Figure 7.8). When imaged using confocal microscopy, all pSmad2/3 localization was nuclear with no diffuse cytoplasmic staining apparent (Figure 7.9**Error! Reference source not found.**).

In the BASAL samples, there were qualitatively no differences in the number of cells with pSmad2/3 nuclear localization or the level of localization between samples dynamically compressed or unloaded. There were qualitatively fewer cells with pSmad2/3 nuclear localization in the statically compressed samples compared to those either dynamically compressed or unloaded.

The constructs treated with TGF-β1, there was a marked increase in pSmad2/3 nuclear localization compared to BASAL conditions, with both a greater number of cells displaying localization and a brighter level of staining. There was also a qualitative increase in the number of cells with pronounced pSmad2/3 nuclear localization in the dynamically compressed samples compared to the statically compressed samples.

In constructs treated with TGF-β1+dexamethasone, there were no observable differences in either the number of cells with nuclear localization or the intensity of staining of pSmad 2/3 compared to the TGF-β1 samples, regardless of mechanical stimulation.

Between media conditions, there were significant differences in the levels of pSmad2/3 detected by Western blotting (Figure 7.10). Samples treated with BASAL media had significantly less pSmad2/3 protein compared to the other media groups

($p<0.001$). In a pairwise comparison, dynamic compression increased pSmad2/3 protein levels over static compression slightly for the samples treated with both BASAL (1.9-fold) and TGF-β1 (1.4-fold) media ($p=0.011$ and $p=0.005$ respectively). There were no in pSmad2/3 differences detected between static and dynamic compression in the TGF-β1+dexamethasone groups.

In general, the IHC complemented the Western blotting results, with the exception of the modulation of Smad2/3 phosphorylation by dynamic compression. IHC showed no differences between the response to dynamic compression of samples treated with TGF-β1 only and those treated with both TGF-β1 and dexamethasone. In both media conditions, dynamic compression upregulated pSmad2/3 localization to the nucleus demonstrated by in increase in the number of pSmad2/3 cells as well as in intensity of staining. Western blotting did not correspond clearly with the IHC findings for the samples treated with both TGF-β1 and dexamethasone, showing no significant regulation of Smad phosphorylation by dynamic compression.

Overall, both the IHC and Western blotting demonstrated that dynamic compression increased TGF-β signaling through the Smad2/3 pathway. While preliminary, dynamic compression increased Smad2/3 phosphorylation and nuclear localization, as well as increase the number of cells responding with TGF-β1 signaling.

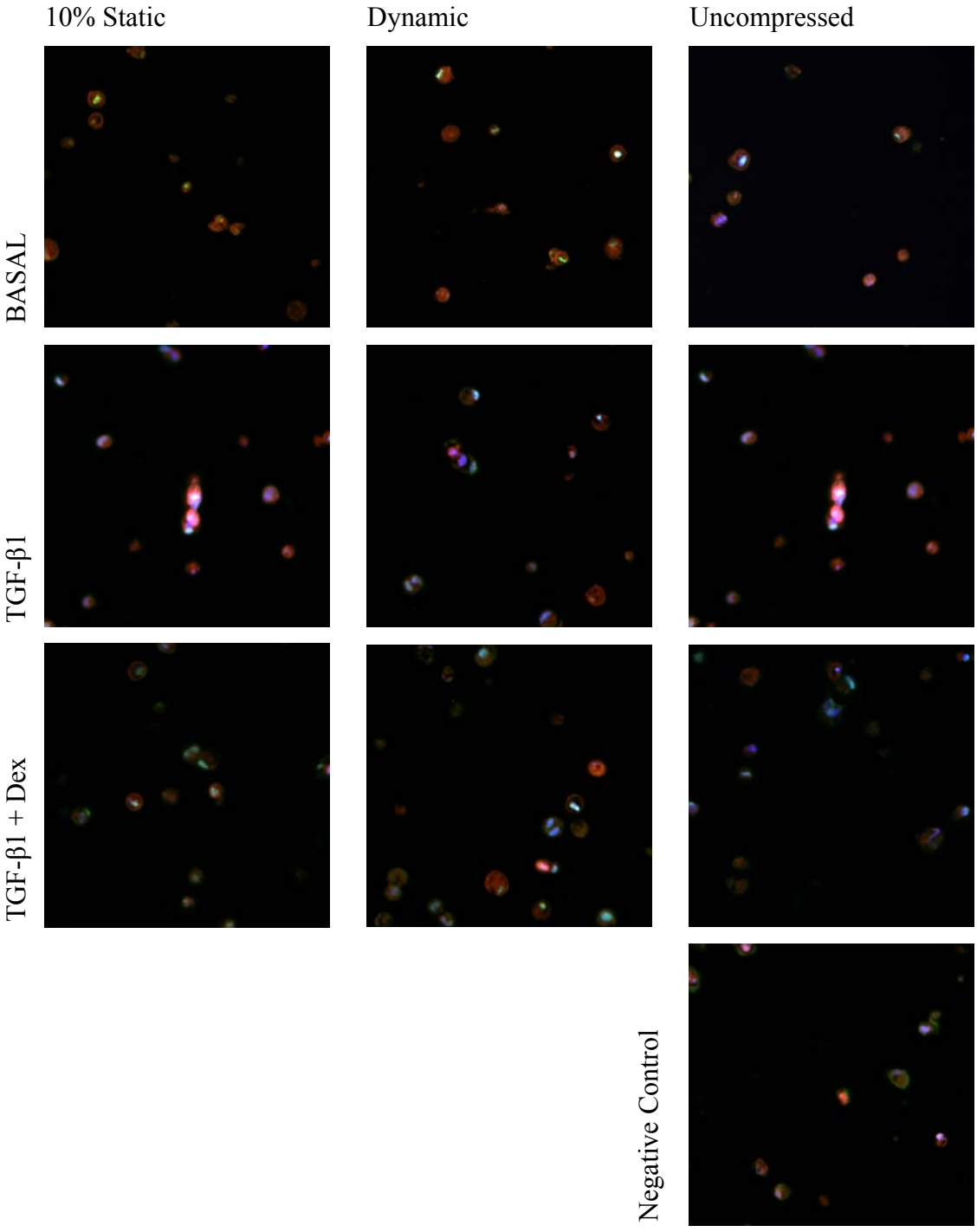

Figure 7.8: Phosphorylated Smad2/3 immunohistochemical staining after 1 hour of mechanical stimulation.

Constructs were cultured for 16 days prior to mechanical stimulation. Representative sections shown. Negative control replaces primary antibody with non-immune rabbit IgG. Images taken at 20X magnification via fluorescence microscopy. (n=4)

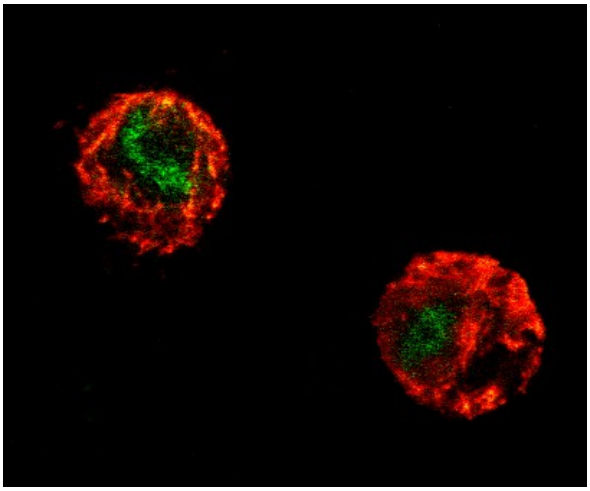

Figure 7.9: Phosphorylated Smad 2/3 (pSmad 2/3) immunohistochemical staining.

pSmad 2/3 localization was primarily nuclear for all conditions. Constructs were cultured for 16 days prior to mechanical stimulation. Unloaded construct stimulated with TGF-β1+ DEX shown and representative of positive pSmad 2/3 staining. Image taken at 100X magnification via confocal microscopy. (n=4)

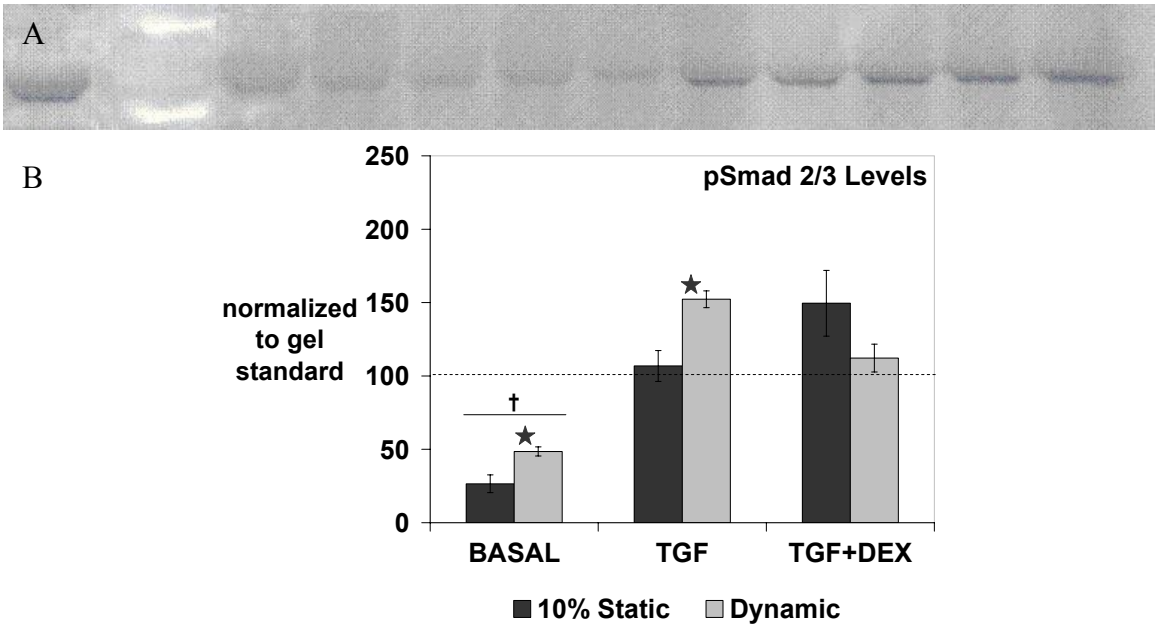

Figure 7.10: Phosphorylated Smad 2/3 (pSmad 2/3) levels.

pSmad 2/3 levels were measured by Western blotting and normalized by gel background and a standard on each gel. Constructs were cultured for 16 days prior to mechanical stimulation. (A) Representative blot for the TGF samples with the normalizing standard in the lane 1 (discussed in appendix E), molecular weight marker in lane 2, static samples in lanes 3-7, and dynamic samples in lanes 8-12. (B) Dashed line indicates 100% of gel standard. ★ indicates $P < 0.05$ vs. respective static group for relative pSmad 2/3 levels. † indicates $P < 0.05$ vs. other media groups. (mean±S.E.M, n=5)

TGF-β Receptor Type I

Between media conditions, there were significant differences in the levels of TβRI detected by Western blotting (Figure 7.11). Samples treated with TGF-β1 media had significantly more TβRI protein compared to the other media groups ($p<0.001$). Dynamic compression increased TβRI protein levels over static compression slightly for the samples treated with both BASAL (1.7-fold) and TGF-β1 (1.2-fold) media ($p=0.006$ and $p=0.038$ respectively). There were no differences between static and dynamic compression detected in the TGF-β1+dexamethasone groups.

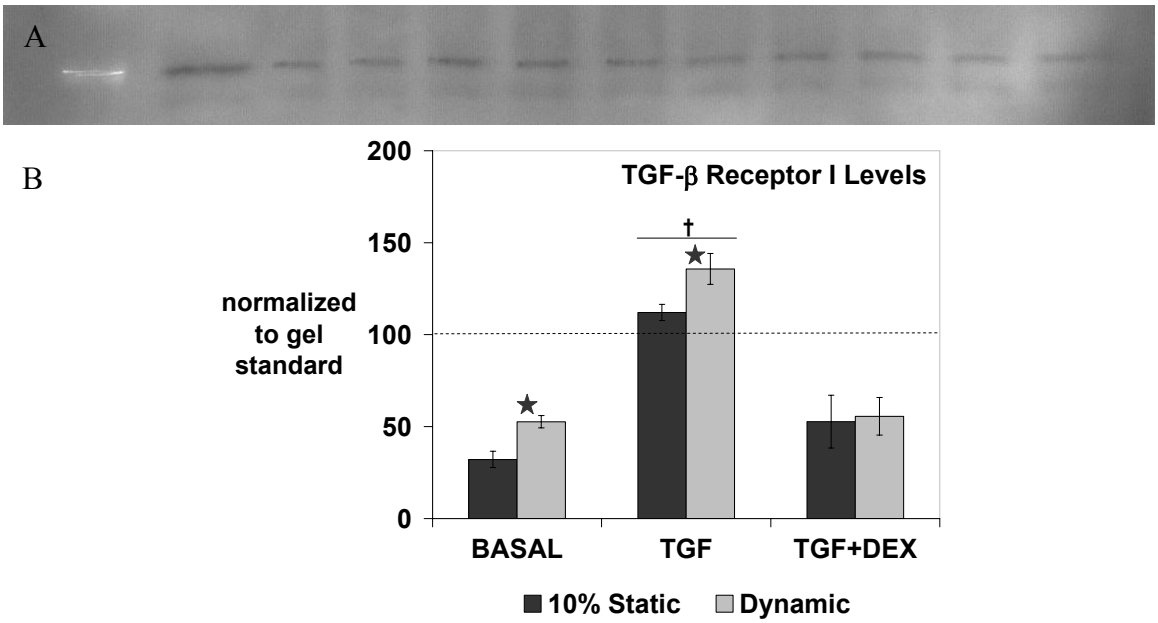

Figure 7.11: TGF-β Receptor I (TGF-β RI) levels.

TGF-β RI levels were measured by Western blotting and normalized by gel background and a standard on each gel. Constructs were cultured for 16 days prior to mechanical stimulation. (A) Representative blot for the TGF samples with the normalizing standard in the left lane (discussed in appendix E). (B) Dashed line indicates 100% of gel standard. ★ indicates $P < 0.05$ vs. respective static group for relative pSmad 2/3 levels. † indicates $P < 0.05$ vs. other media groups. (mean±S.E.M, n=5)

7.3.3 Long Term Loading

DNA

There were no differences in DNA content with time or mechanical stimulus (Figure 7.12).

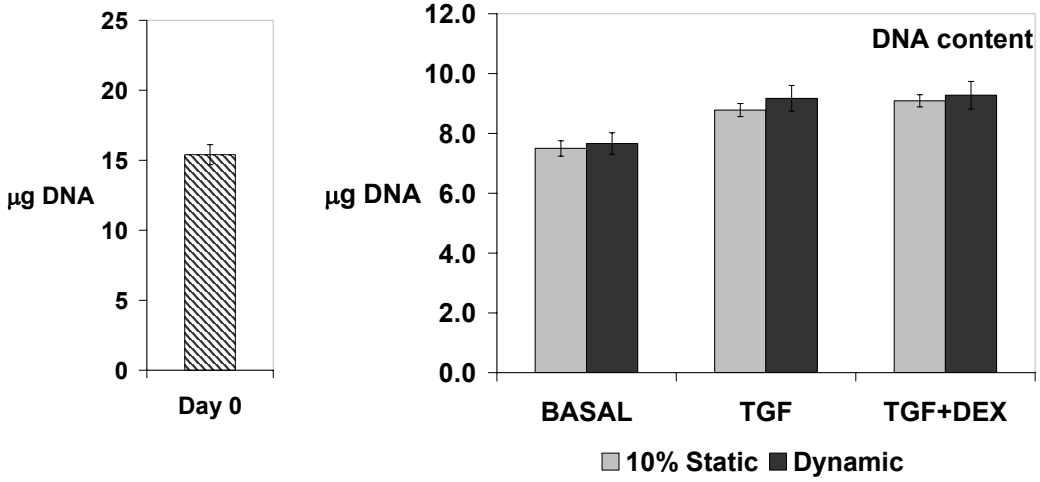

Figure 7.12: DNA content after loading from day 8 to day 16.
Samples were loaded 12 hours per day. (mean±S.E.M, n=4-8)

sGAG per DNA

Between media conditions, there were significant differences in the levels of sGAG accumulated per cell (Figure 7.13). Samples treated with BASAL media had significantly less sGAG accumulated per cell than samples treated with either TGF-β1 or TGF-β1+dexamethasone ($p<0.001$). Samples treated with TGF-β1+dexamethasone had significantly more sGAG accumulated per cell than samples treated with either BASAL media or TGF-β1 ($p<0.001$).

Analyzed with a pairwise comparison, dynamic compression inhibited sGAG accumulation per cell over static compression for the samples treated with TGF-β1 (0.5-fold, $p<0.001$). There were no differences detected in either the BASAL or TGF-β1+dexamethasone groups with dynamic compression.

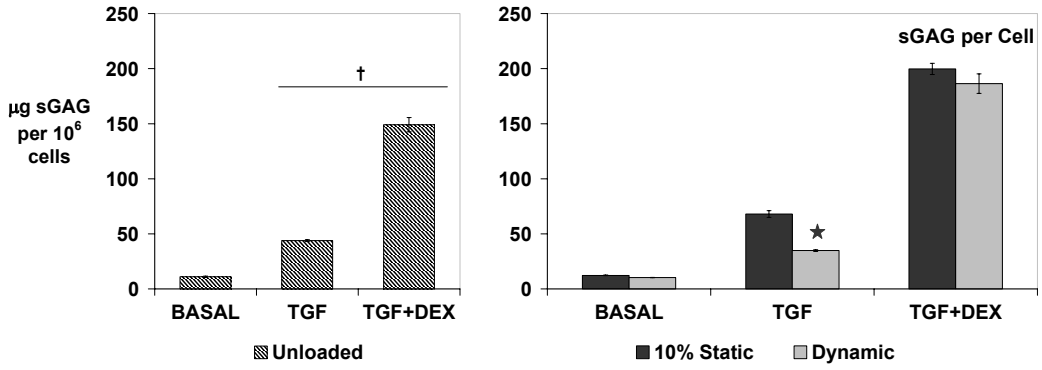

Figure 7.13: sGAG per DNA accumulation after loading from day 8 to day 16.
Samples were loaded 12 hours per day. ★ indicates $P < 0.05$ vs. respective static group. † indicates $P < 0.05$ vs. other BASAL groups. (mean±S.E.M, n=4-8)

Collagen I / II Content

There was considerably less collagen I and collagen II in the samples treated with BASAL media compared to the other media conditions (Figure 7.14). There were no observable differences between the TGF-β1 or TGF-β1+DEX samples in the amount of collagen accumulated. Between mechanical stimulation groups, there were no observable differences in the amounts or types of collagen accumulated in the samples treated with TGF-β1. There were no observable differences in the amounts or types of collagen accumulated in the unloaded and statically loaded samples treated with TGF-β1+dexamethasone, there was observably less collagen I and more collagen II in the dynamically loaded samples.

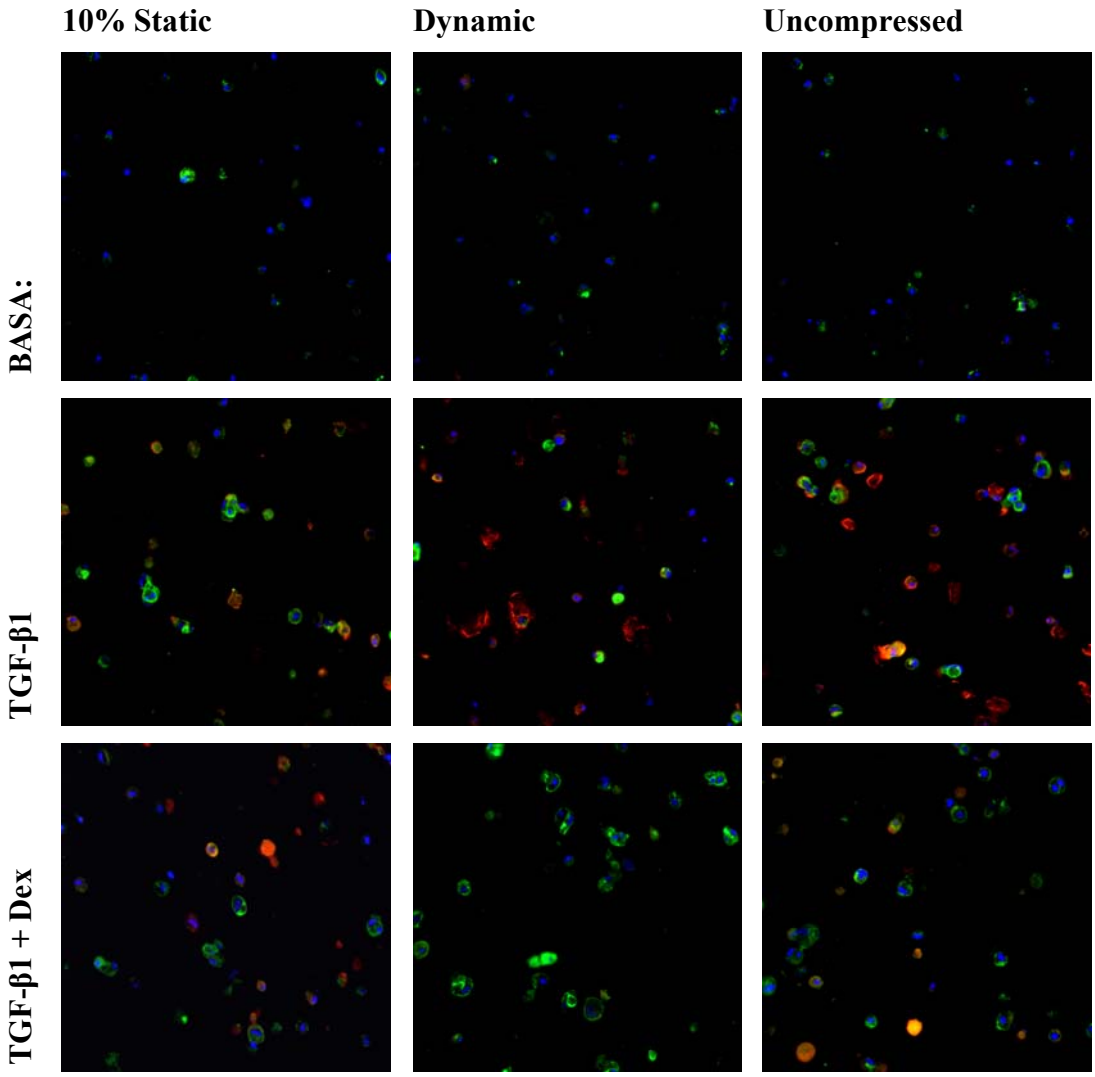

Figure 7.14: Collagen I / II co-localization after loading from day 8 to day 16.

Samples were loaded 12 hours per day. Collagen I shown in RED, Collagen II in GREEN and DNA in BLUE. Images taken at 20X magnification via fluorescence microscopy. (N=4)

7.4 DISCUSSION

Overall, the addition of TGF-β1 increased cell viability, gene expression, matrix synthesis and sGAG content over basal media. The addition of dexamethasone further enhanced all three. There was little stimulation of gene expression or matrix synthesis at day 8 with mechanical loading in chondrogenic media, although there was significant upregulation of gene expression in BASAL medium. On day 16, there was significant stimulation by dynamic loading compared to static loading for chondrogenic groups. The level of stimulation was also dependent on media condition, with the samples treated with basal media being the least responsive and the samples treated with TGF-β1 and dexamethasone being the most responsive. Overall, both collagens I and II gene expressions were more responsive to dynamic loading than aggrecan expression.

Differences between the responsiveness to mechanical stimulation of samples cultured 8 days before loading compared to those cultured 16 days before loading could be the result of multiple factors. One potential reason in the differing response to loading could be that the differentiation states of the cells in the various media formulations may alter their response to mechanical loading. The greater the level of chondrogenic differentiation the more similar in response the cells might be to that of a terminally differentiation chondrocyte. Also, the different levels of matrix accumulation could have affected both the biochemical signaling from the extracellular matrix involved in dynamic loading, as well as the local mechanical stimuli resulting from the macroscopic loading. The accumulation and structure of the pericellular and further removed extracellular matrix has been shown to affect the deformation of chondrocytes in hydrogel cuture[49]. Chondrocytes have been shown to be deformable before a pericellular

matrix has been developed (i.e. in freshly seeded cultures) and after an interconnected ECM has been established, with little to no deformation occurring with the formation of a just pericellular matrix due to stress shielding of the surrounding matrix[49,214]. This has been proposed as an explanation for the observed loss and subsequent redevelopment of mechanoregulation of chondrocytes in agarose.

Overall, total Smad2/3 levels seemed to be largely unaffected by media condition or mechanical stimulation, with only the TGF-β1+DEX samples responding significantly to dynamic compression. While the levels seemed largely stable, the localization of the Smad2/3 proteins was dependent on both media condition and mechanical stimulation. The addition of TGF-β1, and furthermore dexamethasone, increased nuclear localization of Smad2/3, as well as the application of dynamic compression. Due to the interference of agarose and potentially extracellular matrix components, the levels of cytoplasmic localization versus nuclear localization were not able to be analyzed via Western blotting.

Compared to total Smad2/3 localization, pSmad2/3 was primarily localized to the nucleus as evidenced by both IHC and Western blotting. There was an increase Smad2/3 phosphorylation in the samples treated with TGF-β1 and TGF-β1+DEX compared to BASAL samples. Phosphorylation of Smad2/3 increased in both BASAL and TGF-β1 samples, with no significant effect on the TGF-β1+DEX samples. One possible explanation for the discrepancy between the IHC and Western blotting results could be that the amount of ECM in the TGF-β1+DEX samples interfered with isolating the intracellular proteins from the agarose/ECM material. The lack of enhanced phosphorylation of Smad2/3 in the TGF-β1+DEX samples could be due to saturation of the TGF-β signaling pathway. There may be a functional limit to the amount of TGF-β

signaling in the BMSCs. Alternatively, the timing of the activation of the Smad proteins by mechanical stimulation may not be similar in all media conditions. Kim *et al.* found that TGF-β1 increased phosphorylation of Smad2 by 15 minutes, with peaked activation occurring between 15 and 60 minutes[215]. The singular timepoint of 60 minutes evaluated in the current study does not address the temporal variations in Smad activation in the different media conditions. Overall, the IHC and Western blotting results were consistent.

The pSmad2/3 localization to the nucleus is consistent with the generally accepted paradigm for TGF-β signaling[173]. There was also an increase in TβRI protein expression in the TGF-β1 samples, as well as an upregulation by dynamic compression in both BASAL and TGF-β1 samples. The results of this study demonstrate that dynamic loading can alter gene expression, matrix synthesis rates and intracellular phosphorylation for bovine BMSCs. However the response of the cells to dynamic loading depends on both media supplementation and the duration of unloaded culture.

CHAPTER 8 CONCLUSIONS AND RECOMMENDATIONS

8.1 SUMMARY

The study presented in Chapter 3 investigated the differences in the response of BACs to various commonly used tissue engineering scaffolds: agarose, alginate, type I collagen, fibrin and PGA. The study examined the nature of the proteoglycan / GAG matrices synthesized by chondrocytes seeded in these different scaffold materials. In addition to differences in total GAG content and distribution, FACE analysis revealed differences in CS/DS GAG fine structure among different scaffold materials. Overall, the internal Δ-disaccharide profile of GAGs in alginate constructs least resembled that of native articular cartilage, whereas the profile in agarose constructs most closely resembled that of articular cartilage. Striking differences were seen in the levels of unsulfated ΔDi-0S and disulfated ΔDi-4,6S between scaffold types, revealing a tradeoff between incorporation of unsulfated ΔDi-0S and disulfated ΔDi-4,6S into newly synthesized proteoglycans. While differences were detected between scaffold environments, further investigation would be necessary to identify the causes of the observed differences in sulfation patterns (*e.g.*, altered sulfotransferase activity, altered ratios of proteoglycan species, etc.). This study illustrated the dependency of the metabolic behavior of BACs on scaffold environment. Articular chondrocytes seeded into different scaffolds exhibited differences in proliferation, the quantity of matrix accumulated and the fine structure of the newly synthesized glycosaminoglycans. Specifically, BACs in agarose synthesized a disaccharide matrix most similar to that of

native articular cartilage, as well as accumulating a greater amount of sGAG compared to other scaffold types.

The studies in Chapter 4 explored the influences of various ion-channel pathways on the response of BACs to dynamic and static compression. The objectives of the studies were to investigate the dose-dependent inhibition of protein and sGAG synthesis by inhibitors of four different ion-channel signaling pathways in articular cartilage explants, the recovery of protein and sGAG synthesis by the four ion-channel inhibitors in articular cartilage explants and the response of chondrocytes seeded in agarose to dynamic compression when cultured with each of these inhibitors. The ion-channel inhibitors examined were 4-Aminopyridine (4AP), a voltage-dependent K+ channel blocker, Nifedipine (Nf), an L-type voltage sensitive calcium channel blocker, Gadolinium (Gd), an inhibitor of cation-selective stretch-activated ion-channels, and Thapsigargin (Tg), a natural plant product which depletes the Ca2+ store in the sarcoplasmic and endoplasmic reticula by inhibiting ATP-dependent Ca2+ pumps. Overall, treatment with the inhibitors more significantly affected sGAG synthesis suggesting that these ion-channels influence proteoglycan production or processing. Inhibition of Ca2+ channels by Nf affected protein synthesis, with little effect on sGAG synthesis, a unique response of the four inhibitors examined. In contrast to the compression independent selective inhibition of protein synthesis by Nf, the upregulation of protein synthesis due to dynamic stimulation was unaffected, while the upregulation of sGAG synthesis was blocked. A potential reason for the inhibition of mechanically-stimulated upregulation of sGAG synthesis may be due to a critical role in the mechanoregulation of proteoglycan production by Ca2+ channel signaling. Overall, the

studies presented in Chapter 4 suggest that different ion-channels play distinct, yet cooperative, roles to convert the same mechanical signals into different cellular responses, but that the roles of these ion channels in 3D are less distinct than in 2D culture experiments. These studies led us to examine a more specific pathway, the TGF-β signaling pathway.

The studies in Chapter 5 explored the influence of the TGF-β signaling pathway on the response of BACs to dynamic and static compression. The effects of dynamic and static compressive loading on BAC gene expression and matrix synthesis in the presence of the TGF-β signaling inhibitor SB431542 were examined, as well as the dose and recovery response to the inhibitor. SB431542 selectively inhibited protein synthesis over sGAG synthesis in BAC agarose constructs. Synthesis returned to BASAL levels 2 days after removal from the inhibitor. Dynamic compression has been documented to upregulate chondrocyte gene and matrix expression in 3D culture[216-218]. The addition SB431542 abrogated stimulation of all genes and matrix syntheses stimulated by dynamic compression in the BASAL samples, with no significant effect on the statically compressed samples. These findings suggest that TGF-β signaling may be integral in the mechanotransduction involved in the dynamic compression of BACs in 3D culture.

The studies in Chapter 6 investigated the influences of various culture parameters on the chondrogenic differentiation of bovine BMSCs. It has been well established that the parameters of culturing progenitor cell populations affects the differentiation capacity of these cells[201,202]. The studies investigated whether these factors such as passaging, seeding density, growth factor supplementation and scaffold can significantly impact BMSC differentiation. In all studies, chondrogenesis was highest in the TGF-β1+DEX

groups. While a dependency on passage number was not clear for all media conditions, passage 3 cells provided the highest level of chondrogenesis in the TGF-β1+DEX samples. For the TGF-β1 groups (with and without dexamethasone), constructs seeded at $25x10^6$ cells/mL had the highest chondrogenic response. Also, in general, the chondrogenic response of BMSCs was higher in agarose than in alginate. These studies illustrated that these culturing factors can significantly impact BMSC differentiation and should be considered when developing cell-based therapies for cartilage repair, and led us to define specific conditions for use in subsequent studies involving the mechanical stimulation of BMSCs.

The studies in Chapter 7 explored the interaction between TGF-β supplementation and mechanical loading on the chondrogenic differentiation of bovine BMSCs. It has been suggested that the combination of chondrogenic media and dynamic compressive loading may enhance chondrogenesis of BMSCs over the addition of exogenous factors alone[79]. Similar to the previous chapter, TGF-β1 enhanced chondrogenesis over BASAL conditions, with the addition of dexamethasone further enhancing chondrogenesis. There was a marked difference in the response of constructs to loading depending on the preculture duration. After 8 days of preculture, there was no significant regulation of matrix synthesis rates and an inhibition of aggrecan gene expression with dynamic compression in the TGF-β1 and TGF-β1+DEX groups, but a stimulation in BASAL. After 16 days of preculture, dynamic compression upregulated both collagen I and collagen II gene expression in both TGF-β1 groups, with aggrecan expression only being upregulated in the TGF-β1+DEX group and no regulation of the BASAL groups. Complementing the gene expression data, protein synthesis was upregulated by dynamic

compression in both TGF-β1 groups, while proteoglycan expression was only upregulated in the TGF-β1+DEX group. Interestingly, dynamic loading stimulated pSmad2/3 and TβR1 levels for both the BASAL and TGF-β1 groups, but not for the TGF-β1+DEX group, perhaps due to a saturation in TGF-β signaling with this media supplementation. Long term dynamic loading between days 8 and 16 yielded an inhibition in sGAG accumulation in the TGF-β1 samples, compared to static controls. These results suggest that the response of BMSCs in agarose culture to dynamic loading is dependent on either cell differentiation state, matrix accumulation or a combination of both.

8.2 CONCLUSIONS

The work presented in this dissertation demonstrates that there are marked differences between the responses of BACs and bovine BMSCs to mechanical stimulation in 3D culture. In theory, the BACs are a committed cell source, already expressing chondrogenic genes and proteins upon being released from their native environment and seeded into 3D agarose culture. Upon seeding into agarose, the signaling pathways necessary for maintenance of the chondrocyte phenotype are functional in the presence of the FBS media. Sox9, aggrecan and collagen II gene expression levels are high upon introduction into 3D culture[187,219]. Conversely, the BMSCs are a progenitor cell source, with the ability to differentiate into multiple cells types (multilineage potential was not examined within the scope of this work)[220]. Upon seeding into 3D culture and introduction of TGF-β1, the cells experience a shift in

cellular activity, moving from a proliferative state to a differentiating state[185,221]. TGF-β1 upregulates Sox9, considered the first master chondrogenic factor. Upon Sox9 upregulation, a complex series of largely unknown downstream events work in concert to shift the progenitor cell phenotype towards that of a differentiated chondrocte[220].

Distinct differences between BACs and BMSCs in their gene and phenotypic expression over time were found. Mauck *et al.* found that the amount of sGAG and the equilibrium modulus of BMSCs seeded into agarose and cultured for 10 weeks were lower than those of BACs from the same animal donor[190]. In the BMSC samples, both sGAG content and equilibrium modulus were found to plateau with time in the BMSC constructs, suggesting that diminished capacity is not the result of delayed differentiation. While this dissertation did not focus on a direct comparison between the matrices produced by both cells types, it is possible that there are structural differences in the matrices as well as overall accumulation amounts.

The extent of an ECM has been shown to influence chondrocyte deformation in 3D agarose culture. Knight *et al.* have demonstrated that the stiffness of isolated chondrons (chondrocytes with attached pericellular matrix intact) seeded into agarose is higher than that of the surrounding extracellular agarose environment, leading to stress shielding of the chondrocytes during loading[214]. The possibility exists that the level of cellular deformation between the two cell types, and even within the BMSC population cultured in different media formulations, is different at a given time and a given differentiation state. Safranin O staining of BMSCs in agarose showed the beginning of a more interconnected endogenously produced ECM only after 16 days of culture in the TGF-β1+DEX group (Figure 6.13). At day 16, the constructs treated with TGF-β1 only

resembled more similarly the TGF-β1+DEX day 8 samples. Irrespective of differentiation state, the degree of mechanostimulation will be affected by these varying amounts of accumulated matrix[49,214,222]. Interpretation of the effects of dynamic compression between the different media conditions must be kept in perspective realizing that the local mechanical environments may be different.

The addition of dexamethasone to the chondrogenic media greatly influenced both the gene expression and matrix synthesis of the differentiating BMSCs. Glucocorticoids, including dexamethasone, affect gene expression by transcriptional and posttranscriptional mechanisms by binding to specific receptors that belong to the superfamily of nuclear receptors (classical mechanism). The glucocorticoid/receptor complex acts as a ligand-dependent transcriptional factor to either activate or repress the transcription of certain genes[223,224]. Dexamethasone is a glucocorticoid that is typically added to both chondrogenic and osteogenic cultures to stimulate the osteochondral phenotype[225,226]. Dexamethasone has been found to upregulate cFOS mRNA expression in osteoblasts through a mechanism involving binding to a soluble glucocorticoid receptor intracellularly and interacting with cFOS mRNA[227]. Locker *et al.* found that dexamethasone induced Sox9 upregulation in the pluripotent mesoblastic C1 line[228]. While the mechanisms of dexamethasone in the chondrogenic studies presented in this dissertation are unknown, positive regulation though Smad2/3 or Sox9, as well as negative regulation of the inhibitory Smads and SMURFs, are possibilities.

Complimentary to our findings, Huang *et al.* found that cyclic compressive loading promoted gene expressions of Sox9, c-Jun, and both TGF-beta receptors and productions of their corresponding proteins in rabbit BMSCs in 3D agarose culture[176].

TβRI has been shown to cause receptor-activated Smad2/3 phosphorylation at the C-terminal SSXS motif, causing dissociation from the receptor and association with the common mediator Smad4[172,229,230]. Upon heteromeric complex formation, translocation to the nucleus occurs leading to interaction with various DNA-binding co-factors and co-modulators to activate transcription. The study presented in Chapter 5 demonstrated that there is an interaction, or a series of interactions, between TGF-β signaling and dynamic compression in BACs cultured in agarose. The study presented in Chapter 7 illustrated an increase in TβRI protein expression in BMSCs treated with TGF-β1, as well as an upregulation by dynamic compression in both BASAL and TGF-β1 samples. The suggestion of an interaction in both cell systems has been substantiated. While speculative, there are multiple potential regulatory mechanisms through which TGF-β1 signaling and mechanical stimulation interact. The mechanisms fall into one of two categories: the influence on mechanotransduction by the TGF-β signaling pathway or the influence on TGF-β signaling by mechanical stimulation.

The first category of potential mechanisms involves the potential modulation of mechanotransduction by the TGF-β signaling pathway, either directly or indirectly. TGF-β and its signaling pathway may be increasing the sensitivity of the BACs and BMSCs to loading. TGF-β signaling may lead to pSmad activation of mechanosensitive proteins, such as focal adhesion kinase (FAK) and paxillin, which might therefore increase the mechanosensitivity of the cells[181-183]. Another potential mechanism involves the interaction of Smad2/3, in combination with Smad4, with Sox9. In differentiating cells, TGF-β1 and TGF-β3 have been shown to upregulate Sox9 gene expression. This upregulation of Sox9 expression is indicative of chondrogenesis in MPC populations.

Sox9 has been shown to bind to the promoter region of type II collagen, enhancing transcription and collagen II mRNA expression. Smad3 has been found to enhance the transcriptional activity of Sox9 and the expression of the α1 (II) collagen (COL2A1) gene by forming a transcriptional complex with Sox9 and binding to the promoter region of COL2A1[186]. While Sox9 levels parallel COL2A1 in differentiating cells, Aigner *et al.* found no positive correlation between Sox9 and COL2A1 expression levels in adult articular chondrocytes[187]. Possibly, dynamic compression may upregulate chondrocytic gene expression and production through mechanisms similar to those utilized in cells undergoing chondrogenic differentiation including upregulation of Sox9 levels. If this was the case, inhibiting TGF-β signaling during mechanical stimulation would be analogous to depriving a differentiating cell of the growth factor.

The second category of potential mechanisms involves the modulation of the TGF-β signaling pathway by mechanical stimulation. One direct mechanism may involve the stimulation of TGF-β production by mechanical stimulation. Also, mechanical stimulation may upregulate the production of proteolytic moieties such as plasmin and stromelysin-1, leading to the activation of latent TGF-β1, either endogenously produced (both BACs and BMSCs) or introduced into the culture system in the FBS (BACs only)[179,180,231]. Both chondrocytes and BMSCs have been found to affected by TGF-β concentrations in the media[77,184,185]. Also, in either cell system, stimulation of TβR1 is one potential mechanism for the modulation of dynamic loading via TGF-β signaling. An increase in the available supply of TβR1 could potentially lead to a greater level of Smad2/3 activation, amplifying the signaling occurring as a result of TGF-β1 exogenous stimulation. Another possible mechanism for regulation of

chondrogenesis by mechanical stimulation is an increase in the phosphorylation of the Smad2/3 proteins and/or its translocation to the nucleus via alterations in the intracellular space, either separating or bringing together certain proteins and molecules.

The studies in chapters 4, 5 and 7 demonstrated that the upregulation of protein expression and proteoglycan expression by dynamic compression in chondrocytes and chondroprogenitors do not necessarily parallel one another. The study presented in chapter 4 showed that there were differences in the effects of perturbing various ion-channels on protein and proteoglycan expression in BACs. Specifically, inhibiting L-type voltage Ca^{2+} signaling (with Nf) differentially inhibited protein synthesis over proteoglycan synthesis; conversely, inhibition of voltage-dependent K^{+} signaling (with 4AP) inhibited sGAG synthesis over protein synthesis. In chapter 5, collagen II gene expression in BACs was found to be modulated by 3 hours of dynamic compression, whereas aggrecan gene expression was not. Both protein and sGAG syntheses were upregulated with 20 hours of dynamic compression, with both upregulations being abrogated by the addition of the TGF-β signaling antagonist, SB431542. The study presented in chapter 7 demonstrated that the BMSCs response to dynamic compression was dependent on preculture duration and media supplementation. Dynamic compression of BMSCs cultured with both TGF-β1 and dexamethasone upregulated only collagen II gene expression and protein synthesis after 8 days of preculture. After 16 days of preculture, both protein and proteoglycan expressions were upregulated by dynamic compression in BMSCs cultured in the same media. Taken together, these data suggest that the upregulation of protein and proteoglycan synthesis is independent, with some overlap.

The upregulation of TβRI gene expression in BACs with dynamic compression and TβRI protein expression in BMSCs by dynamic compression suggests that the intersection of TGF-β signaling and dynamic compression may occur at the TGF-β receptor level. This is consistent with observations in the literature that dynamic compression increases expression of (both receptors?) by rabbit BMSCs.(cite recent Huang paper—in press?) If dynamic compression increases TβRI protein expression independent of the TGF-β signaling pathway, this could lead to an increase in TGF-β ligand binding and thus upregulation of subsequent TGF-β signaling through Smad phosphorylation. However, other results are inconsistent with this model. Specifically, introduction of the TGF-β signaling inhibitor SB431542 not only blocked the increases in matrix genes by dynamic compression but also blocked the increase in TβRI gene expression, indicating that receptor regulation is not independent of TGF-β signaling. Therefore, it appears likely that the upregulation of TβRI gene expression in chondrocytes and TβRI protein expression in BMSCs depended on an increase in TGF-β signaling. Simply put, an upregulation of TβRI availability is not what is being initially modulated by dynamic compression. An alternative hypothesis that has not yet been explored is that the mechanism of regulation occurs intracellularly, through an upregulation of the accessory TGF-β receptor, betaglycan (TGF-β receptor III).

Betaglycan is a transmembrane glycoprotein with large extracellular regions that bind TGF-β and very similar cytoplasmic regions without any identifiable signaling motif[232]. The extracellular portion of betaglycan contains both heparin sulfate and chondroitin sulfate chains and binds to TGF-β via its core protein[233]. One of the known functional roles of betaglycan is as a positive regulator of TGF-β signaling. Betaglycan

increases the affinity of the binding of TGF-β ligands to the TGF-β type II receptor (TβRII), enhancing the cell's responsiveness to TGF-β[234]. Lopez-Casillas *et al.* found that this effect appears to be mediated by a "presentation complex" formed by betaglycan, TGF-β and TβRII[232,234]. In contrast to the membrane bound form of betaglycan, soluble betaglycan has been shown to have a negative regulatory effect on TGF-β ligand binding to TβRII through competitive inhibition, thus downregulating TGF-β signaling[235]. Betaglycan has been found to be transcriptionally upregulated during skeletal muscle differentiation[236], as well being involved in the deregulation of activin signaling during cancer metastasis[237].

Mechanical loading could thus increase chondrocyte and chondroprogenitor sensitivity to TGF-β by upregulating betaglycan transmembrane expression and downregulating soluble betaglycan, possibly through the p38-MAPK pathways which have been shown to regulate proteoglycan expression[77]. Through an increase in the availability of betaglycan on the cell surface and a decrease in the soluble betaglycan competing for the TGF-β ligand, there would be an increase in TGF-β ligand binding to TβRII and subsequent TβRI – TβRII - ligand complex formation. The increase in TβRI – TβRII - ligand complex would lead to an upregulation of Smad2 and Smad3 phosphorylation, Smad2/3-Smad4 complex formation and localization to the nucleus, and ultimately enhanced gene transcription.

These studies have illustrated a potential connection between dynamic compression and TGF-β signaling in both chondrocytes and chondroprogenitors. Understanding the relationship between mechanical loading and TGF-β signaling may provide potential targets for manipulating cell differentiation, as well as for treating

diseased and injured cartilage. To this end, these findings are important for understanding *in vitro* development of 3D scaffolds for cartilage regeneration. It has been hypothesized that the loading environment in the knee is too harsh to allow an immature construct lacking mechanical integrity to survive and develop into a tissue capable of successful load bearing[8]. Facilitating a tissue-engineered construct capable of functioning successfully in vivo will involve matching mechanical and biochemical properties of native cartilage as closely as possible.

Clearly TGF-β is important for articular chondrocytes and BMSCs, but only one of many growth factor mediated signaling pathway that regulate articular chondrocyte metabolism. These studies establish a paradigm for exploring interactions between mechanical stimulation and a specific growth factor mediated signaling pathway. While *in vitro* mechanical stimulation may end up improving both the mechanical and biochemical properties of constructs, it may not prove to be practical or even feasible for purposes other than scientific investigation. Understanding the pathways through which mechanotransduction occurs offers the possibility of regulating these mechanisms biochemically, as opposed to biomechanically.

8.3 Recommendations and Future Work

The work presented in this dissertation has added to the current body of knowledge on articular chondrocytes, progenitor cells, growth factor supplementation and mechanical stimulation. Coupled with extensive literature on articular cartilage and mechanical stimulation, these studies begin to aid in creating a foundation for

understanding the transduction of mechanical stimuli. These studies establish another potential mechanism for mechanotransduction in 3D culture, signaling through interaction with the TGF-β pathway.

The study presented in chapter 3 investigating the differences in the ECM produced by chondrocytes in different tissue engineering scaffold demonstrated that there were differences in both the total amount of sGAG accumulated, as well as in the composition of the GAG matrix. While the functional implications of altered Δ-disaccharide sulfation patterns in native or engineered cartilage are unknown, there is evidence of structure-function relationships in other tissues and with other sulfated GAGs. Variations in the sulfation of GAGs has been shown to alter the binding of nutrients, chemokines and growth factors, thereby influencing cell migration, differentiation, and matrix production[144-146].

While the use of the inhibitor SB431542 proved useful in determining whether there may be an interaction between TGF-β signaling and dynamic compression, in general, the use of chemical inhibitors is best utilized in concert with other means of discerning signaling through a particular pathway. External ligand agonists, constitutively active and dominant negative forms of proteins are commonly employed to investigate particular signaling pathways. When you perturb a system to attempt to understand it, you run the risk of biasing the system. For this reason it is important to address a question from multiple directions. Using the already well established paradigm for TGF-β signaling through Smad phosphorylation and translocation, different point in this signaling path need to be perturbed to yield a better understanding the interaction (or interactions) between mechanotransduction and TGF-β signaling. The use of external

ligand agonists and constitutively active TβRI would help elucidate the influences from growth factor shedding, growth factor activation and upregulation and activation of TβRI. Protein zymography could also be used to look at the regulation of matrix enzymes by either loading or TGF-β supplementation, addressing the role of TGF-β activation in the interaction between mechanotransduction and TGF-β signaling. Use of both dominant negative mutations of Smad2/Smad3, as well as constitutively phosphorylated Smad2/Smad3, in the presence of mechanical stimulation may help understand the role of these proteins in mechanical stimulation. Blocking TGF-β signaling external to the cell through the use of ligand agonists would address whether mechanical stimulation affects TGF-β signaling by modulating the activation of latent forms of TGF-β though an upregulation of proteolytic factors.

Without the use of additional sophisticated biochemical techniques, a more thorough examination of target protein expression would be useful in investigating at which aspects of TGF-β signaling are regulated by mechanical stimulation in both BACs and BMSCs. In the study presented in the dissertation, mechanical loading influenced total Smad2/3, pSmad2/3 and TβRI protein and gene expression levels. A more exhaustive study looking at these signaling moieties in combination with better characterizing the structural properties of the ECM would provide better insight into the interaction between TGF-β1 signaling and mechanical loading. As previously discussed, the level of ECM directly affects the deformation of cells encapsulated by hydrogel scaffolding.

While somewhat speculative, the potential role of betaglycan in the anabolic stimulation of dynamic compression would be interesting to explore. Either an increase

in betaglycan at the cell membrane or a decrease in soluble betaglycan could lead to increased TGF-β signaling, and preliminary studies to examine both aspects would be fairly straightforward. Levels of soluble betaglycan could be examined through Western blotting for the protein, as well as its fragments, in the media from BAC agarose gels subjected to either dynamic compression, static compression or unloaded in the presence and absence of TGF-β inhibition with SB431542. A downregulation in soluble betaglycan and betaglycan fragments with dynamic compression in both the presence and absence of the inhibitor would support the hypothesis that TGF-β signaling is modulated by a downregulation in soluble, competitive betaglycan. Additionally, the betaglycan (glycosylated protein ~250kDa, core protein ~120kDa) associated with the BAC agarose constructs should be Western blotted after rinsing the excess soluble betaglycan out of the construct. To more sensitively address the rate of betaglycan synthesis, the culture media could be supplemented with 35S-sulfate (which would be incorporated into newly synthesized betaglycan). The newly synthesized betalycan could then be immunoprecipitated from conditioned culture media, and the IPed protein could be assessed via scintillation counting to determine the 35S-sulfate incorporation. To complement the protein expression data, the betaglycan mRNA expression could be analyzed with real-time RT PCR to determine the effect of loading on betaglycan gene expression. If transmembrane betaglycan expression is upregulated by dynamic compression in both the presence and absence of the TGF-β inhibitor, it is likely that the regulation of the transmembrane proteoglycan is occurring independent of the Smad signaling pathway. While these assaying techniques are fairly simple, they would be largely indicative of whether betaglycan is participating in the interaction between TGF-β

signaling and dynamic compression in BACs. If such a role were substantiated, further studies would need to be performed to elucidate the connection between dynamic compression and betaglycan upregulation.

These current findings also have broader implications for the targeting of therapeutics. Stimulation of matrix synthesis by either biomechanical or biochemical stimulus has been shown to depend on the matrix environment as well as the cell type. Future intervention suggested by the seemingly inherent susceptibility of articular cartilage to osteoarthritic degradation may focus on early treatment of the cartilage to delay the onset of degradation. However, it is important to recognize the need for a thorough investigation of the potential effects of biochemical or biomechanical treatments. The current studies have shown differential effects of physiologically relevant stimuli on cells from different tissues, with differential effects. Therefore, consideration of the effects of a specific treatment on the target tissue as well as neighboring tissues will be necessary to ensure net positive effects on the overall health of the knee joint.

APPENDIX A MATERIALS AND REAGENTS

Product	Vendor	Location
Collagen I Antibody	Abcam	Cambridge, MA
Collagen II Antibody	Abcam	Cambridge, MA
PGA felts	Albany International	Mansfield, MA
e-aminocaproic acid	Acros Organics	Fairlawn, NJ
L-5-^{3}H-proline	American Radiolabeled Chemicals	St. Louis, MO
SYBR Green Master Mix	Applied Biosystems	Foster City, CA
Glass Electrophoresis Plates	Bio-Rad	Hercules, CA
Dissacharide standards	Calbiochem	La Jolla, CA
Chondroitinase ABC	Calbiochem	La Jolla, CA
Chondroitinase AC	Calbiochem	La Jolla, CA
Hyaluronidase	Calbiochem	La Jolla, CA
4-Aminopyridine	Calbiochem	La Jolla, CA
Nifedipine	Calbiochem	La Jolla, CA
Thapsigargin	Calbiochem	La Jolla, CA
Protease Inhibitor Cocktail Set I	Calbiochem	La Jolla, CA
Rat-tail collagen I	Collaborative Biomed	Bedford, MA
T-75 Flasks	Corning	Corning, NY
0.22 mm Polyethersulfone Filter	Corning	Corning, NY
EDAS 120 Imaging System	Eastman Kodak	New Haven, CT
Proteinase K	EMD Chemicals	Gibbstown, NJ
b-Mercaptoethanol	EMD Chemicals	Gibbstown, NJ
24-well Plates	Falcon	Franklin Lakes, CA
48-well Plates	Falcon	Franklin Lakes, CA
Triton X-100	Fisher Scientific	Pittsburg, PA
Sodium Dodecyl Sulfate	Fisher Scientific	Pittsburg, PA
Mono gels and running buffer	Glyko	Novato, CA
Fetal Bovine Serum	Hyclone	Logan, UT
Bovine Fibrinogen	ICN Biomedical	Irvine, CA
Thrombin	ICN Biomedical	Irvine, CA
Ecolume	ICN Biomedical	Irvine, CA

High Glucose Dulbecco's Modified Eagle's Medium	Invitrogen	Carlsbad, CA
HEPES Buffer	Invitrogen	Carlsbad, CA
AP-conj anti-Biotin	Invitrogen	Carlsbad, CA
Non-essential Amino Acids	Invitrogen	Carlsbad, CA
Gentamicin	Invitrogen	Carlsbad, CA
Fungizone (Amphotericin B)	Invitrogen	Carlsbad, CA
Phosphate Buffered Saline	Invitrogen	Carlsbad, CA
Collagenase Type II	Invitrogen	Carlsbad, CA
Trypsin	Invitrogen	Carlsbad, CA
Antibiotic/Antimycotic	Invitrogen	Carlsbad, CA
Forward and Reverse Primers	Invitrogen	Carlsbad, CA
Biotin SP-conj anti-Rb IgG	Jackson Immuno	
Polysulfone	JM Machining	Lawrenceville, GA
p-DAB	JT Baker	Phillipsburg, NJ
Chloramine T	Mallinckrodt	Paris, KY
Red FDA Rubber	McMaster Carr	Atlanta, GA
Microcon YM-30	Millipore	
4 mm Biopsy Punch	Miltex	York, PA
6 mm Biopsy Punch	Miltex	York, PA
LIVE/DEAD® Assay Kit	Molecular Probes	Eugene, OR
Labeled Goat a-Rabbit IgG Antibody	Molecular Probes	Eugene, OR
Labeled Goat a-Mouse IgG Antibody	Molecular Probes	Eugene, OR
Phalloidin	Molecular Probes	Eugene, OR
2-Aminoacridone HCl	Molecular Probes	Eugene, OR
^{35}S-sodium sulfate	MP Biomedicals	Irvine, CA
rh bFGF	PeproTech	Rocky Hill, NJ
rh IGF-I	PeproTech	Rocky Hill, NJ
rh PDGF-AB	PeproTech	Rocky Hill, NJ
rh TGF-b1	PeproTech	Rocky Hill, NJ
Promega Reverse Transcription Kit	Promega	Madison, WI
Alginic acid	Pronova	Oslo, Norway
Qiagen Rneasy Mini Kit	Qiagen	Valencia, CA
Qiagen Qiashredders	Qiagen	Valencia, CA
Calf Stifle Joints	Research 87	Marlborough, MA
TWEEN-20	Sigma	St. Louis, MO
Gadolinium	Sigma	St. Louis, MO
L-proline	Sigma	St. Louis, MO
L-ascorbic acid	Sigma	St. Louis, MO

Bovine Serum Albumin	Sigma	St. Louis, MO
Agarose	Sigma	St. Louis, MO
Ammonium Acetate	Sigma	St. Louis, MO
Agarase	Sigma	St. Louis, MO
1,9-Dimethylmethlyene Blue	Sigma	St. Louis, MO
Hoechst 33258 Dye	Sigma	St. Louis, MO
Chondroitin Sulfate	Sigma	St. Louis, MO
Calf Thymus DNA	Sigma	St. Louis, MO
Hydroxyproline	Sigma	St. Louis, MO
Goat Serum	Sigma	St. Louis, MO
Rabbit Serum	Sigma	St. Louis, MO
Safranin O	Sigma	St. Louis, MO
Tris Base	Sigma	St. Louis, MO
Glycine	Sigma	St. Louis, MO
Sodium Chloride	Sigma	St. Louis, MO
Sodium Fluoride	Sigma	St. Louis, MO
Sodium Orthovanadate	Sigma	St. Louis, MO
Sodium Cyanoborohydride	Sigma	St. Louis, MO
SB431542	Tocris	
No. 12 Razor Blades	VWR Scientific	West Chester, PA
#22 Scalpel Blade	VWR Scientific	West Chester, PA

APPENDIX B TISSUE CULTURE METHODS

B.1 ARTICULAR CHONDROCYTES IN GEL CULTURE

Bovine articular chondrocytes were isolated from the stifle joints of immature (<5 weeks) donor animals. Tissue was excised from the patellofemoral grooves, minced and digested in DMEM with 0.2% collagenase for 24 h in a 37°C, 5% CO_2 incubator. After centrifugation at 160 x g, cells were washed twice with Ca^{2+}, Mg^{2+} -free PBS and counted with either a Coulter counter or a Vi-Cell Cell Viability Analyzer. Cells were seeded into a hydrogel or on polyglycolic acid (PGA) felts.

Media were changed every two days. After culture period, the constructs were weighed, lyophilized, reweighed, and digested in 1ml of 100mM ammonium acetate buffer with 250 μg/mL Proteinase K at 60°C for 24 hours. Portions of each digest were assayed for total DNA using the Hoechst 33258 assay with calf thymus DNA as a standard and sGAG using the DMMB assay with shark cartilage CS as a standard.

B.2 BONE MARROW STROMAL CELLS ISOLATION AND PASSAGING

BMSCs were isolated from both the femoral and tibial diaphyses of 2-4 week old calves obtained within 24 hours of slaughter. After removal of all fascia and muscle from the bones, the bones were cut at the mid-diaphysis with a sterile bone saw. Marrow was removed from the medullary canal and transferred to a 50ml conical with sterile PBS plus 1% antibiotic/antimycotic (A/A; 100U/mL penicillin, 100ug/mL streptomycin, 250 ng/mL Amphotericin). Marrow was sequentially passed through large bore (25mL) and

small bore (5mL) pipets to disrupt large pieces. Marrow was then sequentially passed through 16- and 18-gauge needles for further homogenization. Marrow suspension was centrifuged at 300 x g for 15 minutes. The separated fatty layer was removed and discarded. The cell pellet was resuspended in Ca^{2+}, Mg^{2+} -free PBS, passed through a 20-gauge needle and filtered through a 100μm nylon filter. Mononuclear cells were counted using a hemacytometer using the Trypan Blue exclusion method after lysing red blood cells with the addition of 4% acetic acid.

Cells were plated in T-flasks at 5 x 10^3 mononuclear cells per cm^2 in passaging medium (consisting of low glucose DMEM, 10% FBS, 1% A/A, 1ng/mL bFGF). Nonadherent cells were removed during media change three days later. Medium was changes every three days thereafter. Cells were cultured until confluent (~ 2 weeks, P1), detached with 0.05% trypsin/1mM EDTA, and replated at 5 x 10^3 cells per cm^2. Cells were cultured until confluence and either replated or seeded into either 2% alginate gels or 3% agarose. Media were changed every two days. After 20 and 40 days, constructs were weighed, lyophilized, reweighed, and digested in 1ml of 100mM ammonium acetate buffer with 250 μg/mL Proteinase K at 60°C for 24 hours.

B.3 TISSUE ENGINEERING SCAFFOLDS AND MEDIA

Specific Aim 1

Agarose constructs were assembled by autoclaving 3% LMP agarose in 1X Ca^{2+}, Mg^{2+} -free PBS and then cooling the solution to 42°C. An equal volume of cells suspended at 30 x10^6 cells/mL in 2X DMEM and 20% FBS was added, and the solution was cooled in custom molds. Alginate constructs were similarly assembled by autoclaving 1.5% alginic acid in 1X Ca^{2+}, Mg^{2+} -free PBS to solubilize and sterilize the alginate, cooling the solution to 37°C, adding 30x10^6 cells/mL in Ca^{2+}, Mg^{2+} -free PBS and polymerizing the gels in the molds with 102 mM $CaCl_2$. Collagen constructs were assembled by suspending 15x10^6 cell/mL in a solution containing 10% FBS, 0.5x DMEM and 2 mg/mL acid solubilized rat tail collagen type I and titrating the solution to neutral pH with 0.1M NaOH. Constructs were allowed to polymerize in a 37°C, 5% CO_2 incubator for 30 minutes before transfer to 24 well plates with 2ml of media. Fibrin constructs were assembled by suspending cells in a solution of bovine fibrinogen, FBS, aminocaproic acid (ACA), and DMEM. Bovine thrombin was dissolved in 40 mM $CaCl^2$, and 100 µl of the thrombin solution was placed into each well of a polycarbonate mold (12 mm diameter by 3 mm deep), followed by 200 µl of the cell/fibrinogen mixture. Final concentrations in the constructs were 50 mg/mL fibrinogen, 50 U/mL thrombin, 10% FBS, 2 mg/mL ACA, and 15x10^6 cells/mL. Constructs were allowed to polymerize in a 37°C, 5% CO2 incubator for 30 min and then removed from the molds and transferred to 24-well culture dishes containing 2 mL of culture medium (described below). PGA felts (45 mg/cm^3 polymer density; 12-15 µm fiber thickness; 10 mm diameter by 2 mm thickness) were prewetted overnight in high-glucose DMEM

containing 10% FBS. PGA felts were then seeded by repeatedly pipetting 1 mL of cell suspension ($1.2x10^6$ cells/mL) onto each felt and culturing on a shaker plate at 300 rpm for 24 hours. The felts were then transferred to 2 mL each of culture medium in culture dish wells that had been pre-coated with a thin layer of 1% agarose.

Constructs and native cartilage samples (n=8 per group per endpoint) were cultured in 24 well plates with 2 mL of DMEM containing 10% FBS, 0.1mM NEAA, 4mM L-glutamine, 5 μg/mL gentamicin sulfate and 50 μg/mL ascorbic acid. As in previous studies on dorsal root ganglia, smooth muscle cells and chondrocytes, aminocaproic acid (2 mg/mL) was added to the media of fibrin constructs to inhibit proteolytic degradation.

Specific Aim 2

Agarose constructs were assembled by autoclaving 4% LMP agarose in 1X Ca^{2+}, Mg^{2+} -free PBS and then cooling the solution to 42°C, for a final agarose concentration of 2%. An equal volume of BAC cells were suspended at $20x10^6$ cells/mL in 1X Ca^{2+}, Mg^{2+} -free PBS, and the solution was cooled in custom molds.

Constructs were cultured in 24 well plates with 2 mL of DMEM containing 10% FBS, 0.1mM NEAA, 4mM L-glutamine, 5 μg/mL gentamicin sulfate and 50 μg/mL ascorbic acid. Inhibitors were added as specified in chapter 4.

Specific Aim 3

Agarose constructs were assembled by autoclaving 3% LMP agarose in 1X Ca^{2+}, Mg^{2+} -free PBS, cooling the solution to 42°C, and suspending the BAC cell pellet in the

appropriate volume yielding $20x10^6$ cells per mL of agarose. Agarose constructs were cast in 3mm thick sheets between two electrophoresis plates and punched to a 4mm diameter using biopsy punches.

Constructs were cultured in 24 well plates with 2 mL of DMEM containing 10% FBS, 0.1mM NEAA, 4mM L-glutamine, 5 μg/mL gentamicin sulfate and 50 μg/mL ascorbic acid. The inhibitor SB431542 was added as specified in chapter 5.

Specific Aim 4

Alginate constructs were assembled by autoclaving 2% LVG Pronova Alginate in Ca^{2+}, Mg^{2+}-free PBS and then cooling the solution to 37°C. Cells were pelleted down and resuspended in the alginate solution. The cell solution was polymerized using 100mM $CaCl^2$ solution in 11mm diameter by 3mm thick constructs. Once polymerized, the constructs were washed in PBS to remove any excess $CaCl^2$ solution before being moved to media.

Gels were cultured in 24 well plates containing basal media consisting of high glucose DMEM plus antibiotic/antimycotic, non-essential amino acids, 1% ITS+ Premix, 50μg/mL ascorbate and 0.4mM proline (BASAL), basal media plus 10ng/mL TGF-β1 (TGF-β1), or basal media plus 10ng/mL TGF-β1 and 100nM dexamethasone (TGF-β1+DEX). Media were changed every two days.

For the ***passaging*** study, BMSCs were expanded in monolayer for 2, 3 and 4 passages (P2, P3, P4 respectively). After each passage, cells were seeded at $25x10^6$ cells/mL and cultured in BASAL, TGF-β1or TGF-β1+DEX medium for 7 days. For the ***seeding density*** study, passage 3 BMSC consructs were seeded at three concentrations:

12.5x10^6 (LOW), 25x10^6 (MED) and 50x10^6 (HIGH) cells/mL. Gels were cultured in BASAL, TGF-β1or TGF-β1+DEX medium for 10 days. For the ***time course*** study, passage 3 BMSC gels were seeded at 25x10^6 cells/mL and cultured in BASAL or TGF-β1+DEX medium for 2, 4, 7 and 14 days.

Specific Aims 5

Agarose constructs were assembled by autoclaving 3% LMP agarose in 1X Ca^{2+}, Mg^{2+} -free PBS, cooling the solution to 42°C, and suspending the BMSC cell pellet in the appropriate volume yielding 20x10^6 cells per mL of agarose. Agarose constructs were cast in 3mm thick sheets between two electrophoresis plates and punched to a 6mm diameter using biopsy punches.

Constructs were cultured in 24 well plates containing basal media consisting of high glucose DMEM plus antibiotic/antimycotic, non-essential amino acids, 1% ITS+ Premix, 50μg/mL ascorbate and 0.4mM proline (BASAL), basal media plus 10ng/mL TGF-β1 (TGF-β1), or basal media plus 10ng/mL TGF-β1 and 100nM dexamethasone (TGF-β1+DEX). Media were changed every two days.

APPENDIX C FLUOROPHORE-ASSISTED CARBOHYDRATE ELECTROPHORESIS (FACE)

C.1 MATERIALS

Glycosaminoglycan preparation from gels, tissues and proteoglycans

1. Proteinase K (>20 Units/mg)
2. 100 mM ammonium acetate, pH 7.0, freshly prepared
3. Absolute ethanol, pre-cooled to –20°C
4. Microcon Centrifugal Filter Devices (YM-3) [Amicon]
5. Tabletop micro-centrifuge

Glycosaminoglycan lyase digestion

a. Looking at chondroitin sulfate disaccharides:

1. Chondroitinase ABC (Proteus vulgaris) [Calbiochem 230681], dissolved in tissue culture water at 1.5 units/mL (or comparable) and stored in 100 µl aliquots at –80°C for up to 3 months
2. Chondroitinase AC II (Arthrobacter aurenscens) [Calbiochem 230683], dissolved in tissue culture water at 1.5 units/mL (or comparable) and stored in 100 µl aliquots at –80°C for up to 3 months
3. Hyaluronidase (Streptomyces hyaluronlyticus) [Calbiochem 389561], dissolved in tissue culture water at 20 units/mL (or comparable) and stored in 100 µl aliquots at –80°C for up to 3 months
4. 50 mM ammonium acetate, pH 7.0, freshly prepared
5. Micro-centrifuge tubes (1 mL capacity)

b. Looking at keratan sulfate disaccharides:

1. Keratanase (Pseudomonas) [Calbiochem 422402], dissolved in tissue culture water at 5 units/mL (or comparable) and stored in 100 µl aliquots at –80°C
2. Hyaluronidase (Streptomyces hyaluronlyticus) [Calbiochem 389561], dissolved in tissue culture water at 20 units/mL (or comparable) and stored in 100 µl aliquots at –80°C for up to 3 months
3. 50 mM ammonium acetate, pH 7.0, freshly prepared
4. Micro-centrifuge tubes (1 mL capacity)

c. Looking at dermatan sulfate disaccharides:

1. Chondroitinase B (Flavobacterium heparinum) [Calbiochem 230684], dissolved in tissue culture water at 5 units/mL (or comparable) and stored in 100 µl aliquots at –80°C

2. Hyaluronidase (Streptomyces hyaluronlyticus) [Calbiochem 389561], dissolved in tissue culture water at 20 units/mL (or comparable) and stored in 100 µl aliquots at –80°C for up to 3 months.
3. 50 mM ammonium acetate, pH 7.0, freshly prepared
4. Micro-centrifuge tubes (1 mL capacity)

Fluorescent labeling of lyase digestion products

1. 2-aminoacridone (AMAC) [Molecular Probes Inc.]
2. Dimethylsulfoxide (DMSO) (99.7%)
3. Acetic Acid (ACS grade, absolute)
4. Sodium cyanoborohydride (95%) [Sigma Chemical Co]
5. Oven or heating block at 37°C

FACE™ gel electrophoresis of fluorotagged lyase digestion products

1. Mono™ composition gel cassettes [Glyko, Inc.], stored at 4°C until use
2. Mono™ gel running buffer [Glyko, Inc.], freshly prepared in 1.5 L di-H_2O and cooled to 4°C
3. Electrophoresis apparatus [Glyko, Inc.]
4. High voltage power supply

Gel imaging and product quantification

1. UV transilluminator (300-360 nm)
2. Kodak digital science Electrophoresis Documentation and Analysis System

C.2 EXPERIMENTAL PROCEDURE

Glycosaminoglycan preparation from gels, tissues and proteoglycans

1. Digest gels, tissue or proteoglycans normally using either 500 µl proteinase K or papain solution.
2. After full digestion, remove 250 µl of the digest solution to reserve for the DNA and sGAG assay (for determination of total sGAG amount, see note C.1). This 250 µl amount will not be referenced anymore in this protocol.
3. To the remaining 250 µl of digest solution, add 750 µl of ice-cold ethanol (for a final concentration of 75% v/v) and store at –20°C for a minimum of 4 hours.
4. Pellet precipitate in a tabletop micro-centrifuge at 15,000g for 20 minutes.
5. Re-dissolve pellets in tissue culture water (volume depending on amount of expected sGAG, see note C.1).
6. Using the DMMB assay, quantify the amount of sGAG in the re-dissolved solution.

Glycosaminoglycan lyase digestion

a. Looking at chondroitin sulfate disaccharides:

1. Aliquot 5 μg portions of GAG into micro-centrifuge tubes and dry in the speedvac. (See note C.2)
2. Re-suspend dried aliquots in 100 μl of 50 mM ammonium acetate buffer and digest at 37°C for 16 hours with 10 mUnits of Chondroitinase ABC, 10 mUnits of Chondroitinase AC and 10 mUnits of Hyaluronidase. (See note C.2)
3. Cool the digests on ice. Add 900 μl of ice-cold ethanol (for a final concentration of 90% v/v) and store at –20°C for a minimum of 2 hours.
4. Pellet precipitate in a tabletop micro-centrifuge at 15,000g for 20 minutes. The Δdisaccharides are recovered in the supernatant and dried in the speedvac.

b. Looking at keratan sulfate disaccharides:

1. Aliquot 5 μg portions of GAG into micro-centrifuge tubes and dry in the speedvac. (See note C.2)
2. Re-suspend dried aliquots in 100 μl of 50 mM ammonium acetate buffer and digest at 37°C for 16 hours with 20 mUnits of Keratanase and 10 mUnits of Hyaluronidase. (See note C.2)
3. Cool the digests on ice. Add 900 μl of ice-cold ethanol (for a final concentration of 90% v/v) and store at –20°C for a minimum of 2 hours.
4. Pellet precipitate in a tabletop micro-centrifuge at 15,000g for 20 minutes. The Δdisaccharides are recovered in the supernatant and dried in the speedvac.

c. Looking at dermatan sulfate disaccharides:

1. Aliquot 5 μg portions of GAG into micro-centrifuge tubes and dry in the speedvac. (See note C.2)
2. Re-suspend dried aliquots in 100 μl of 50 mM ammonium acetate buffer (pH 7.0) and digest at 37°C for 16 hours with 20 mUnits of Chondroitinase B and 10 mUnits of Hyaluronidase. (See note C.2)
3. Cool the digests on ice. Add 900 μl of ice-cold ethanol (for a final concentration of 90% v/v) and store at –20°C for a minimum of 2 hours.
4. Pellet precipitate in a tabletop micro-centrifuge at 15,000g for 20 minutes. The Δdisaccharides are recovered in the supernatant and dried in the speedvac.

Fluorescent labeling of lyase digestion products

1. Check for prepared AMAC solution. If none is available, make up a 0.1 M solution of AMAC by adding 1 mL of DMSO/acetic acid (85:15, v/v) to 25 mg of AMAC reagent. Aliquot 50 μl portions for storage at –80°C for a maximum of 3 months. (See note C.3)
2. Add 5 μl of AMAC solution to the dried lyase products. Vortex samples and set aside.

3. Prepare a 0.5 M solution of Na-cyanoborohydride in tissue culture water. Add a 10 µl portion to each sample. Vortex to mix and centrifuge for a few seconds to force the samples to the bottom of their tubes.
4. Fluorotag for 16-20 hours at 37°C. Make sure samples are covered with foil to keep out light. (See note C.3)
5. After completion of fluorotagging, cool samples to room temperature. Add 15 µl of heated glycerol. Heating the glycerol makes pipeting much easier. The samples can be analyzed immediately or stored for up to 6 months at –80°C. (See note C.3)

FACE™ gel electrophoresis of fluorotagged lyase digestion products

1. Fill the electrophoresis tank with pre-cooled running buffer and set into a large container of ice to maintain tank and buffer temperature as close to 4°C as possible before and during the run.
2. Remove the pre-cast Mono™ composition gel from its package. Wash the loading wells extensively with running buffer, making sure not to leave any air bubbles in the wells. Place the cassette into the electrophoresis tank. (See note C.4)
3. Load a 5 µl portion of the standard mixture and a 4-6 µl portion of the samples per well. Electrophoresis is carried out at 500 V, with a starting current of ~25 mA per gel and a final current of ~10 mA per gel.
4. Terminate electrophoresis when the salt front nears the bottom of the gel, which is usually achieved after ~60-65 minutes, depending on temperature of the running buffer. (See note C.4)

Gel imaging and product quantification

1. After completion of the electrophoresis, one gel cassette at a time is removed from the tank. Turn the cassette upside down (well down) and wash the wells extensively with de-ionized water to remove any excess fluorotag. Keeping the cassette upside down, wash the glass plates as well. (See note C.5)
2. Place the gel cassette on the transilluminator box with the appropriate light guard, placing the wells on the light guard. (See note C.5)
3. Turn the camera on. Open the software and acquire the camera. Settings are as follows: SYBR Green, 8.5"x11.5", and 1s exposure. It is a good idea to take numerous pictures varying the exposure time from 0.5s to 1.5s. (See note C.5)
4. Take picture/pictures. After straightening and cropping image, save these images.
5. Using the image analysis software, export the net intensities to Excel. Based on the standard lane, convert intensities to pmol values.

C.3 NOTES

Glycosaminoglycan preparation from gels, tissues and proteoglycans

1. Traditional methods of digestion using proteinase K, papain and/or agarase (suspended in tissue culture water) may be employed in this step in place of the ammonium acetate buffer solution. The purpose of the ammonium acetate buffer is to provide an optimal environment for the enzymatic digestion with proteinase K, but may have an effect on other assays (Hoechst). Longer digestion times may need to be employed with other methods.
2. The GAG precipitation step using 75% ethanol may lose a small percentage of the overall GAGs. Unprocessed digest solution should be reserved for the DNA assay and sGAG assay to get an accurate quantification.
3. The separation of GAGs from other protease products, such as collagen peptides, is usually required. These protease products can interfere with the lyase digestion and the recovery of products. However, unsulfated chondroitin and/or short chains of hyaluronan and chondroitin/dermatan sulfate are poorly recovered after ethanol precipitation. Buffer salts and protein products can be alternatively removed by the centrifugation of digests in MicroCon 3 devices (15 minutes at 9,500g at room temperature). The GAG peptides are retained on the filters, recovered in water and dried for further processing.
4. The volume used to re-suspend the GAGs in tissue culture water should be determined based on experience. When a high content of sGAGs is expected, more suspension volume may be used. An acceptable starting volume for unknown amounts is 0.5 mL.

Glycosaminoglycan lyase digestion

1. Anywhere from 1-10 μg portions of sGAG can be analyzed using the FACE method. The enzyme amounts have been optimized for 5 μg portions of sGAG.
2. Using the speedvac is preferable over the lyophilizer. The speedvac keeps the GAGs at the bottom of the tubes, as opposed to drying the GAGs onto the sides of the tubes.
3. Disaccharide digestion may not proceed to completion if the GAGs are insufficiently dissolved before digestion. This can be improved by several short cycles of agitation using a vortex mixer and a 10-minute incubation at 37°C prior to the addition of the lyase.
4. Different enzymes have different levels of pH that optimize digestion. The pH 7.0 was chosen because it is between the pH optimums for the different enzymes. Depending on the specific aim with digestion, the pH may be altered to optimize one enzyme over another. Information about the specifics of the different enzymes can be found in the manufacturers' catalogs. The pH can be monitored by the inclusion of 10 μl of 0.05% phenol red in the digestion buffer.
5. Additional lyases are commercially available. It should be noted that each enzyme has distinct substrate specificity and cleavage modes that will result in a mixture of Δdi- and oligosaccharide products from the GAG chain interior. Conditions for optimal resolution of products generated by these enzymes by FACE will need to be established.

Fluorescent labeling of lyase digestion products

1. AMAC is a fluorescent reagent. It should not be handled under the fluorescent lights of the lab. Take care to dim the direct light when handling the AMAC. Always wear gloves and a lab coat as the AMAC tends to get everywhere.
2. If the AMAC is not stored in –80°C conditions, the acetic acid solution will evaporate off, leaving the solution at an unknown concentration.
3. The Na-cyanoborohydride (Na-CBH) solution should be made up fresh every time and with extreme caution. Na-CBH will turn to cyanide if inhaled, so it is a good idea to wear a face mask and work in the fume hood when preparing this solution. Fresh reagents minimize the decomposition of the reducing agent prior to fluorotagging. There is a Na-CBH waste under the sink in the Levenston lab.
4. Once the samples have begun the fluorotagging process, they should be kept out of direct light.
5. The glycerol can be heated in a 1.5 mL tube to make its addition easier and quicker.
6. After the addition of glycerol, they can be stored at –80°C for up to 6 months. At any temperature less that –80°C, the solution may evaporate off of the samples

FACE™ gel electrophoresis of fluorotagged lyase digestion products

1. Glyko recommends mixing the packet of Mono™ buffer with 1000 mL of di-H_2O, rinsing the packet with 100 mL of di-H_2O and bringing the solution up to a final volume of 1.5 L di-H_2O. This is to insure the correct concentration of buffer.
2. Every time a gel or pair of gels is to be run, freshly chilled running buffer should replace the previous buffer. New ice should be used to keep the electrophoresis tank chilled. The duration of the electrophoresis is dependent on the temperature of the running buffer and tank. Also, the 40% PAGE gels will tend to melt if great care is not taken to always replace the running buffer with freshly chilled buffer and to re-pack the tank in ice. It is a good idea to practice with only running one gel at a time (and using the glass plate on the opposite side), as two gels tends to heat up rather quickly.
3. Electrophoresis times should be monitored to adjust for variable rates of sample migration on different gel batches, obtained from the supplier.

Gel imaging and product quantification

1. Excess fluorotag will mask the intensity of the samples if it isn't washed away. The cassette should be placed on the light guard with the wells overlapping the guard.
2. A shorter exposure time will allow for the quantification of brighter band and a longer exposure time will allow for the quantification of less intense bands. If bands run together (as is occasionally the case with chondroitin-4 and chondroitin-6 sulfates), the software separates them using a Gaussian distribution. As long as the software can distinguish the bands repeatably and the intensity of the bands fall within the linear standard curve, the results can be considered trustworthy. If the bands are in general too bright, the gel should be re-run loading less sample in the wells.
3. A sample containing a range of concentrations (20-300 pmol) of Δdisaccharide standards are to be included on every face gel to generate a standard curve of pixel densities per pmol of saccharide for product identification and quantification in

experimental samples. It is recommended that the amount of each individual Δdisaccharide as provided by the supplier be validated first. This can also be performed by FACE analysis. Portions of Δdisaccharide standards (1 nmol of each) and 1 nmol of glucose should be fluorotagged and electrophoretically separated. Based on the known glucose standard, the actual amounts of the Δdisaccharide standards can be determined.

APPENDIX D MECHANICAL LOADING SYSTEM

D.1 DESIGN

The mechanical loading system was custom designed (Figure 12) to impose the compression protocols (all designing done by Stacy Imler and Andrew Martinez, Georgia Institute of Technology). The entire system fit on a shelf within an incubator (Forma Scientific, Marietta, OH) maintained at 37ºC and 5% carbon dioxide. The compression chambers were made of polysulfone (all materials and machining done by JM Machining, Lawrenceville, GA), and a single chamber held up to eight samples. The samples resided in the individual wells of the bottom part of the assembly that were 0.620" in diameter and 0.50" deep. Four chambers could either be loaded into the mechanical loading frame or used alone to impose static compression. The top part of the chamber assembly contained stainless steel platens that were 0.375" in diameter by 0.50" long. To impart static compression, spacers made of stainless steel were machined to specific heights in order to compress the samples to a given height. To impart oscillatory compression, the translation of motion from the table to the samples was done using an L-shaped bracket that was made of 6061 aluminum. The tops of the chambers affixed directly to the bracket, while the bottom of the chamber sat stationary on the base plate.

The application of oscillatory compression was attained by controlling the motion of the 404XR square rail linear table (Parker Automation, Irwin, PA). The BE231 servo motor was driven by the VIX500AE servo drive (both Parker Automation, Rohnert Park, CA). Using the Galil WSDK Programming Software, the sinusoidal input for table motion was sent to the Galil DMC-2113 servo controller (Galil Motion Control, Rocklin,

CA). The position of the bracket was detected using a linear encoder that was mounted external to the linear table.

Figure X: Custom designed compressive loading system

D.2 Set-up Protocol for Dynamic Loading

1. Check the system out before you load your samples
    a. If the control box and computer are OFF, power them both ON.
    b. Open up WSDK
    c. Open up the terminal in the top toolbar
2. Type in MO to disable the motor
3. Check the PID parameters by typing in KP?, KI?, and KD?
4. Set P/I/D parameters to 3/0/30 by typing KP3, KI0, KD30 [BLUE frame]
    2.5/0/18 by typing KP2.5, KI0, KD18 [GOLD frame]
5. Set the voltage offset to -0.055 by typing OF-0.055 [BLUE frame]
    0.055 by typing OF0.055 [GOLD frame]
6. Set the mode to single loop by typing DV0

7. In the right window (program window), open the program for the oscillatory compression = CIRCLES_FORE_ORIGINAL_SLOW

8. Download the program to the controller by hitting the download button

9. Type in XQ to execute the program to check for stability

    a. If stable, type in ST to stop the execution. The motor will still be enabled at this point until you type in MO. Continue to step 10.

    b. If unstable, hit the kill switch and exit out of all software. Cycle the power on the control box and start from the beginning.

10. Raise the platform to a location that is reasonable for you to get your cassettes loaded.

    a. Do this by setting the speed to 3000 counts/sec by typing SP3000

    b. Set acceleration and deceleration to 25600 counts/sec^2 by typing AC25600 and DC25600

    c. Also, disable the Off-on-error command that was in the oscillatory compression program by typing in OE0.

    d. Remember ↑- and ↓+ AND 1 count = 0.1 μm. I usually raise the platform by 5000 or 10000 counts at a time

    e. Define current position as 0 by typing DP0

    f. Raise platform by typing in PAxxx and then BG

11. Disable the motor by typing MO

12. Load your cassettes in the hood

13. Take the rig out of the incubator and place cassettes in the RIG

14. Manually push down on the platform until it is in contact with the tops of the cassettes. Simultaneously, type in DP0 to reset the new zero position.

15. Enable the motor by typing SH

16. Raise platform by typing PA-40000 and then BG so that you can get your cassettes out

17. Return platform to the zero point by typing PA0 and then BG. Check position by typing in TP because it often doesn't make it all the way to zero. Retype PA0 to get the platform as close to zero as possible.

18. Download the CIRCLES program

19. Type in XQ to check for stability

20. Type in ST. Also, disable the Off-on-error command that was in the oscillatory compression program by typing in OE0

21. Raise platform by typing PA-40000 and then BG so that you can get your cassettes in the RIG

22. Place cassettes in the RIG and return the platform close to the tops of the cassettes (within 1000 counts). Do this gradually until you get to -1000 counts.

23. Disable the motor by typing MO.

24. Lightly screw in the large bolts (5/16" allen wrench) such that they are attached to the cassette tops

25. Unscrew the small alignment screws (M4 allen wrench) and take them out of the assembly

26. Fully tighten the large bolts

27. Enable the motor by typing SH

28. Slide the spacers out from the assembly

    a. If the spacers don't slide out so easily, raise the platform by 1000 counts to release the pressure from the assembly.

    b. Do not raise the platform beyond 2000 counts! This corresponds to 200 μm from the 10% static offset. Your samples my float out from under the platens if they are raised too high!

29. Return the platform to the zero point by typing PA0 and then BG.

30. Check that the tuning parameters and the binary parameters (from Useful Commands) are correct.

31. Download the CIRCLES program

32. Type in XQ to start the loading.

D.3 DYNAMIC COMPRESSION PROGRAM

This program is written in the Galil WSDK software and programming language. The program utilizes the circle (CR) function to impart a sinusoidal motion. The commands that control the specific motion are: vector speed (VS) and circle (CR). Vector speed is an integer that is a product of: $1.024*(2\pi Rf)$. R is the radius in linear encoder counts (1 count = 0.1 μm) of the circle. In the sinusoidal application, R represents the amplitude of the sine wave. f is the frequency in Hz. The value of 1.024 represents necessary compensation for a lag in time between the controller and the command, as stated in the Galil literature. The circle command is composed of three arguments: CR $R,\theta,\Delta\theta$. R is the same value from the VS command. θ is where on the circle the motion will begin from in degrees. Δθ is the number of degrees around a circle that the command will follow. In the program θ is set at -90° to begin at a 0 position, and Δθ is set at 360° to complete a single circle. The CR command exists in a jump (JP) loop, and therefore is commanded to continue until manually stopped.

```
#CIRCLES_FORE_ORIG_SLOW
VMAN
SH
OE1
ER 1200
DP0
VA 680000
VD 680000
VS 5787
CR 900,-90,360
BGS
#L
CR 900,-90,360
#WAIT ; JP #WAIT ; _LM=0
JP#L
EN
```

APPENDIX E WESTERN BLOTTING PROTOCOL

E.1 BUFFERS AND SOLUTIONS

RADIOIMMUNOPRECIPITATION (RIPA) BUFFER

Pre-made solution: 150mM Tris (pH 7.2), 150mM NaCl, 1% Triton X-100, 1% deoxycholate, 0.1% SDS, 5mM NaF

Add fresh: 2mM Na_3VO_4 (activated), 1% Calbiochem protease inhibitor stock

ELECTRODE BUFFER

50mM Tris Base, 384mM Glycine, 0.2% SDS

TRANSFER BUFFER

25mM Tris Base, 192 mM Glycine, 200mL MeOH

10X TRIS BUFFERED SALINE (TBS)

200mM Tris Base, 1.37M NaCl, pH to 7.6

TBS WITH TWEEN

1X TBS, 0.1% TWEEN-20

BLOCKING SOLUTION

1X TBS, 0.1% TWEEN-20, 1% dry non-fat milk

BLOTTO WITH TWEEN

1X TBS, 0.1% TWEEN-20, 5% dry non-fat milk

SAMPLE BUFFER

200µL Tris-glycine SDS 2X buffer (Invitrogen #LC2676), 200uL 6M Urea, 0.012g DTT

E.2 AGAROSE GEL TAKE-DOWN

Preparation

1. Prepare RIPA buffer. Make sure to add protease inhibitors.
2. Aliquot out RIPA buffer into 1.5 mL Eppendorf tubes that have been labeled.
    a. Use 0.5 mL of RIPA buffer for a 6 mm diameter x 3 mm thick gel.
    b. Store aliquots at 4°C until needed.
3. Have liquid nitrogen and ice on hand.

Take-down Part I

4. Immediately after experiment has completed, put gels into RIPA buffer.
    a. Using a non-serrated blunt nose forceps, crush the agarose gel until it is semi-homogenized. Work quickly.
    b. Clean forceps between groups to minimize cross-contamination.
    c. After homogenization, seal all caps.
    d. Place into liquid nitrogen until frozen.

e. Move out of nitrogen and onto ice.

Take-down Part II

5. Homogenize samples.
    a. Take samples off of ice to thaw, but keep cool once thawed.
    b. Vortex each sample for 15 seconds. Use a timer to be consistent.
    c. Let sit on ice for 10 minutes.
    d. Vortex each sample again for 15 second.
6. Concentrate samples.
    a. Quickly centrifuge agarose to the bottom of the tube.
    b. Pipet the supernatant (with as little agarose as possible) into a Microcon filter device (YM-30 used for Smads and TGF-β Receptor I).
    c. Centrifuge for 30 min at 14,000 x g.
    d. Remove assembly from centrifuge. Separate vial from sample reservoir.
    e. Place sample reservoir upside down in a new vial.
    f. Centrifuge for 3 minutes at 2000 x g to transfer concentrate to vial.

Quantify protein or DNA

7. Use either a μ-BCA kit to quantify total protein OR the Hoechst dye assay to quantify total DNA.
    a. Protein cannot be quantified after sample loading buffer is added (with reducing agent), but DNA can.

Storage of sample

8. Add sample loading buffer (either 2X or 6X depending on concentration).
9. Store at -20°C.

E.3 WESTERN BLOTTING

1. Boil samples for 4 minutes prior to loading for separating.
2. SDS-PAGE: Run samples on a Novex 4-12% gel in electrode buffer at 180 volts for approximately 1 hour at room temperature.
    a. On each gel was a molecular weight standard, as well as a standard for included for normalization purposes. A consistent amount of the same standard was loaded onto each gel for comparison between gels. The standard was processed in the same way as the samples and consisted of unloaded gels seeded with BMSCs and treated to 10ng/mL TGF-β1.
3. Transfer: Transfer proteins onto nitrocellulose membrane in transfer buffer at 30 volts for 90 minutes at room temperature.
4. Block membrane for 1 hour in blocking solution at room temperature.
5. Incubate membranes in primary antibody (in Blotto with TWEEN) overnight at room temperature. Working concentrations of antibodies used:
    a. Smad 2/3 1:1000
    b. pSmad 2/3 1:1000
    c. TGF-β Receptor I 1:1000
6. Wash in TBS with TWEEN three times for 5 minutes each.

7. Incubate for 1 hour in secondary antibody in Blotto with Tween.
    a. Secondary antibody used: Biotin SP-conjugated anti-rabbit IgG
    b. Dilution of secondary: 1:10,000
8. Wash in TBS with TWEEN three times for 5 minutes each.
9. Incubate for 1 hour in tertiary antibody in Blotto with Tween.
    a. Secondary antibody used: AP conjugated anti-Biotin
    b. Dilution of tertiary: 1:10,000
10. Wash in TBS with TWEEN three times for 10 minutes each.
11. Develop with ECL for 7 minutes.
    a. 1mL ECL per membrane
12. Dry membranes.
13. Image using the Fuju Film Phosphoimager
    a. Plate used: FLA Fluor State 2340
    b. Software used: Image Reader Software
    c. Sample mode: Fluor 473, Filter Y520, 16 bit gradation, 50 resolution, F10 sensitivity
14. File exported to a bitmap and analyzed using Photoshop.

APPENDIX D IMMUNOHISTOCHEMISTRY PROTOCOL

D.1 FIXED FROZEN SAMPLE PREPARATION

At time of harvest, constructs were rinsed in PBS and fixed in 10% neutral buffered formalin (NBF) for 4hr at room temperature. Samples were then transferred to 30% sucrose for 48hrs at 4C, embedded in OCT, and frozen in liquid nitrogen-cooled isopentane. Frozen blocks were sectioned to 7μm using a cryostat and placed on superfrost plus slides. Prior to immunostaining, frozen sections were thawed and dried for 20min. at room temperature. Following fixation in acetone for 5min., slides were dried for at least 5 min., and rehydrated in PBS.

D.2 FORMALIN FIXED, PARAFFIN EMBEDDED SAMPLE PREPARATION

At time of harvest, constructs were rinsed in PBS and fixed in 10% NBF for 48hr at 4C. Samples were then processed for dehydration and infiltration by paraffin in a Thermo Shandon Pathcenter, sectioned to 4μm on a rotary microtome, placed on superfrost plus slides, and dried at 37C overnight. Prior to immunostaining, sections were deparaffinized and rehydrated through xylene and graded alcohols in a Leica Autostainer XL. Slides probed for Smad2/3 and p-Smad2 underwent antigen retrieval involving incubation in 10mM citrate pH 6.0 buffer and heat in a pressure cooker for 10min.

D.3 IMMUNOHISTOCHEMISTRY

Slides were loaded into Sequenza staining racks with ~500μL PBS and rinsed 3 times with 300μL PBS. Frozen sections probed for collagen I and collagen II underwent enzymatic antigen retrieval with 0.5x trypsin at 37C for 15min. Paraffin-embedded sections probed for Smad2/3 or p-Smad2 were treated with 0.1U/mL chondroitinase ABC at 37C for 30min. Slides were then rinsed 3 times with 300μL PBS and blocked for 1hr at room temperature with 2% normal goat serum, 0.1% gelatin, 0.5% Tween-20, and 1% BSA in PBS. A solution of rabbit anti-collagen II (1:100) and mouse anti-collagen I (1:100) was prepared with 1% BSA/0.1% Gelatin/PBS. Alternatively, rabbit anti-Smad2/3 (1:100) or rabbit anti-p-Smad2 (1:1000) was prepared. Similar solutions were prepared with 10μg/mL non-immune rabbit IgG (collagen co-stained slides were also treated with 10μg/mL non-immune mouse IgG) as negative controls. Samples were incubated with 150μL of primary antibody solution for 1hr at room temperature, and then rinsed 3 times with 300μL PBS. A secondary antibody solution was prepared with goat anti-rabbit AlexaFluor488 (1:100) in PBS with 1.25μg/mL DAPI as a nuclear counterstain. For collagen I/II co-stained slides goat anti-mouse AlexaFluor594 was included (1:100), and for Smad2/3 and p-Smad2 stained slides Alexafluor 546-Phalloidin was added at 100μg/mL. Samples were incubated with 200μL of secondary antibody solution for 1hr at room temperature in the dark. Slides were then rinsed 3 times with 300μL PBS, mounted in gel-mount, and coverslipped.

D.4 IMAGING

Images of individual channels were captured using a Nikon E600 epifluorescent microscope fit with a CCD camera and filters for FITC, TRITC, and DAPI. QCapture software was used to adjust exposure times for each channel. Adobe Photoshop image analysis software was used to consistently apply brightness and contrast adjustments and to combine images.

APPENDIX E STATISTICAL ANALYSIS

Unless specified, the data were analyzed with a multi-factor General Linear Model using Minitab Release 12.23 (Minitab Inc., State College, PA). A Tukey's Test for post-hoc analysis was performed if necessary. A value of $p<0.05$ indicated significance.

Reference List

1. Iannone,F. & Lapadula,G. The pathophysiology of osteoarthritis. *Aging Clin. Exp. Res.* **15**, 364-372 (2003).

2. Buckwalter,J.A., Saltzman,C. & Brown,T. The impact of osteoarthritis: implications for research. *Clin. Orthop. Relat Res.* S6-15 (2004).

3. Malemud,C.J. & Goldberg,V.M. Future directions for research and treatment of osteoarthritis. *Front Biosci.* **4**, D762-D771 (1999).

4. Gao,J. & Caplan,A.I. Mesenchymal stem cells and tissue engineering for orthopaedic surgery. *Chir Organi Mov* **88**, 305-316 (2003).

5. von der,M.K., Gauss,V., von der,M.H. & Muller,P. Relationship between cell shape and type of collagen synthesised as chondrocytes lose their cartilage phenotype in culture. *Nature* **267**, 531-532 (1977).

6. Caplan,A.I. Mesenchymal stem cells. *J. Orthop. Res.* **9**, 641-650 (1991).

7. Caplan,A.I. & Bruder,S.P. Mesenchymal stem cells: building blocks for molecular medicine in the 21st century. *Trends Mol. Med.* **7**, 259-264 (2001).

8. Hung,C.T., Mauck,R.L., Wang,C.C., Lima,E.G. & Ateshian,G.A. A paradigm for functional tissue engineering of articular cartilage via applied physiologic deformational loading. *Ann. Biomed. Eng* **32**, 35-49 (2004).

9. Poole,A.R. *et al.* Composition and structure of articular cartilage: a template for tissue repair. *Clin. Orthop. Relat Res.* S26-S33 (2001).

10. Ateshian,G.A. & Hung,C.T. Patellofemoral joint biomechanics and tissue engineering. *Clin. Orthop. Relat Res.* 81-90 (2005).

11. Frenkel,S.R. & Di Cesare,P.E. Scaffolds for articular cartilage repair. *Ann. Biomed. Eng* **32**, 26-34 (2004).

12. Cremer,M.A., Rosloniec,E.F. & Kang,A.H. The cartilage collagens: a review of their structure, organization, and role in the pathogenesis of experimental arthritis in animals and in human rheumatic disease. *J. Mol. Med.* **76**, 275-288 (1998).

13. Alford,J.W. & Cole,B.J. Cartilage restoration, part 1: basic science, historical perspective, patient evaluation, and treatment options. *Am. J. Sports Med.* **33**, 295-306 (2005).

14. Alford,J.W. & Cole,B.J. Cartilage restoration, part 2: techniques, outcomes, and future directions. *Am. J. Sports Med.* **33**, 443-460 (2005).

15. Bayliss,M.T., Osborne,D., Woodhouse,S. & Davidson,C. Sulfation of chondroitin sulfate in human articular cartilage. The effect of age, topographical position, and zone of cartilage on tissue composition. *J. Biol. Chem.* **274**, 15892-15900 (1999).

16. Eyre,D.R. & Muir,H. The distribution of different molecular species of collagen in fibrous, elastic and hyaline cartilages of the pig. *Biochem. J.* **151**, 595-602 (1975).

17. Plaas,A.H., West,L.A., Wong-Palms,S. & Nelson,F.R. Glycosaminoglycan sulfation in human osteoarthritis. Disease-related alterations at the non-reducing termini of chondroitin and dermatan sulfate. *J. Biol. Chem.* **273**, 12642-12649 (1998).

18. Hascall,V.C. & Sajdera,S.W. Physical properties and polydispersity of proteoglycan from bovine nasal cartilage. *J. Biol. Chem.* **245**, 4920-4930 (1970).

19. Frenkel,S.R. *et al.* Transforming growth factor beta superfamily members: role in cartilage modeling. *Plast. Reconstr. Surg.* **105**, 980-990 (2000).

20. Eyre,D.R. & Muir,H. The distribution of different molecular species of collagen in fibrous, elastic and hyaline cartilages of the pig. *Biochem. J.* **151**, 595-602 (1975).

21. Sandy,J.D. & Plaas,A.H. Age-related changes in the kinetics of release of proteoglycans from normal rabbit cartilage explants. *J. Orthop. Res.* **4**, 263-272 (1986).

22. Morales,T.I. & Hascall,V.C. Correlated metabolism of proteoglycans and hyaluronic acid in bovine cartilage organ cultures. *J. Biol. Chem.* **263**, 3632-3638 (1988).

23. Ilic,M.Z., Handley,C.J., Robinson,H.C. & Mok,M.T. Mechanism of catabolism of aggrecan by articular cartilage. *Arch. Biochem. Biophys.* **294**, 115-122 (1992).

24. Lark,M.W. *et al.* Cell-mediated catabolism of aggrecan. Evidence that cleavage at the "aggrecanase" site (Glu373-Ala374) is a primary event in proteolysis of the interglobular domain. *J. Biol. Chem.* **270**, 2550-2556 (1995).

25. Ilic,M.Z., Haynes,S.R., Winter,G.M. & Handley,C.J. Kinetics of release of aggrecan from explant cultures of bovine cartilage from different sources and from animals of different ages. *Acta Orthop. Scand. Suppl* **266**, 33-37 (1995).

26. Sandy,J.D., Flannery,C.R., Neame,P.J. & Lohmander,L.S. The structure of aggrecan fragments in human synovial fluid. Evidence for the involvement in osteoarthritis of a novel proteinase which cleaves the Glu 373-Ala 374 bond of the interglobular domain. *J. Clin. Invest* **89**, 1512-1516 (1992).

27. Roughley,P.J. Articular cartilage and changes in arthritis: noncollagenous proteins and proteoglycans in the extracellular matrix of cartilage. *Arthritis Res.* **3**, 342-347 (2001).

28. Scully,S.P., Lee,J.W., Ghert,P.M.A. & Qi,W. The role of the extracellular matrix in articular chondrocyte regulation. *Clin. Orthop. Relat Res.* S72-S89 (2001).

29. Knudson,C.B. & Knudson,W. Hyaluronan and CD44: modulators of chondrocyte metabolism. *Clin. Orthop. Relat Res.* S152-S162 (2004).

30. Sandell,L.J. & Aigner,T. Articular cartilage and changes in arthritis. An introduction: cell biology of osteoarthritis. *Arthritis Res.* **3**, 107-113 (2001).

31. van der Kraan,P.M., Buma,P., van Kuppevelt,T. & van den Berg,W.B. Interaction of chondrocytes, extracellular matrix and growth factors: relevance for articular cartilage tissue engineering. *Osteoarthritis. Cartilage.* **10**, 631-637 (2002).

32. Martin,J.A., Brown,T., Heiner,A. & Buckwalter,J.A. Post-traumatic osteoarthritis: the role of accelerated chondrocyte senescence. *Biorheology* **41**, 479-491 (2004).

33. Brommer,H. *et al.* Influence of age, site, and degenerative state on the speed of sound in equine articular cartilage. *Am. J. Vet. Res.* **66**, 1175-1180 (2005).

34. Shelbourne,K.D., Jari,S. & Gray,T. Outcome of untreated traumatic articular cartilage defects of the knee: a natural history study. *J. Bone Joint Surg. Am.* **85-A Suppl 2**, 8-16 (2003).

35. Jurvelin,J., Kiviranta,I., Tammi,M. & Helminen,J.H. Softening of canine articular cartilage after immobilization of the knee joint. *Clin. Orthop. Relat Res.* 246-252 (1986).

36. Gorevic,P.D. Osteoarthritis. A review of musculoskeletal aging and treatment issues in geriatric patients. *Geriatrics* **59**, 28-32 (2004).

37. Buckwalter,J.A., Martin,J. & Mankin,H.J. Synovial joint degeneration and the syndrome of osteoarthritis. *Instr. Course Lect.* **49**, 481-489 (2000).

38. Butler,D.L., Shearn,J.T., Juncosa,N., Dressler,M.R. & Hunter,S.A. Functional tissue engineering parameters toward designing repair and replacement strategies. *Clin. Orthop. Relat Res.* S190-S199 (2004).

39. Redman,S.N., Oldfield,S.F. & Archer,C.W. Current strategies for articular cartilage repair. *Eur. Cell Mater.* **9**, 23-32 (2005).

40. Gillogly,S.D., Voight,M. & Blackburn,T. Treatment of articular cartilage defects of the knee with autologous chondrocyte implantation. *J. Orthop. Sports Phys. Ther.* **28**, 241-251 (1998).

41. Steadman,J.R. *et al.* The microfracture technique in the treatment of full-thickness chondral lesions of the knee in National Football League players. *J. Knee. Surg.* **16**, 83-86 (2003).

42. Easley,M.E. & Scranton,P.E., Jr. Osteochondral autologous transfer system. *Foot Ankle Clin.* **8**, 275-290 (2003).

43. Chow,J.C., Hantes,M.E., Houle,J.B. & Zalavras,C.G. Arthroscopic autogenous osteochondral transplantation for treating knee cartilage defects: a 2- to 5-year follow-up study. *Arthroscopy* **20**, 681-690 (2004).

44. Minas,T. & Nehrer,S. Current concepts in the treatment of articular cartilage defects. *Orthopedics* **20**, 525-538 (1997).

45. Haapala,J. *et al.* Coordinated regulation of hyaluronan and aggrecan content in the articular cartilage of immobilized and exercised dogs. *J. Rheumatol.* **23**, 1586-1593 (1996).

46. Bird,J.L., Platt,D., Wells,T., May,S.A. & Bayliss,M.T. Exercise-induced changes in proteoglycan metabolism of equine articular cartilage. *Equine Vet. J.* **32**, 161-163 (2000).

47. Mauck,R.L. *et al.* Functional tissue engineering of articular cartilage through dynamic loading of chondrocyte-seeded agarose gels. *J. Biomech. Eng* **122**, 252-260 (2000).

48. Sah,R.L. *et al.* Biosynthetic response of cartilage explants to dynamic compression. *J. Orthop. Res.* **7**, 619-636 (1989).

49. Lee,D.A. *et al.* Chondrocyte deformation within compressed agarose constructs at the cellular and sub-cellular levels. *J. Biomech.* **33**, 81-95 (2000).

50. Mauck,R.L. *et al.* Functional tissue engineering of articular cartilage through dynamic loading of chondrocyte-seeded agarose gels. *J. Biomech. Eng* **122**, 252-260 (2000).

51. Buschmann,M.D., Gluzband,Y.A., Grodzinsky,A.J. & Hunziker,E.B. Mechanical compression modulates matrix biosynthesis in chondrocyte/agarose culture. *J. Cell Sci.* **108 (Pt 4)**, 1497-1508 (1995).

52. Davisson,T., Kunig,S., Chen,A., Sah,R. & Ratcliffe,A. Static and dynamic compression modulate matrix metabolism in tissue engineered cartilage. *J. Orthop. Res.* **20**, 842-848 (2002).

53. Yellowley,C.E., Jacobs,C.R. & Donahue,H.J. Mechanisms contributing to fluid-flow-induced Ca2+ mobilization in articular chondrocytes. *J. Cell Physiol* **180**, 402-408 (1999).

54. Guilak,F. *et al.* Mechanically induced calcium waves in articular chondrocytes are inhibited by gadolinium and amiloride. *J. Orthop. Res.* **17**, 421-429 (1999).

55. Wu,Q.Q. & Chen,Q. Mechanoregulation of chondrocyte proliferation, maturation, and hypertrophy: ion-channel dependent transduction of matrix deformation signals. *Exp. Cell Res.* **256**, 383-391 (2000).

56. Sharma,B. & Elisseeff,J.H. Engineering structurally organized cartilage and bone tissues. *Ann. Biomed. Eng* **32**, 148-159 (2004).

57. Rahaman,M.N. & Mao,J.J. Stem cell-based composite tissue constructs for regenerative medicine. *Biotechnol. Bioeng.* **91**, 261-284 (2005).

58. Benya,P.D. & Shaffer,J.D. Dedifferentiated chondrocytes reexpress the differentiated collagen phenotype when cultured in agarose gels. *Cell* **30**, 215-224 (1982).

59. Caplan,A.I. Mesenchymal stem cells. *J. Orthop. Res.* **9**, 641-650 (1991).

60. Bosnakovski,D. *et al.* Chondrogenic differentiation of bovine bone marrow mesenchymal stem cells in pellet cultural system. *Exp. Hematol.* **32**, 502-509 (2004).

61. Huang,C.Y., Reuben,P.M., D'Ippolito,G., Schiller,P.C. & Cheung,H.S. Chondrogenesis of human bone marrow-derived mesenchymal stem cells in agarose culture. *Anat. Rec.* **278A**, 428-436 (2004).

62. Steinert,A. *et al.* Chondrogenic differentiation of mesenchymal progenitor cells encapsulated in ultrahigh-viscosity alginate. *J. Orthop. Res.* **21**, 1090-1097 (2003).

63. Yang,I.H. *et al.* Comparison of Phenotypic Characterization between "Alginate Bead" and "Pellet" Culture Systems as Chondrogenic Differentiation Models for Human Mesenchymal Stem Cells. *Yonsei Med. J.* **45**, 891-900 (2004).

64. Stevens,M.M., Marini,R.P., Martin,I., Langer,R. & Prasad,S., V. FGF-2 enhances TGF-beta1-induced periosteal chondrogenesis. *J. Orthop. Res.* **22**, 1114-1119 (2004).

65. Caplan,A.I. Mesenchymal stem cells. *J. Orthop. Res.* **9**, 641-650 (1991).

66. Roelen,B.A. & Dijke,P. Controlling mesenchymal stem cell differentiation by TGFBeta family members. *J. Orthop. Sci.* **8**, 740-748 (2003).

67. Pittenger,M.F. *et al.* Multilineage potential of adult human mesenchymal stem cells. *Science* **284**, 143-147 (1999).

68. Mackay,A.M. *et al.* Chondrogenic differentiation of cultured human mesenchymal stem cells from marrow. *Tissue Eng* **4**, 415-428 (1998).

69. Miyazono,K. Positive and negative regulation of TGF-beta signaling. *J. Cell Sci.* **113 (Pt 7)**, 1101-1109 (2000).

70. Moustakas,A., Souchelnytskyi,S. & Heldin,C.H. Smad regulation in TGF-beta signal transduction. *J. Cell Sci.* **114**, 4359-4369 (2001).

71. Nakao,A. *et al.* TGF-beta receptor-mediated signalling through Smad2, Smad3 and Smad4. *EMBO J.* **16**, 5353-5362 (1997).

72. Mehra,A. & Wrana,J.L. TGF-beta and the Smad signal transduction pathway. *Biochem. Cell Biol.* **80**, 605-622 (2002).

73. Yonekura,A. *et al.* Transforming growth factor-beta stimulates articular chondrocyte cell growth through p44/42 MAP kinase (ERK) activation. *Endocr. J.* **46**, 545-553 (1999).

74. Rosado,E., Schwartz,Z., Sylvia,V.L., Dean,D.D. & Boyan,B.D. Transforming growth factor-beta1 regulation of growth zone chondrocytes is mediated by multiple interacting pathways. *Biochim. Biophys. Acta* **1590**, 1-15 (2002).

75. Hirota,Y. *et al.* Activation of specific MEK-ERK cascade is necessary for TGFbeta signaling and crosstalk with PKA and PKC pathways in cultured rat articular chondrocytes. *Osteoarthritis. Cartilage.* **8**, 241-247 (2000).

76. Watanabe,H., de Caestecker,M.P. & Yamada,Y. Transcriptional cross-talk between Smad, ERK1/2, and p38 mitogen-activated protein kinase pathways regulates transforming growth factor-beta-induced aggrecan gene expression in chondrogenic ATDC5 cells. *J. Biol. Chem.* **276**, 14466-14473 (2001).

77. Grimaud,E., Heymann,D. & Redini,F. Recent advances in TGF-beta effects on chondrocyte metabolism. Potential therapeutic roles of TGF-beta in cartilage disorders. *Cytokine Growth Factor Rev.* **13**, 241-257 (2002).

78. Wakitani,S. *et al.* Mesenchymal cell-based repair of large, full-thickness defects of articular cartilage. *J. Bone Joint Surg. Am.* **76**, 579-592 (1994).

79. Huang,C.Y., Hagar,K.L., Frost,L.E., Sun,Y. & Cheung,H.S. Effects of cyclic compressive loading on chondrogenesis of rabbit bone-marrow derived mesenchymal stem cells. *Stem Cells* **22**, 313-323 (2004).

80. Elder,S.H., Goldstein,S.A., Kimura,J.H., Soslowsky,L.J. & Spengler,D.M. Chondrocyte differentiation is modulated by frequency and duration of cyclic compressive loading. *Ann. Biomed. Eng* **29**, 476-482 (2001).

81. Elder,S.H., Kimura,J.H., Soslowsky,L.J., Lavagnino,M. & Goldstein,S.A. Effect of compressive loading on chondrocyte differentiation in agarose cultures of chick limb-bud cells. *J. Orthop. Res.* **18**, 78-86 (2000).

82. Angele,P. *et al.* Cyclic, mechanical compression enhances chondrogenesis of mesenchymal progenitor cells in tissue engineering scaffolds. *Biorheology* **41**, 335-346 (2004).

83. Mauney,J.R. *et al.* Mechanical stimulation promotes osteogenic differentiation of human bone marrow stromal cells on 3-D partially demineralized bone scaffolds in vitro. *Calcif. Tissue Int.* **74**, 458-468 (2004).

84. Plaas,A.H., West,L.A., Wong-Palms,S. & Nelson,F.R. Glycosaminoglycan sulfation in human osteoarthritis. Disease-related alterations at the non-reducing termini of chondroitin and dermatan sulfate. *J. Biol. Chem.* **273**, 12642-12649 (1998).

85. Hascall,V.C. & Sajdera,S.W. Physical properties and polydispersity of proteoglycan from bovine nasal cartilage. *J. Biol. Chem.* **245**, 4920-4930 (1970).

86. Eyre,D.R. & Muir,H. The distribution of different molecular species of collagen in fibrous, elastic and hyaline cartilages of the pig. *Biochem. J.* **151**, 595-602 (1975).

87. Morales,T.I. & Hascall,V.C. Correlated metabolism of proteoglycans and hyaluronic acid in bovine cartilage organ cultures. *J. Biol. Chem.* **263**, 3632-3638 (1988).

88. Ilic,M.Z., Handley,C.J., Robinson,H.C. & Mok,M.T. Mechanism of catabolism of aggrecan by articular cartilage. *Arch. Biochem. Biophys.* **294**, 115-122 (1992).

89. Lark,M.W. *et al.* Cell-mediated catabolism of aggrecan. Evidence that cleavage at the "aggrecanase" site (Glu373-Ala374) is a primary event in proteolysis of the interglobular domain. *J. Biol. Chem.* **270**, 2550-2556 (1995).

90. Ilic,M.Z., Haynes,S.R., Winter,G.M. & Handley,C.J. Kinetics of release of aggrecan from explant cultures of bovine cartilage from different sources and from animals of different ages. *Acta Orthop. Scand. Suppl* **266**, 33-37 (1995).

91. Sandy,J.D., Flannery,C.R., Neame,P.J. & Lohmander,L.S. The structure of aggrecan fragments in human synovial fluid. Evidence for the involvement in osteoarthritis of a novel proteinase which cleaves the Glu 373-Ala 374 bond of the interglobular domain. *J. Clin. Invest* **89**, 1512-1516 (1992).

92. Brown,M.P., West,L.A., Merritt,K.A. & Plaas,A.H. Changes in sulfation patterns of chondroitin sulfate in equine articular cartilage and synovial fluid in response to aging and osteoarthritis. *Am. J. Vet. Res.* **59**, 786-791 (1998).

93. Plaas,A.H., Wong-Palms,S., Roughley,P.J., Midura,R.J. & Hascall,V.C. Chemical and immunological assay of the nonreducing terminal residues of chondroitin sulfate from human aggrecan. *J. Biol. Chem.* **272**, 20603-20610 (1997).

94. Rizkalla,G., Reiner,A., Bogoch,E. & Poole,A.R. Studies of the articular cartilage proteoglycan aggrecan in health and osteoarthritis. Evidence for molecular heterogeneity and extensive molecular changes in disease. *J. Clin. Invest* **90**, 2268-2277 (1992).

95. Visco,D.M., Johnstone,B., Hill,M.A., Jolly,G.A. & Caterson,B. Immunohistochemical analysis of 3-B-(-) and 7-D-4 epitope expression in canine osteoarthritis. *Arthritis Rheum.* **36**, 1718-1725 (1993).

96. Slater,R.R., Jr., Bayliss,M.T., Lachiewicz,P.F., Visco,D.M. & Caterson,B. Monoclonal antibodies that detect biochemical markers of arthritis in humans. *Arthritis Rheum.* **38**, 655-659 (1995).

97. Carlson,C.S. *et al.* Osteoarthritis in cynomolgus macaques. II. Detection of modulated proteoglycan epitopes in cartilage and synovial fluid. *J. Orthop. Res.* **13**, 399-409 (1995).

98. Cs-Szabo,G., Roughley,P.J., Plaas,A.H. & Glant,T.T. Large and small proteoglycans of osteoarthritic and rheumatoid articular cartilage. *Arthritis Rheum.* **38**, 660-668 (1995).

99. Plaas,A.H., West,L.A., Wong-Palms,S. & Nelson,F.R. Glycosaminoglycan sulfation in human osteoarthritis. Disease-related alterations at the non-reducing termini of chondroitin and dermatan sulfate. *J. Biol. Chem.* **273**, 12642-12649 (1998).

100. Trowbridge,J.M. & Gallo,R.L. Dermatan sulfate: new functions from an old glycosaminoglycan. *Glycobiology* **12**, 117R-125R (2002).

101. Trowbridge,J.M., Rudisill,J.A., Ron,D. & Gallo,R.L. Dermatan sulfate binds and potentiates activity of keratinocyte growth factor (FGF-7). *J. Biol. Chem.* **277**, 42815-42820 (2002).

102. Deepa,S.S., Umehara,Y., Higashiyama,S., Itoh,N. & Sugahara,K. Specific molecular interactions of oversulfated chondroitin sulfate E with various heparin-binding growth factors. Implications as a physiological binding partner in the brain and other tissues. *J. Biol. Chem.* **277**, 43707-43716 (2002).

103. Kawashima,H. *et al.* Oversulfated chondroitin/dermatan sulfates containing GlcAbeta1/IdoAalpha1-3GalNAc(4,6-O-disulfate) interact with L- and P-selectin and chemokines. *J. Biol. Chem.* **277**, 12921-12930 (2002).

104. Mizuguchi,S. *et al.* Chondroitin proteoglycans are involved in cell division of Caenorhabditis elegans. *Nature* **423**, 443-448 (2003).

105. Ragan,P.M. *et al.* Chondrocyte extracellular matrix synthesis and turnover are influenced by static compression in a new alginate disk culture system. *Arch. Biochem. Biophys.* **383**, 256-264 (2000).

106. Sun,D., Aydelotte,M.B., Maldonado,B., Kuettner,K.E. & Kimura,J.H. Clonal analysis of the population of chondrocytes from the Swarm rat chondrosarcoma in agarose culture. *J. Orthop. Res.* **4**, 427-436 (1986).

107. Petit,B. *et al.* Characterization of crosslinked collagens synthesized by mature articular chondrocytes cultured in alginate beads: comparison of two distinct matrix compartments. *Exp. Cell Res.* **225**, 151-161 (1996).

108. Cao,Y. *et al.* Comparative study of the use of poly(glycolic acid), calcium alginate and pluronics in the engineering of autologous porcine cartilage. *J. Biomater. Sci. Polym. Ed* **9**, 475-487 (1998).

109. Kawasaki,K., Ochi,M., Uchio,Y., Adachi,N. & Matsusaki,M. Hyaluronic acid enhances proliferation and chondroitin sulfate synthesis in cultured chondrocytes embedded in collagen gels. *J. Cell Physiol* **179**, 142-148 (1999).

110. Rotter,N. *et al.* Cartilage reconstruction in head and neck surgery: comparison of resorbable polymer scaffolds for tissue engineering of human septal cartilage. *J. Biomed. Mater. Res.* **42**, 347-356 (1998).

111. Schuman,L. *et al.* Chondrocyte behaviour within different types of collagen gel in vitro. *Biomaterials* **16**, 809-814 (1995).

112. Hunter,C.J., Imler,S.M., Malaviya,P., Nerem,R.M. & Levenston,M.E. Mechanical compression alters gene expression and extracellular matrix synthesis by chondrocytes cultured in collagen I gels. *Biomaterials* **23**, 1249-1259 (2002).

113. Haisch,A. *et al.* [Tissue engineering of human cartilage tissue for reconstructive surgery using biocompatible resorbable fibrin gel and polymer carriers]. *HNO* **44**, 624-629 (1996).

114. Buschmann,M.D., Gluzband,Y.A., Grodzinsky,A.J., Kimura,J.H. & Hunziker,E.B. Chondrocytes in agarose culture synthesize a mechanically functional extracellular matrix. *J. Orthop. Res.* **10**, 745-758 (1992).

115. Mauck,R.L. *et al.* Functional tissue engineering of articular cartilage through dynamic loading of chondrocyte-seeded agarose gels. *J. Biomech. Eng* **122**, 252-260 (2000).

116. Hauselmann,H.J. *et al.* Phenotypic stability of bovine articular chondrocytes after long-term culture in alginate beads. *J. Cell Sci.* **107 (Pt 1)**, 17-27 (1994).

117. Mok,S.S., Masuda,K., Hauselmann,H.J., Aydelotte,M.B. & Thonar,E.J. Aggrecan synthesized by mature bovine chondrocytes suspended in alginate. Identification of two distinct metabolic matrix pools. *J. Biol. Chem.* **269**, 33021-33027 (1994).

118. Heywood,H.K., Sembi,P.K., Lee,D.A. & Bader,D.L. Cellular utilization determines viability and matrix distribution profiles in chondrocyte-seeded alginate constructs. *Tissue Eng* **10**, 1467-1479 (2004).

119. Mauck,R.L. *et al.* Functional tissue engineering of articular cartilage through dynamic loading of chondrocyte-seeded agarose gels. *J. Biomech. Eng* **122**, 252-260 (2000).

120. Herbert,C.B., Bittner,G.D. & Hubbell,J.A. Effects of fibinolysis on neurite growth from dorsal root ganglia cultured in two- and three-dimensional fibrin gels. *J. Comp Neurol.* **365**, 380-391 (1996).

121. Grassl,E.D., Oegema,T.R. & Tranquillo,R.T. Fibrin as an alternative biopolymer to type-I collagen for the fabrication of a media equivalent. *J. Biomed. Mater. Res.* **60**, 607-612 (2002).

122. Hunter,C.J., Mouw,J.K. & Levenston,M.E. Dynamic compression of chondrocyte-seeded fibrin gels: effects on matrix accumulation and mechanical stiffness. *Osteoarthritis. Cartilage.* **12**, 117-130 (2004).

123. Vanderploeg,E.J., Imler,S.M., Brodkin,K.R., García,A.J. & Levenston,M.E. Oscillatory tension differentially modulates matrix metabolism and cytoskeletal organization in chondrocytes and fibrochondrocytes. *Journal of Biomechanics* (2004).

124. Lipman,J.M. Fluorophotometric quantitation of DNA in articular cartilage utilizing Hoechst 33258. *Anal. Biochem.* **176**, 128-131 (1989).

125. Farndale,R.W., Sayers,C.A. & Barrett,A.J. A direct spectrophotometric microassay for sulfated glycosaminoglycans in cartilage cultures. *Connect. Tissue Res.* **9**, 247-248 (1982).

126. Enobakhare,B.O., Bader,D.L. & Lee,D.A. Quantification of sulfated glycosaminoglycans in chondrocyte/alginate cultures, by use of 1,9-dimethylmethylene blue. *Anal. Biochem.* **243**, 189-191 (1996).

127. Rosenberg,L. Chemical basis for the histological use of safranin O in the study of articular cartilage. *J. Bone Joint Surg. Am.* **53**, 69-82 (1971).

128. Calabro,A., Benavides,M., Tammi,M., Hascall,V.C. & Midura,R.J. Microanalysis of enzyme digests of hyaluronan and chondroitin/dermatan sulfate by fluorophore-assisted carbohydrate electrophoresis (FACE). *Glycobiology* **10**, 273-281 (2000).

129. Calabro,A., Hascall,V.C. & Midura,R.J. Adaptation of FACE methodology for microanalysis of total hyaluronan and chondroitin sulfate composition from cartilage. *Glycobiology* **10**, 283-293 (2000).

130. Calabro,A. *et al.* Fluorophore-assisted carbohydrate electrophoresis (FACE) of glycosaminoglycans. *Osteoarthritis. Cartilage.* **9 Suppl A**, S16-S22 (2001).

131. Jackson,P. High-resolution polyacrylamide gel electrophoresis of fluorophore-labeled reducing saccharides. *Methods Enzymol.* **230**, 250-265 (1994).

132. Jackson,P. Polyacrylamide gel electrophoresis of reducing saccharides labeled with the fluorophore 2-aminoacridone: subpicomolar detection using an imaging system based on a cooled charge-coupled device. *Anal. Biochem.* **196**, 238-244 (1991).

133. Sauerland,K., Plaas,A.H., Raiss,R.X. & Steinmeyer,J. The sulfation pattern of chondroitin sulfate from articular cartilage explants in response to mechanical loading. *Biochim. Biophys. Acta* **1638**, 241-248 (2003).

134. Hunter,C.J., Mouw,J.K. & Levenston,M.E. Dynamic compression of chondrocyte-seeded fibrin gels: effects on matrix accumulation and mechanical stiffness. *Osteoarthritis. Cartilage.* **12**, 117-130 (2004).

135. Loeser,R.F. Integrin-mediated attachment of articular chondrocytes to extracellular matrix proteins. *Arthritis Rheum.* **36**, 1103-1110 (1993).

136. Scully,S.P., Lee,J.W., Ghert,P.M.A. & Qi,W. The role of the extracellular matrix in articular chondrocyte regulation. *Clin. Orthop.* S72-S89 (2001).

137. Kim,S.J., Kim,E.J., Kim,Y.H., Hahn,S.B. & Lee,J.W. The modulation of integrin expression by the extracellular matrix in articular chondrocytes. *Yonsei Med. J.* **44**, 493-501 (2003).

138. Ma,P.X. & Langer,R. Morphology and mechanical function of long-term in vitro engineered cartilage. *J. Biomed. Mater. Res.* **44**, 217-221 (1999).

139. Hutmacher,D.W. Scaffolds in tissue engineering bone and cartilage. *Biomaterials* **21**, 2529-2543 (2000).

140. Grande,D.A., Halberstadt,C., Naughton,G., Schwartz,R. & Manji,R. Evaluation of matrix scaffolds for tissue engineering of articular cartilage grafts. *J. Biomed. Mater. Res.* **34**, 211-220 (1997).

141. Hutmacher,D.W. Scaffolds in tissue engineering bone and cartilage. *Biomaterials* **21**, 2529-2543 (2000).

142. Grande,D.A., Halberstadt,C., Naughton,G., Schwartz,R. & Manji,R. Evaluation of matrix scaffolds for tissue engineering of articular cartilage grafts. *J. Biomed. Mater. Res.* **34**, 211-220 (1997).

143. Grande,D.A., Halberstadt,C., Naughton,G., Schwartz,R. & Manji,R. Evaluation of matrix scaffolds for tissue engineering of articular cartilage grafts. *J. Biomed. Mater. Res.* **34**, 211-220 (1997).

144. Kawashima,H. *et al.* Oversulfated chondroitin/dermatan sulfates containing GlcAbeta1/IdoAalpha1-3GalNAc(4,6-O-disulfate) interact with L- and P-selectin and chemokines. *J. Biol. Chem.* **277**, 12921-12930 (2002).

145. Kawashima,H. *et al.* Oversulfated chondroitin/dermatan sulfates containing GlcAbeta1/IdoAalpha1-3GalNAc(4,6-O-disulfate) interact with L- and P-selectin and chemokines. *J. Biol. Chem.* **277**, 12921-12930 (2002).

146. Sugahara,K. *et al.* Recent advances in the structural biology of chondroitin sulfate and dermatan sulfate. *Curr. Opin. Struct. Biol.* **13**, 612-620 (2003).

147. Carter,D.R. *et al.* The mechanobiology of articular cartilage development and degeneration. *Clin. Orthop. Relat Res.* S69-S77 (2004).

148. Mauck,R.L. *et al.* Functional tissue engineering of articular cartilage through dynamic loading of chondrocyte-seeded agarose gels. *J. Biomech. Eng* **122**, 252-260 (2000).

149. Ragan,P.M. *et al.* Down-regulation of chondrocyte aggrecan and type-II collagen gene expression correlates with increases in static compression magnitude and duration. *J. Orthop. Res.* **17**, 836-842 (1999).

150. Burton-Wurster,N., Vernier-Singer,M., Farquhar,T. & Lust,G. Effect of compressive loading and unloading on the synthesis of total protein, proteoglycan, and fibronectin by canine cartilage explants. *J. Orthop. Res.* **11**, 717-729 (1993).

151. Mauck,R.L. *et al.* Functional tissue engineering of articular cartilage through dynamic loading of chondrocyte-seeded agarose gels. *J. Biomech. Eng* **122**, 252-260 (2000).

152. Buschmann,M.D., Gluzband,Y.A., Grodzinsky,A.J. & Hunziker,E.B. Mechanical compression modulates matrix biosynthesis in chondrocyte/agarose culture. *J. Cell Sci.* **108 (Pt 4)**, 1497-1508 (1995).

153. Mow,V.C., Kuei,S.C., Lai,W.M. & Armstrong,C.G. Biphasic creep and stress relaxation of articular cartilage in compression? Theory and experiments. *J. Biomech. Eng* **102**, 73-84 (1980).

154. Yellowley,C.E., Jacobs,C.R. & Donahue,H.J. Mechanisms contributing to fluid-flow-induced Ca2+ mobilization in articular chondrocytes. *J. Cell Physiol* **180**, 402-408 (1999).

155. Valhmu,W.B. & Raia,F.J. myo-Inositol 1,4,5-trisphosphate and Ca(2+)/calmodulin-dependent factors mediate transduction of compression-induced signals in bovine articular chondrocytes. *Biochem. J.* **361**, 689-696 (2002).

156. Wohlrab,D., Lebek,S., Kruger,T. & Reichel,H. Influence of ion channels on the proliferation of human chondrocytes. *Biorheology* **39**, 55-61 (2002).

157. Wohlrab,D., Wohlrab,J., Reichel,H. & Hein,W. Is the proliferation of human chondrocytes regulated by ionic channels? *J. Orthop. Sci.* **6**, 155-159 (2001).

158. Tanaka,N. *et al.* Cyclic mechanical strain regulates the PTHrP expression in cultured chondrocytes via activation of the Ca2+ channel. *J. Dent. Res.* **84**, 64-68 (2005).

159. DiBattista,J.A., Dore,S., Morin,N. & Abribat,T. Prostaglandin E2 up-regulates insulin-like growth factor binding protein-3 expression and synthesis in human articular chondrocytes by a c-AMP-independent pathway: role of calcium and protein kinase A and C. *J. Cell Biochem.* **63**, 320-333 (1996).

160. Greisberg,J.K., Wolf,J.M., Wyman,J., Zou,L. & Terek,R.M. Gadolinium inhibits thymidine incorporation and induces apoptosis in chondrocytes. *J. Orthop. Res.* **19**, 797-801 (2001).

161. Clark,C.C., Iannotti,J.P., Misra,S. & Richards,C.F. Effects of thapsigargin, an intracellular calcium-mobilizing agent, on synthesis and secretion of cartilage collagen and proteoglycan. *J. Orthop. Res.* **12**, 601-611 (1994).

162. Lipman,J.M. Fluorophotometric quantitation of DNA in articular cartilage utilizing Hoechst 33258. *Anal. Biochem.* **176**, 128-131 (1989).

163. Enobakhare,B.O., Bader,D.L. & Lee,D.A. Quantification of sulfated glycosaminoglycans in chondrocyte/alginate cultures, by use of 1,9-dimethylmethylene blue. *Anal. Biochem.* **243**, 189-191 (1996).

164. Duncan,R.L. & Hruska,K.A. Chronic, intermittent loading alters mechanosensitive channel characteristics in osteoblast-like cells. *Am. J. Physiol* **267**, F909-F916 (1994).

165. Wu,L.N. *et al.* Morphological and biochemical characterization of mineralizing primary cultures of avian growth plate chondrocytes: evidence for cellular processing of Ca2+ and Pi prior to matrix mineralization. *J. Cell Biochem.* **57**, 218-237 (1995).

166. Lai,C.C., Hong,K., Kinnell,M., Chalfie,M. & Driscoll,M. Sequence and transmembrane topology of MEC-4, an ion channel subunit required for mechanotransduction in Caenorhabditis elegans. *J. Cell Biol.* **133**, 1071-1081 (1996).

167. Tavernarakis,N. & Driscoll,M. Molecular modeling of mechanotransduction in the nematode Caenorhabditis elegans. *Annu. Rev. Physiol* **59**, 659-689 (1997).

168. Tavernarakis,N. & Driscoll,M. Mechanotransduction in Caenorhabditis elegans: the role of DEG/ENaC ion channels. *Cell Biochem. Biophys.* **35**, 1-18 (2001).

169. Hjelmeland,M.D. *et al.* SB-431542, a small molecule transforming growth factor-beta-receptor antagonist, inhibits human glioma cell line proliferation and motility. *Mol. Cancer Ther.* **3**, 737-745 (2004).

170. Inman,G.J. *et al.* SB-431542 is a potent and specific inhibitor of transforming growth factor-beta superfamily type I activin receptor-like kinase (ALK) receptors ALK4, ALK5, and ALK7. *Mol. Pharmacol.* **62**, 65-74 (2002).

171. Laping,N.J. *et al.* Inhibition of transforming growth factor (TGF)-beta1-induced extracellular matrix with a novel inhibitor of the TGF-beta type I receptor kinase activity: SB-431542. *Mol. Pharmacol.* **62**, 58-64 (2002).

172. Heldin,C.H., Miyazono,K. & ten Dijke,P. TGF-beta signalling from cell membrane to nucleus through SMAD proteins. *Nature* **390**, 465-471 (1997).

173. Lutz,M. & Knaus,P. Integration of the TGF-beta pathway into the cellular signalling network. *Cell Signal.* **14**, 977-988 (2002).

174. Buschmann,M.D., Gluzband,Y.A., Grodzinsky,A.J. & Hunziker,E.B. Mechanical compression modulates matrix biosynthesis in chondrocyte/agarose culture. *J. Cell Sci.* **108 (Pt 4)**, 1497-1508 (1995).

175. Huang,C.Y., Hagar,K.L., Frost,L.E., Sun,Y. & Cheung,H.S. Effects of cyclic compressive loading on chondrogenesis of rabbit bone-marrow derived mesenchymal stem cells. *Stem Cells* **22**, 313-323 (2004).

176. Huang,C.Y., Reuben,P.M. & Cheung,H.S. Temporal expression patterns and corresponding protein inductions of early responsive genes in rabbit bone marrow-derived mesenchymal stem cells under cyclic compressive loading. *Stem Cells* **23**, 1113-1121 (2005).

177. Mehra,A., Attisano,L. & Wrana,J.L. Characterization of Smad phosphorylation and Smad-receptor interaction. *Methods Mol. Biol.* **142**, 67-78 (2000).

178. Tschumperlin,D.J. *et al.* Mechanotransduction through growth-factor shedding into the extracellular space. *Nature* **429**, 83-86 (2004).

179. Maeda,S., Dean,D.D., Gay,I., Schwartz,Z. & Boyan,B.D. Activation of latent transforming growth factor beta1 by stromelysin 1 in extracts of growth plate chondrocyte-derived matrix vesicles. *J. Bone Miner. Res.* **16**, 1281-1290 (2001).

180. Pedrozo,H.A. *et al.* Potential mechanisms for the plasmin-mediated release and activation of latent transforming growth factor-beta1 from the extracellular matrix of growth plate chondrocytes. *Endocrinology* **140**, 5806-5816 (1999).

181. Luettich,K. & Schmidt,C. TGFbeta1 activates c-Jun and Erk1 via alphaVbeta6 integrin. *Mol. Cancer* **2**, 33 (2003).

182. You,L. & Kruse,F.E. Differential effect of activin A and BMP-7 on myofibroblast differentiation and the role of the Smad signaling pathway. *Invest Ophthalmol. Vis. Sci.* **43**, 72-81 (2002).

183. Wang,S.E., Wu,F.Y., Shin,I., Qu,S. & Arteaga,C.L. Transforming growth factor {beta} (TGF-{beta})-Smad target gene protein tyrosine phosphatase receptor type kappa is required for TGF-{beta} function. *Mol. Cell Biol.* **25**, 4703-4715 (2005).

184. Makhijani,N.S., Bischoff,D.S. & Yamaguchi,D.T. Regulation of proliferation and migration in retinoic acid treated C3H10T1/2 cells by TGF-beta isoforms. *J. Cell Physiol* **202**, 304-313 (2005).

185. Caplan,A.I. & Mosca,J.D. Orthopaedic gene therapy. Stem cells for gene delivery. *Clin. Orthop.* S98-100 (2000).

186. Furumatsu,T., Tsuda,M., Taniguchi,N., Tajima,Y. & Asahara,H. Smad3 induces chondrogenesis through the activation of SOX9 via CREB-binding protein/p300 recruitment. *J. Biol. Chem.* **280**, 8343-8350 (2005).

187. Aigner,T. *et al.* SOX9 expression does not correlate with type II collagen expression in adult articular chondrocytes. *Matrix Biol.* **22**, 363-372 (2003).

188. Lisignoli,G. *et al.* Cellular and molecular events during chondrogenesis of human mesenchymal stromal cells grown in a three-dimensional hyaluronan based scaffold. *Biomaterials* **26**, 5677-5686 (2005).

189. Romanov,Y.A., Darevskaya,A.N., Merzlikina,N.V. & Buravkova,L.B. Mesenchymal stem cells from human bone marrow and adipose tissue: isolation, characterization, and differentiation potentialities. *Bull. Exp. Biol. Med.* **140**, 138-143 (2005).

190. Mauck,R.L., Yuan,X. & Tuan,R.S. Chondrogenic differentiation and functional maturation of bovine mesenchymal stem cells in long-term agarose culture. *Osteoarthritis. Cartilage.* (2005).

191. Bosnakovski,D. *et al.* Chondrogenic differentiation of bovine bone marrow mesenchymal stem cells in pellet cultural system. *Exp. Hematol.* **32**, 502-509 (2004).

192. Bosnakovski,D. *et al.* Isolation and multilineage differentiation of bovine bone marrow mesenchymal stem cells. *Cell Tissue Res.* **319**, 243-253 (2005).

193. Abdel-Hamid,M., Hussein,M.R., Ahmad,A.F. & Elgezawi,E.M. Enhancement of the repair of meniscal wounds in the red-white zone (middle third) by the injection of bone marrow cells in canine animal model. *Int. J. Exp. Pathol.* **86**, 117-123 (2005).

194. Lennon,D.P., Edmison,J.M. & Caplan,A.I. Cultivation of rat marrow-derived mesenchymal stem cells in reduced oxygen tension: effects on in vitro and in vivo osteochondrogenesis. *J. Cell Physiol* **187**, 345-355 (2001).

195. Bosnakovski,D. *et al.* Chondrogenic differentiation of bovine bone marrow mesenchymal stem cells in pellet cultural system. *Exp. Hematol.* **32**, 502-509 (2004).

196. Huang,C.Y., Reuben,P.M., D'Ippolito,G., Schiller,P.C. & Cheung,H.S. Chondrogenesis of human bone marrow-derived mesenchymal stem cells in agarose culture. *Anat. Rec.* **278A**, 428-436 (2004).

197. Steinert,A. *et al.* Chondrogenic differentiation of mesenchymal progenitor cells encapsulated in ultrahigh-viscosity alginate. *J. Orthop. Res.* **21**, 1090-1097 (2003).

198. Caplan,A.I. Mesenchymal stem cells. *J. Orthop. Res.* **9**, 641-650 (1991).

199. Enobakhare,B.O., Bader,D.L. & Lee,D.A. Quantification of sulfated glycosaminoglycans in chondrocyte/alginate cultures, by use of 1,9-dimethylmethylene blue. *Anal. Biochem.* **243**, 189-191 (1996).

200. Rosenberg,L. Chemical basis for the histological use of safranin O in the study of articular cartilage. *J. Bone Joint Surg. Am.* **53**, 69-82 (1971).

201. Sotiropoulou,P.A., Perez,S.A., Salagianni,M., Baxevanis,C.N. & Papamichail,M. CHARACTERIZATION OF THE OPTIMAL CULTURE CONDITIONS FOR CLINICAL SCALE PRODUCTION OF HUMAN MESENCHYMAL STEM CELLS. *Stem Cells* (2005).

202. Zhou,D.H. *et al.* [The expansion and biological characteristics of human mesenchymal stem cells]. *Zhonghua Er. Ke. Za Zhi.* **41**, 607-610 (2003).

203. Awad,H.A., Halvorsen,Y.D., Gimble,J.M. & Guilak,F. Effects of transforming growth factor beta1 and dexamethasone on the growth and chondrogenic differentiation of adipose-derived stromal cells. *Tissue Eng* **9**, 1301-1312 (2003).

204. Siebler,T., Robson,H., Shalet,S.M. & Williams,G.R. Dexamethasone inhibits and thyroid hormone promotes differentiation of mouse chondrogenic ATDC5 cells. *Bone* **31**, 457-464 (2002).

205. Mushtaq,T., Farquharson,C., Seawright,E. & Ahmed,S.F. Glucocorticoid effects on chondrogenesis, differentiation and apoptosis in the murine ATDC5 chondrocyte cell line. *J. Endocrinol.* **175**, 705-713 (2002).

206. Hall,F.L. *et al.* Transforming growth factor-beta type-II receptor signalling: intrinsic/associated casein kinase activity, receptor interactions and functional effects of blocking antibodies. *Biochem. J.* **316 (Pt 1)**, 303-310 (1996).

207. Pittenger,M.F. *et al.* Multilineage potential of adult human mesenchymal stem cells. *Science* **284**, 143-147 (1999).

208. Miyazono,K. Positive and negative regulation of TGF-beta signaling. *J. Cell Sci.* **113 (Pt 7)**, 1101-1109 (2000).

209. Moustakas,A., Souchelnytskyi,S. & Heldin,C.H. Smad regulation in TGF-beta signal transduction. *J. Cell Sci.* **114**, 4359-4369 (2001).

210. Nakao,A. *et al.* TGF-beta receptor-mediated signalling through Smad2, Smad3 and Smad4. *EMBO J.* **16**, 5353-5362 (1997).

211. Watanabe,H., de Caestecker,M.P. & Yamada,Y. Transcriptional cross-talk between Smad, ERK1/2, and p38 mitogen-activated protein kinase pathways regulates transforming growth factor-beta-induced aggrecan gene expression in chondrogenic ATDC5 cells. *J. Biol. Chem.* **276**, 14466-14473 (2001).

212. Elder,S.H., Goldstein,S.A., Kimura,J.H., Soslowsky,L.J. & Spengler,D.M. Chondrocyte differentiation is modulated by frequency and duration of cyclic compressive loading. *Ann. Biomed. Eng* **29**, 476-482 (2001).

213. Elder,S.H., Kimura,J.H., Soslowsky,L.J., Lavagnino,M. & Goldstein,S.A. Effect of compressive loading on chondrocyte differentiation in agarose cultures of chick limb-bud cells. *J. Orthop. Res.* **18**, 78-86 (2000).

214. Knight,M.M., Ghori,S.A., Lee,D.A. & Bader,D.L. Measurement of the deformation of isolated chondrocytes in agarose subjected to cyclic compression. *Med. Eng Phys.* **20**, 684-688 (1998).

215. Kim,H.S., Luo,L., Pflugfelder,S.C. & Li,D.Q. Doxycycline inhibits TGF-beta1-induced MMP-9 via Smad and MAPK pathways in human corneal epithelial cells. *Invest Ophthalmol. Vis. Sci.* **46**, 840-848 (2005).

216. Mauck,R.L., Nicoll,S.B., Seyhan,S.L., Ateshian,G.A. & Hung,C.T. Synergistic action of growth factors and dynamic loading for articular cartilage tissue engineering. *Tissue Eng* **9**, 597-611 (2003).

217. Mauck,R.L. *et al.* Functional tissue engineering of articular cartilage through dynamic loading of chondrocyte-seeded agarose gels. *J. Biomech. Eng* **122**, 252-260 (2000).

218. Mow,V.C., Wang,C.C. & Hung,C.T. The extracellular matrix, interstitial fluid and ions as a mechanical signal transducer in articular cartilage. *Osteoarthritis. Cartilage.* **7**, 41-58 (1999).

219. Goldring,M.B., Tsuchimochi,K. & Ijiri,K. The control of chondrogenesis. *J. Cell Biochem.* (2005).

220. Caplan,A.I. Mesenchymal stem cells. *J. Orthop. Res.* **9**, 641-650 (1991).

221. Johnstone,B., Hering,T.M., Caplan,A.I., Goldberg,V.M. & Yoo,J.U. In vitro chondrogenesis of bone marrow-derived mesenchymal progenitor cells. *Exp. Cell Res.* **238**, 265-272 (1998).

222. Hing,W.A., Sherwin,A.F. & Poole,C.A. The influence of the pericellular microenvironment on the chondrocyte response to osmotic challenge. *Osteoarthritis. Cartilage.* **10**, 297-307 (2002).

223. Evans,R.M. The steroid and thyroid hormone receptor superfamily. *Science* **240**, 889-895 (1988).

224. Mangelsdorf,D.J. *et al.* The nuclear receptor superfamily: the second decade. *Cell* **83**, 835-839 (1995).

225. Shur,I., Socher,R. & Benayahu,D. Dexamethasone regulation of cFos mRNA in osteoprogenitors. *J. Cell Physiol* **202**, 240-245 (2005).

226. Kim,H. *et al.* In vivo bone formation by human marrow stromal cells in biodegradable scaffolds that release dexamethasone and ascorbate-2-phosphate. *Biochem. Biophys. Res. Commun.* **332**, 1053-1060 (2005).

227. Engelbrecht,Y. *et al.* Glucocorticoids induce rapid up-regulation of mitogen-activated protein kinase phosphatase-1 and dephosphorylation of extracellular signal-regulated kinase and impair proliferation in human and mouse osteoblast cell lines. *Endocrinology* **144**, 412-422 (2003).

228. Locker,M. *et al.* Paracrine and autocrine signals promoting full chondrogenic differentiation of a mesoblastic cell line. *J. Bone Miner. Res.* **19**, 100-110 (2004).

229. Massague,J. & Chen,Y.G. Controlling TGF-beta signaling. *Genes Dev.* **14**, 627-644 (2000).

230. Lagna,G., Hata,A., Hemmati-Brivanlou,A. & Massague,J. Partnership between DPC4 and SMAD proteins in TGF-beta signalling pathways. *Nature* **383**, 832-836 (1996).

231. George,S.J., Johnson,J.L., Smith,M.A., Angelini,G.D. & Jackson,C.L. Transforming growth factor-beta is activated by plasmin and inhibits smooth muscle cell death in human saphenous vein. *J. Vasc. Res.* **42**, 247-254 (2005).

232. Lopez-Casillas,F. *et al.* Structure and expression of the membrane proteoglycan betaglycan, a component of the TGF-beta receptor system. *Cell* **67**, 785-795 (1991).

233. Zhang,L., David,G. & Esko,J.D. Repetitive Ser-Gly sequences enhance heparan sulfate assembly in proteoglycans. *J. Biol. Chem.* **270**, 27127-27135 (1995).

234. Lopez-Casillas,F., Wrana,J.L. & Massague,J. Betaglycan presents ligand to the TGF beta signaling receptor. *Cell* **73**, 1435-1444 (1993).

235. Lopez-Casillas,F., Payne,H.M., Andres,J.L. & Massague,J. Betaglycan can act as a dual modulator of TGF-beta access to signaling receptors: mapping of ligand binding and GAG attachment sites. *J. Cell Biol.* **124**, 557-568 (1994).

236. Lopez-Casillas,F. *et al.* Betaglycan expression is transcriptionally up-regulated during skeletal muscle differentiation. Cloning of murine betaglycan gene promoter and its modulation by MyoD, retinoic acid, and transforming growth factor-beta. *J. Biol. Chem.* **278**, 382-390 (2003).

237. Harrison,C.A., Gray,P.C., Vale,W.W. & Robertson,D.M. Antagonists of activin signaling: mechanisms and potential biological applications. *Trends Endocrinol. Metab* **16**, 73-78 (2005).